#717

GROUND BASED SURVEYS
BELL LABORATORIES H I SURVEY

GR-11A

ASRA-00011

Table of Contents

1. Introduction

2. Errata/Change Log

3. LINKS TO RELEVANT INFORMATION IN THE ONLINE NSSDC INFORMATION SYSTEM

4. Catalog Materials

    a. Associated Documents

    b. Core Catalog Materials

---

1. INTRODUCTION:

The documentation for this data set was originally on paper, kept in NSSDC's Data Set Catalogs (DSCs). The paper documentation in the Data Set Catalogs have been made into digital images, and then collected into a single PDF file for each Data Set Catalog. The inventory information in these DSCs is current as of July 1, 2004. This inventory information is now no longer maintained in the DSCs, but is now managed in the inventory part of the NSSDC information system. The information existing in the DSCs is now not needed for locating the data files, but we did not remove that inventory information.

The offline tape datasets have now been migrated from the original magnetic tape to Archival Information Packages (AIP's).

A prior restoration may have been done on data sets, if a requestor of this data set has questions; they should send an inquiry to the request office to see if additional information exists.

2. ERRATA/CHANGE LOG:

NOTE: Changes are made in a text box, and will show up that way when displayed on screen with a PDF reader.

When printing, special settings may be required to make the text box appear on the printed output.

Version	Date	Person	Page	Description of Change
01				
02				

3 LINKS TO RELEVANT INFORMATION IN THE ONLINE NSSDC INFORMATION SYSTEM:

http://nssdc.gsfc.nasa.gov/nmc/

[NOTE: This link will take you to the main page of the NSSDC Master Catalog. There you will be able to perform searches to find additional information]

4. CATALOG MATERIALS:

a. Associated Documents To find associated documents you will need to know the document ID number and then click here.
http://nssdcftp.gsfc.nasa.gov/miscellaneous/documents/

b. Core Catalog Materials

DELL M1 LABS
C-29431
FITS HEADER

```
FILE 1     RECORD     1      28800 BYTES
SIMPLE  =                    T /
BITPIX  =                   16 /
NAXIS   =                    3 /
NAXIS1  =                  800 /
NAXIS2  =                  400 /
NAXIS3  =                    1 /
CTYPE1  = 'GLON    '           /
CRVAL1  =           0.00000000 /
CDELT1  =         -0.450563204 /
CRPIX1  =           800.000000 /
CROTA1  =           0.00000000 /
CTYPE2  = 'GLAT    '           /
CRVAL2  =           0.00000000 /
CDELT2  =          0.451127820 /
CRPIX2  =           200.500000 /
CROTA2  =           0.00000000 /
CTYPE3  = 'FELO-LSR'           /
CRVAL3  =          -360000.000 /
CDELT3  =           10000.0000 /
CRPIX3  =           0.00000000 /
CROTA3  =           0.00000000 /
BLANK   =               -32768 /
BSCALE  =       2.14450871E-05 /
BZERO   =          0.118645698 /
BUNIT   = 'K-KM/S  '           /
DATAMAX =          0.821336865 /
DATAMIN =         -0.584045470 /
DATE    = '18/05/91'           /
TELESCOP= 'BTL 7M  '           /
HISTORY COMB TITLE HI.0  T*dV -365,-355
HISTORY COMB PARAM ir:200 gi: rc:
END
```

Ground Based Surveys

Bell Laboratories H I Survey

GR-11A ASRA-00011

This data set consists of three tapes. They are 9 track, 6250 BPI, written in FITS* format by VMS fortran. The C tape is an eight millimeter tape, Low density containing all files from the D tapes. The order of data on the C tape is explained below. The D and C numbers along with the number of files on the D tapes follow:

D#	Files	C#	Files	Data Type
D-86842	145	C-29431	1-145	Whole Sky Images
D-86843	211	C-29431	146-290 436-501	South Polar Cap Images R.A. - Velocity Images
D-86844	145	C-29431	291-435	North Polar Cap Images

* When loading data to disk, always specify 'RECORDSIZE=2880' and BLOCKSIZE=(largest blocksize) on the mount command. This will insure fixed length records within the newly created data file. The FITS Reader requires fixed length records.

THE ASTROPHYSICAL JOURNAL SUPPLEMENT SERIES, 79:77–104, 1992 March
© 1992. The American Astronomical Society. All rights reserved. Printed in U.S.A.

THE BELL LABORATORIES H I SURVEY

ANTONY A. STARK,[1] CHARLES F. GAMMIE,[2] ROBERT W. WILSON, JOHN BALLY, AND RICHARD A. LINKE[3]
Radio Physics Research Department, AT&T Bell Laboratories, Holmdel, NJ 07733
AND
CARL HEILES AND MARK HURWITZ
University of California, Berkeley, Berkeley, CA 94720
Received 1990 July 11; accepted 1991 July 19

ABSTRACT

The sky north of $\delta = -40°$ was observed in the 21 cm line of atomic hydrogen with the FWHM = 2° beam of the 20 foot horn reflector at AT&T Bell Laboratories, Crawford Hill. The survey covers a velocity range of 654 km s^{-1} centered on the Galactic standard of rest, with 5.3 km s^{-1} wide filters. Calibration and reduction of the observations are described. The survey is presented as a series of images of the sky, each covering a 10 km s^{-1} wide velocity range. This survey is distinguished by its sensitivity to low surface brightness features ($T_A \approx 50$ mK) and relative freedom from sidelobe contamination. High-velocity clouds are extracted and cataloged automatically. At the resolution of the survey, the lowest H I column density in the sky is 5.7×10^{19} cm^{-2}.

Subject headings: ISM: general — radio lines: atomic — surveys

1. INTRODUCTION

A northern sky 21 cm line survey was made with the 20 foot horn reflector at AT&T Bell Laboratories, Crawford Hill, in order to obtain column densities and velocities of low surface brightness features. These measurements are useful for studying the distribution of high-velocity clouds, estimating the reddening to extragalactic objects, and exploring the relationship between neutral Galactic hydrogen and diffuse background emission at many wavelengths. Observations were made as drift scans along even declinations between $\delta = -40°$ and $\delta = +90°$, at the epoch (1981) of the observations. The horn antenna has a FWHM beam size of 2° at 21 cm. This large beam made it possible to cover the whole visible sky in 66 constant-declination scans. The survey is undersampled in declination (one beamwidth sampling) and oversampled in right ascension (roughly quarter beamwidth sampling). The average rms noise of spectra taken at all declinations is 0.017 K in 5.2 km s^{-1} wide channels, although in some cases baseline problems make the survey unreliable at this level. The release version of the survey contains 19,248 spectra; more were taken but some were excluded under well-defined criteria.

Precise measurements of 21 cm line strengths are complicated by stray radiation, which is the presence of emission in the antenna sidelobes. The magnitude of this effect depends on the structure of the antenna, the illumination of the antenna by the feed, and the orientation of the antenna with respect to the ground and emission features on the sky. For most telescopes, stray radiation can contribute a significant fraction of the total observed 21 cm line emission. For example, Lockman, Jahoda, & McCammon (1986, hereafter LJM), in their NRAO 140 foot (42.7 m) telescope study of regions having low H I column density, found that for some pointings of that antenna more than half of the received signal was from emission in the sidelobes rather than the main beam. The problem is most acute in directions where actual column densities on the sky are lowest, so great care must be taken in the study of low surface brightness features at frequencies where H I emission is strong elsewhere on the sky. The 20 foot horn reflector has a main beam efficiency of 92%, and almost all the remaining sensitivity is in nearby diffraction lobes. In contrast, the main beam efficiency for a typical on-axis parabolic antenna like the 140 foot is of order 80%, with perhaps half of the remaining 20% in distant side lobes. It is the response at large angles from the main beam that causes most of the spillover problem, and in the horn reflector antenna this is very much reduced.

A method of correcting for stray radiation in large antennas has been developed by LJM, using data from the present survey. LJM combine several spectra from the 140 foot telescope by weighted averaging to synthesize a beam like that of the 20 foot horn and take the difference between that synthetic spectrum and the spectrum from the present survey at the same position. They attribute the difference to contamination by stray radiation in the 140 foot telescope. One of the low column density regions they have studied is called "The Hole," and its 20 foot horn spectrum is shown in Figure 1. The total column density toward this feature is 5.67×10^{19} cm^{-2}, the lowest in the survey (and almost certainly the lowest in the sky at this resolution). Appendix A of LJM gives a detailed discussion of their technique.

The present survey covers most of the sky with sensitivity good enough to detect high-velocity clouds as well as essentially all Galactic emission. This paper describes the survey in order to make it generally useful. The instrument and observing methods are described in § 2. In § 3, the baseline removal

[1] Postal address: Smithsonian Astrophysical Observatory, 160 Concord Avenue, Cambridge, MA 02138.
[2] Postal address: Princeton University Observatory, Peyton Hall, Princeton, NJ 08544.
[3] Postal address: NEC Research Institute, Inc., 4 Independence Way, Princeton, NJ 08540.

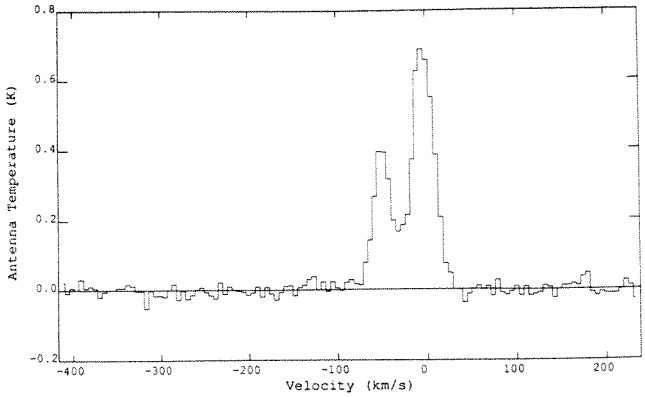

FIG. 1.—Spectrum of the low column density region at (l = 148.1, b = 53.3).

technique is described. The data are presented as images in § 4. A catalog of high-velocity clouds is presented in § 5. The conclusions in § 6 give some preliminary results and present a column density map for H I. The Appendices document machine-readable versions of the survey data.

2. OBSERVING METHODS AND FLAWS IN THE DATA

Observations were made with the 20 foot horn reflector on Crawford Hill during the summer of 1980 and the summer and fall of 1981. Spectra were taken as drift scans, i.e., with the antenna stationary with respect to Earth, and almost all were taken with the antenna pointed at the meridian. The integration time varied with declination—it was adjusted so that the sky moves roughly a quarter beamwidth over the course of the integration. Many of the declination strips were observed more than once. If a declination strip was done more than once, the last occurrence (the one with the largest scan number) is almost always the most reliable, since the instrumentation was monitored and improvements made as the observations were carried out. Some declination strips were repeated because of known errors or instrumental problems in the earlier data. In general only the last version of a declination strip is included in our analysis.

The antenna is described by Crawford, Hogg, & Hunt (1961). It is an offset paraboloid with a large offset angle: the central ray is deflected by an angle of 90° at the primary mirror. The antenna has bilateral symmetry about a single plane which bisects the primary mirror and passes through its focus, but it does not have radial symmetry. The polarization mode where the electric field vector is perpendicular to the symmetry plane is called "transverse" and has a cleaner beam pattern than the other polarization mode where the electric field is parallel to the symmetry plane, called "longitudinal."

The spillover response of this antenna is much better than conventional antenna designs, but it is nevertheless present and not negligible. The sidelobe response was mapped at 21 cm in the transverse polarization by Penzias, Encrenaz, & Wilson (1969). In this polarization the primary beam efficiency is about 92%. The sidelobes have more integrated power in the longitudinal polarization, especially at large angles; the sidelobe patterns in this polarization have been mapped at 2390 MHz by Crawford et al., (1961) and 4080 MHz by Hogg & Wilson (1965). The longitudinal polarization pattern shows two dominant sidelobes, both centered on the plane of antenna symmetry. The larger sidelobe contains roughly 6×10^{-3} of the total antenna response. It is about 18° from the main beam, and when the antenna is pointed toward the meridian in the south, it falls on a region at an hour angle ~ -1.5 h and about the same declination as the main beam. The smaller sidelobe contains roughly 10^{-3} of the total response, and falls about 70° from the main beam on the opposite side, on a region near hour angle $\sim +5$ h and about the same declination as the main beam.

The rectangular-to-circular waveguide coupler (labeled "D" in Fig. 2) was oriented so that for the antenna at 45° elevation angle the receiver is sensitive only to transverse mode, while "over-the-top" at an elevation angle of 135°, the receiver is sensitive only to "longitudinal" mode. At all elevation angles, power at the receiver, P, is a combination of power in the two modes P_t and P_l:

$$P = P_t \cos^2(\mathrm{el} - 45°) + P_l \sin^2(\mathrm{el} - 45°) .$$

Most of the data are therefore predominantly from the better polarization mode. Some of the data north of $\delta = 40°$ (that is, north of the zenith) have much more "longitudinal" polarization than they should, because these data were perversely taken in an "over-the-top" configuration, where the elevation angle of the telescope is more than 90°, causing an increased sidelobe level and spurious features like the one at $l = 190°$, $b = 50°$, $v = 40$ kms^{-1}. When these data are mixed with other data that do not have this problem, the features take on a striped appearance.

For the data discussed here, the receiver was configured with the amplifier Dewar connected to the antenna feed through a

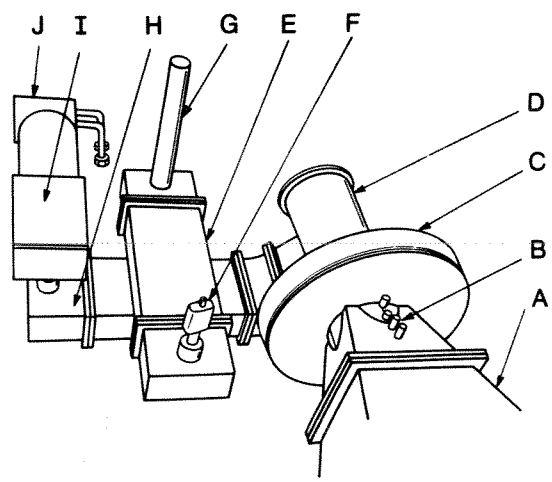

FIG. 2.—Waveguide connections between the receiver and horn antenna. (A) Tapered end of the 20 foot horn. (B) Square taper to circular waveguide conversion. (C) Rotary waveguide choke joint: Parts A and B rotate in elevation with the antenna; the other parts do not. (D) "Ohm coupler"-type circular-to-rectangular waveguide converter. (E) 25.33 dB cross-guide coupler. (F) 10^4 K noise diode. (G) Waveguide termination. (H) Waveguide-to-coax adapter. (I) Receiver dewar. (J) 15 K refrigerator.

directional coupler for the noise diode, as shown in Figure 2. The spectra were frequency-switched by square-wave frequency modulation of the local oscillator. Some earlier data were taken in a load-switched configuration but are not included in the present discussion or the current release of the data.

The first receiver stage was a particularly successful example (BTL #1) of the Weinreb, Fenstermacher, & Harris (1982) cooled FET amplifier design, with a noise temperature of about 6.5 K. It was coupled to an uncooled coaxial-to-waveguide adapter which introduced ~13 K noise. The waveguide and directional coupler introduce another 2 K noise, and back-lobe spillover adds another ~3 K. The antenna system therefore had a noise temperature of about 26 K. Additional sources of noise were the atmospheric emission (2–20 K, depending on elevation), the cosmic background radiation (3 K), and Galactic synchrotron emission (0.3 to ~20 K). The total system noise from all sources was typically 34 K.

The 21 cm signal was downconverted with a computer-controlled local oscillator to an intermediate frequency (IF) band centered at 150 MHz, which was sent by cable to the spectrometer in the control building of the 7 m millimeter-wave antenna. The IF signal was split and sent to two spectrometers: 128 × 250 kHz wide filters (wide-band) and 124 × 25 kHz wide filters (narrow-band). The narrow-band filters were synthesized using a spectrum expander (Henry 1976).

The narrow-band spectrometer only covered a velocity range 654 kms^{-1} wide. In order to optimize the placement of this bandwidth on the Galactic signal, the spectrometer was shifted at regular intervals so that the central channel was within 13.2 kms^{-1} of the Galactic standard of rest (GSR). This was done in two stages. At the beginning of every calibration (roughly every 20 minutes), the LSR velocity of the central channel was calculated by the formula:

$$v_{\mathrm{LSR},c} = 26.375\ \mathrm{kms}^{-1} \times \text{nearest integer}\left[\frac{220}{26.375}\sin(l)\cos(b)\right],$$

where 220 kms^{-1} is the rotation speed of the Galaxy, and 26.375 kms^{-1} is the velocity width of 5 channels, so that shifts in velocity moved the data by multiples of 5 channels. That is, the channel corresponding to 0 kms^{-1} LSR is always a multiple of precisely 5 channels from the center. The second stage of velocity tracking occurs within a single spectrum. During the collection of each spectrum, the local oscillator frequency was recalculated every few seconds in order to compensate for small shifts between the velocity of the antenna and the LSR.

The backend was designed for systems with signal-to-noise ratios smaller than unity. In the Galactic plane, however, the survey data have large signal-to-noise ratios ([H I line + background continuum]/system temperature) $\gtrsim 4$. The available dynamic range of the backend is about 30 dB, whereas the survey data has a dynamic range of 40 dB. Faced with the prospect of losing either the brightest or the faintest points in some spectra, we chose to save the faintest points because the brightest 21 cm lines have been well studied. When a channel in the filter bank falls on a bright part of the spectrum, the amplifiers constituting that channel saturate. This causes the survey to be inaccurate for individual channels brighter than 40 K. Other channels less than 40 K in the same spectrum are not affected. We spent considerable time trying to correct for this problem without success and believe there is no way to make the survey useful for channels with high antenna temperatures.

The system gain and temperature for the survey were absolutely calibrated using a noise diode and directional coupler that were themselves calibrated in the laboratory. The calibration agrees with that of Penzias et al. (1969) within 2% but is independent of that work. Early, unauthorized versions of the survey include data (excluded from the release version) that was calibrated with an unstable noise diode. The system gain was measured about three times per hour, sufficiently often that all H I profiles are accurate within a few percent, except for single channels with $T \gtrsim 40$ K.

Data taken with the frequency-switched reference band above 1420.4 MHz were generally of inferior quality and were excluded when a spectrum taken frequency-switched the other way was available within a circle of radius 55′. Spectra were also excluded if radar contamination was present in the broad-band spectrum or if trouble comments in the observing log were coupled with bad baselines, provided that a spectrum without these problems was present in the data within a circle 55′ in radius.

3. BASELINE REMOVAL

The frequency-switching observing technique used here introduces baseline curvature because the reflected power, gain, and system temperature depend on frequency. The wide-band spectrum with its 32 MHz bandwidth was used to obtain a preliminary estimate of the baseline curvature in the 3.1 MHz wide narrow-band spectrum; the final estimate was obtained from the narrow-band spectrum itself, because some of the baseline curvature is introduced by the spectrum expander.

The preliminary estimate of the baseline curvature was obtained by least-squares fitting a parabolic curve to a number of channels in the wide-band spectrum. A sample wide-band spectrum is shown in Figure 3. In this spectrum the 21 cm line appears as two peaks, one positive and one negative, separated by the frequency-switching interval of 3.1 MHz (equivalent to

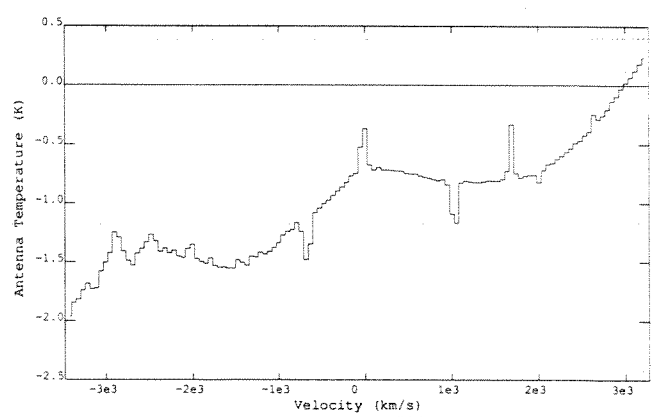

FIG. 3.—Typical wide-band spectrum

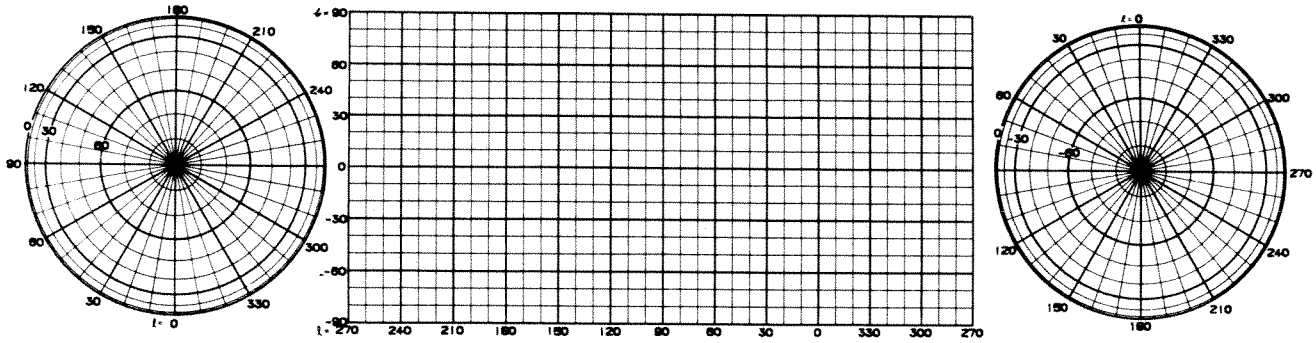

FIG. 7.—Coordinate system for the velocity slice images, for making a transparent overlay

present data were unsuccessful. The spectrum expander causes baseline errors that depend on the measured spectrum itself. This effect is serious in regions where the H I line and background synchrotron emission are intense, and depends not only on the intensity of the H I line but also on its shape.

TABLE 1

PLATE CUTOFF INTENSITIES

Velocity			Intensity (K km s^{-1})		
High	Center	Low	Top	Middle	Bottom
−150	−155	−160	4	4	4
−135	−140	−145	4	4	4
−125	−130	−130	16	4	16
−120	−120	−125	4	16	4
−110	−115	−115	32	4	16
−105	−105	−110	4	32	4
−95	−100	−100	32	4	32
−90	−90	−95	4	64	4
−80	−85	−85	128	4	128
−75	−75	−80	8	128	8
−65	−70	−70	128	8	128
−60	−60	−65	16	128	16
−55	−55	−55	128	64	16
−50	−50	−50	128	32	16
−45	−45	−45	128	64	16
−40	−40	−40	128	64	32
−35	−35	−35	256	64	32
−30	−30	−30	256	64	32
−25	−25	−25	256	64	32
−20	−20	−20	512	128	64
−15	−15	−15	512	256	64
−10	−10	−10	1024	512	128
−5	−5	−5	1024	512	128
0	0	0	512	256	128
5	5	5	1024	512	256
10	10	10	1024	512	256
15	15	15	1024	512	256
20	20	20	512	256	128
25	25	25	512	256	128
30	30	30	512	128	32
35	35	35	512	128	32
40	45	50	4	4	4
55	60	65	4	4	4
70	75	80	4	4	4
N_{tot}			512	1024	4096

NOTE.—All other plates cutoff at 2 K km s^{-1}.

Despite this problem, our procedure for correcting each spectrum on an individual basis appears to be satisfactory at the level of 0.05 K or better in most cases. Figure 4 shows a typical baseline.

Baselines of some spectra are degraded to a fairly significant degree by strong H I emission. This occurs routinely in the Galactic plane, and occasionally at intermediate latitudes. In addition, baselines can be adversely affected by strong interference outside the narrow-band spectrometer, as discussed above. In such cases the baseline is not well represented by a parabolic curve. We made no attempt to correct such cases on an individual basis. As a result, the survey cannot be regarded as absolutely reliable below the 0.1 K level. Figure 5 shows a spectrum with some residual baseline problems. The quality of most spectra is bracketed by Figures 4 and 5.

4. SKY IMAGES

The survey is a scalar function of three dimensions and must be sectioned in order to display it on the page. H I surveys have traditionally been published in the form of individual spectra (Weaver & Williams 1973) or as latitude-velocity contour maps. The present survey is particularly well suited to the study of clouds, which have linewidths of order 10 kms^{-1}, so Figure 6 (Plates 26–89) present the survey in the form of images, each showing a picture of the sky in a 10 kms^{-1} wide range of LSR velocities (a velocity "slice"). The images were

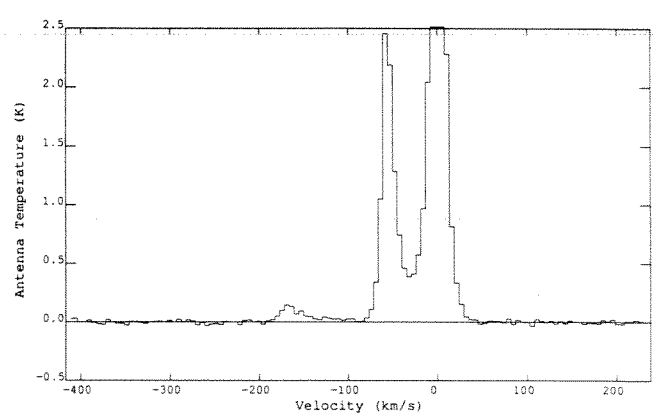

FIG. 8.—Typical spectrum showing high-velocity feature

made using COMB, the Bell Labs single-dish data reduction package. The images are a representation of brightness as a function of the two position coordinates. The brightness at intermediate positions in the image were interpolated using a two-dimensional Gaussian weighting function with a FWHM = 2°.4 that was truncated at 6°.7 diameter. The photographic exposures were made with the dicomed at the NRAO Very Large Array. The velocity slices were obtained by integrating over a 10 kms^{-1} velocity interval centered on the indicated velocity, so the velocity resolution is degraded roughly a factor of 2 from the original data.

Each velocity slice is shown in a group of three projections, two circular and one rectangular, with the central velocity indicated at the far right (except for the total column density image, which has no velocity label). On the left is an orthographic projection [$r = \cos(b)$] of the northern Galactic hemisphere: the north Galactic pole is at the center, and Galactic longitude increases clockwise from the Galactic center, which is at the bottom. The rectangular image at the center is a Galactic coordinate projection, with $l = 270°$ at the left and $l = -90°$ at the right. The Galactic plane runs horizontally across the middle, with positive b above and negative b below. The vertical axis is scaled uniformly in b. The circular image on the right is an orthographic projection of the southern hemisphere, with Galactic longitude increasing counterclockwise from the Galactic center at the top. The coordinate systems are shown explicitly in Figure 7, which is reproduced at the same scale as the images; the reader is invited to make a transparent overlay.

The images are scaled so that the wedge at the bottom of each page runs linearly from zero to a cutoff intensity. The cutoff intensity for each triplet of images is either 2 K kms^{-1} or is listed in Table 1. Due to the high dynamic range in the survey, the data at velocities near the local standard of rest could not be adequately represented on a linear scale in one set of images; in these cases the same velocity slice is shown two or more times with different scales. In some places the temperatures are sufficiently negative that wraparound occurs (e.g., at −275 to −285 kms^{-1}); these areas on the map are bright around the edge and dark in the middle. As discussed in Appendix B, all the images are available in machine-readable FITS format from the National Space Science Data Center A.

5. HIGH-VELOCITY CLOUDS

High-velocity clouds were first observed in the 21 cm line in 1963 (Muller et al. 1966; cf. Verschuur 1975) and have since been observed in absorption at optical and UV wavelengths. Typically they have column densities of a few $\times 10^{19}$ cm^{-2} and velocity widths of a few tens of kilometers per second. A representative spectrum of a high-velocity cloud from the survey is shown in Figure 8, where the high velocity feature is centered at ~ -170 kms^{-1}. Figures 9 and 10 describe the distribution of high-velocity clouds over position on the sky and velocity. Figures 9*a*, 9*b*, and 9*c* are maps of the integrated column density in high-velocity clouds, according to a definition discussed below. As far as we know, this is the most completely sampled map of high-velocity clouds available to date. Other surveys (Giovanelli 1980; Hulsbosch & Wakker 1988) use smaller beams but are significantly undersampled. Recent absorption-line work by Colgan, Salpeter, & Terzian (1990) implies that the present survey is also representative in the sense that there is little high-velocity material present in a subthermally excited state, which would not be visible in emission. Most of the high-velocity material is concentrated within ~50° of the point $l = 120°$, $b = 15°$, as has been known for some time. The majority of the clouds are in the north Galactic hemisphere. Figure 10 is an attempt to show this effect: it compares the average of all spectra taken at $b > 20°$ with the average of all spectra taken at $b < -20°$ and shows that there is more high-velocity material at positive b. At some low level of antenna temperature, the values in this graph will be subject to unknown systematic effects, because we do not know about the quality of the baseline fits at levels significantly below the average noise of a single spectrum, and at some level all spectra will have shared baseline problems which do not average out. Velocities with respect to the local standard of rest vary from tens to hundreds of kilometers per second; features with $|V_{\mathrm{lsr}}| \gtrsim 80$ kms^{-1} and $|b| \gtrsim 15°$ have traditionally been called high-velocity clouds.

Only for two of the clouds is anything known about distance. Songaila, Cowie, & Weaver (1988) have bracketed the distance to clouds near $(l, b) = (100°, 50°)$ by looking for Ca K absorption features in stars whose distances are known. These clouds are between 0.3 and 2 kpc distant. The Magellanic Stream, on the other hand, connects continuously with the Magellanic Clouds, so at least some of it is ~50 kpc distant.

High-velocity clouds tend to blend in continuously with the Galactic emission. In order to separate them out and catalog them, we adopted a definition which allows us to state definitely (if somewhat arbitrarily) whether a given emission feature is "high-velocity" or not. We define permitted velocities in the context of a model galaxy where the rotation speed of circular orbits is constant on cylinders and the rotation curve is flat at 220 kms^{-1}. The Galaxy model is bounded by two planes above and below the Galactic plane ($z = 0$) and separated from the Galactic plane by 500 pc $\times R_0/(8.5$ kpc), so that the two planes are about 1 kpc apart and the Galactic plane is sandwiched between them. A line of sight from Earth (with $b \neq 0$) will pierce one of these planes. Between Earth and the point where the line of sight "leaves the Galaxy" by piercing a plane is a line segment, and each point on that line segment has associated with it a velocity which is the projection of the local rotational velocity vector onto the line of sight. The set of those projected circular velocities is then the range of "permitted' velocities on that line of sight. A buffer zone of $40(1 + \cos b)$ kms^{-1} around these velocities is also considered to be "permitted." This definition of high-velocity clouds differs from that of van Woerden, Schwartz, & Hulsbosch et al. (1985), who define as "high-velocity" any cloud lying at $|b| > 15°$ and $|v| > 50$ kms^{-1}. Our definition excludes gas which is near the Galactic plane and rotating with the Galactic rotation curve, but includes gas in the plane at forbidden velocities. Gas which shares the Galactic rotation but is warped well out of the plane is defined by us (and everyone else) to be "high-velocity," even though this material may just be distant spiral arms (Verschuur 1971; Davies 1972).

Table 2 is a catalog of high-velocity objects found in the survey. Naturally it shares the sampling properties of the survey, as described in § 2: it covers only $\delta > -40°$ and has higher sensitivity further from the celestial equator and the horizon;

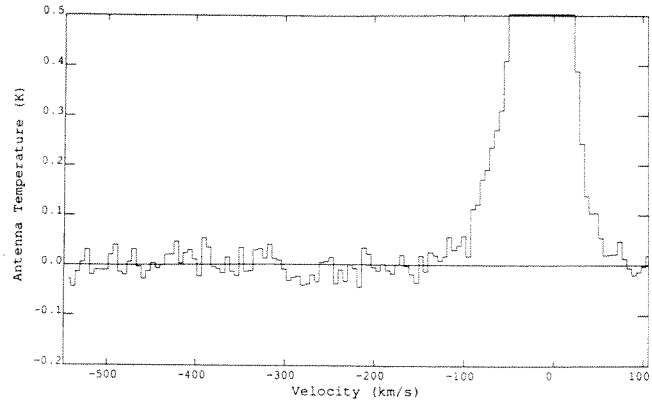

FIG. 4.—A spectrum showing a typical baseline

12.4 channels). The feature appearing at 1700 kms^{-1} is radar interference from Newark Airport, 30 km away. The 3.1 MHz frequency-switching interval was positive in some cases, negative in others; that is, the negative peak may be at either larger or smaller channel numbers than the positive peak. As mentioned in § 2, the latter scheme usually produces better spectra. Consider the former case in which the negative peak is to the right of the positive peak, i.e., at a larger channel number. Let $n_{\rm lsr}$ be the number of the channel with the greatest positive brightness. The numbers of the channels included in the least-squares fit were $n_{\rm lsr} - 6$ to $n_{\rm lsr} - 13$; $n_{\rm lsr} + 7.2$ to $n_{\rm lsr} + 5.2$; and $n_{\rm lsr} + 6 + 12.4$ to $n_{\rm lsr} + 13 + 12.4$. The first interval corresponds to -690 to -320 kms^{-1} relative to the positive peak. The second interval corresponds to 270 to 380 kms^{-1} relative to the positive peak and -380 to -270 kms^{-1} relative to the negative peak. The third interval corresponds to 320–690 kms^{-1} relative to the negative peak. The resulting baseline fits were also applied to the narrow-band spectrum before the final estimate of baseline curvature was obtained.

The final estimate of the baseline curvature was derived from the narrow-band spectrum itself. A parabolic curve was least-squares fitted to each spectrum using an iterative technique. Only a limited number of channels were included in each fit, and this number evolved by iteration. For the first iteration, no channel was included if it was within four channels of a channel having $T > 0.12$ K or if it was within 10 channels of a channel having $T > 1.0$ K. However, the first two and the last two channels of the set of 124 were always included in the fit, no matter what their temperature. After the first least-squares fit, any channel having a residual greater than 3 times the rms deviation, and any channel within 10 channels of a channel having residual greater than 1.0 K, were excluded from the next iteration. The iterations were continued, using this method, until repeated iterations excluded no additional channels.

The presence of strong radar interference in the wide-band spectrum could introduce baseline curvature in the narrow spectrum that is not well-represented by a parabola. (The radar signal in Fig. 3 is a mild example.) Some of the auxiliary variables in the data header, I_{15} and R_7–R_9, provide information on the presence of such interference (see Appendix A). This information helps to locate narrow-band spectra having poorly defined baselines. I_{15} indicates the direction of frequency switching. If $I_{15} = 1$, the reference band was below the frequency of the 21 cm line; if $I_{15} = 2$, it was above. The data with $I_{15} = 2$ were all taken early in the survey and tend to have more profound baseline problems than the $I_{15} = 1$ data. The frequency-switching direction was changed when it was discovered that switching the other way produced better baselines. R_7, R_8, and R_9 provide information on the presence of interference in the wide-band spectrum. To determine these parameters, a fifth degree polynomial was least-squares fitted to all channels in the wide-band spectrum that were farther than 9 channels (2.25 MHz, or 475 kms^{-1}) from 0 kms^{-1} LSR in either the signal or the reference frequency. After this first iteration of the fit, any channel having a residual greater than 3 times the rms deviation of the fit was excluded from the next iteration. Iterations were continued until no additional channels exceeded 3 times the rms deviation. Those channels that were excluded because of large residuals always had interference. The number of such channels is a measure of the number of interfering signals in the wide-band spectrum; this number is R_9. The rms deviation of all channels further than 9 channels from 0 kms^{-1} LSR is a measure of the strength of the various interfering signals; this is R_7. Sometimes the rms deviation is dominated by a single strong interfering signal, which does not necessarily cause bad baselines; in such cases the sum of the absolute values of the residuals is probably a better measure of the strength of the interference, and this is R_8. Our present experience suggests that R_8 and R_9 offer a guide to baseline quality. R_9 by itself is a reasonably good indicator of baseline quality: if $I_{15} = 1$, then values of R_9 greater than 11 indicate increasingly poor baseline quality; if $I_{15} = 2$ than values of R_9 greater than 21, or perhaps somewhat more, indicate poor baseline quality. A better indicator of bad baselines than R_9 alone is a combination of R_9 with R_7 or R_8.

The procedure used to correct baselines considers only each individual spectrum. This differs from procedures used in earlier surveys, which assumed that baseline parameters vary smoothly with time. These latter procedures are better in principle because the derived baseline corrections are more nearly independent of the presence of weak, high-velocity H I. Unfortunately, considerable efforts to apply such procedures to the

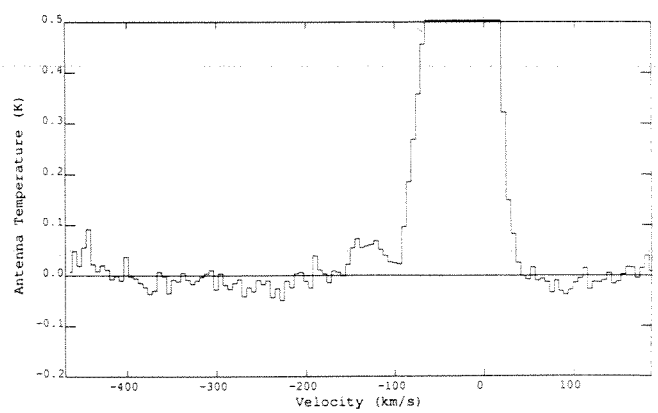

FIG. 5.—A spectrum showing some baseline problems

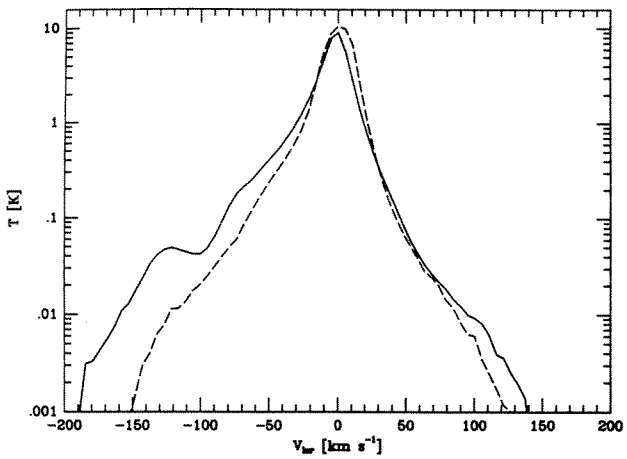

FIG. 10.—Average of all spectra taken at $b > 20$ (*solid line*) and at $b < 20$ (*dashed line*), showing that there is more high-velocity material in the north galactic hemisphere.

the velocity range is approximately ±314 kms^{-1} around 0 kms^{-1} GSR. The catalog was generated automatically, using an algorithm which searched for antenna temperatures above noise level in channels having velocities outside permitted velocity intervals, then linked the resulting detections into spatially extended "clouds." To generate the list of detections in individual spectra, the following process was performed repeatedly on each spectrum. First, the peak channel was identified and checked to make sure its temperature is greater than $T_{\rm pk,min}$ (a parameter of the catalog, to be set as described below). Second, channels around the peak channel were grouped into a "block" of channels and adjacent channels added to that "block" until either the edge channels were below 3 σ, or the "derivative" $|T_{i+1} - T_i|$ exceeded 1.5 σ, where σ is the survey average noise level. The first criterion allows for the possibility that there is no overlap with another cloud in velocity space. This approach to identifying cloud boundaries in velocity space will systematically underestimate the total column density by neglecting emission in the wings, but it is not possible to fit each line with an assumed shape (e.g., Gaussian) since in most cases the profiles are highly irregular. The second criterion allows for the possibility of cloud overlap in velocity space. A sufficiently large change in the derivative, therefore, indicates the beginning of a new "block." Third, having identified a contiguous "block" of "on" channels within the spectrum, it was checked that the peak velocity is outside "permitted" velocities and the integrated intensity is greater than $T_{\rm int,min}$. Finally, if these criteria are satisfied, the block of channels was recorded as a detection, and the velocity range, peak velocity, peak temperature, and integrated intensity were recorded. The process was then repeated on the remaining channels until the peak channel was below $T_{\rm pk,min}$.

Table 2 lists contiguous blocks of "on" channels from groups of spatially adjacent spectra. Connected objects in (l, b, v) were defined as follows. Blocks of "on" channels from adjacent spectra were compared to see if peak velocities for the blocks are within two channels of each other. If they are, the blocks were linked together. After this procedure was repeated for all adjacent pairs of spectra, the resulting linked structures were extracted. For a physical connection between clouds, it is of course necessary but not sufficient that they overlap in (l, b, v).

Columns (2), (3), (4), and (5) in Table 2 give the position of peak brightness for the catalog entry. Columns (6)–(11) are the boundaries of a rectangular prism in l, b, v space which encloses the object. Column (12) is sum of T_A in all "on" channels (see above) associated with this object and is therefore a measure of total flux (in units of K kms^{-1} beam area) and an indicator of the likelihood that the object is real. The average surface brightness in K kms^{-1} of the object is this number divided by the total number of spectra in which the object is detected (col. [14]). Column (13) is the peak antenna temperature of the object (in K). Column (14) is the number of points in which the object is detected. The full list of detections in individual spectra is too long to publish but is available on request.

How many of the blocks and connected structures found by our cataloging algorithm are real? The two critical parameters are $T_{\rm pk,min}$ and $T_{\rm int,min}$. The values of these parameters used to produce Table 2 were set by exploring the noise properties of the survey. The temperature scale was inverted (that is, the data were multiplied by −1) to produce a fake survey with much the same noise properties as the uninverted data. The number of detections in the inverted survey is then an indicator of the number of false detections to expect in the catalog. The total number of "on" blocks detected in individual spectra was taken as the performance indicator, and it was required that the number of detections in the inverted survey be less than 20% of the number of detections in the real survey. This resulted in values of $T_{\rm pk,min} = 3.0\ \sigma$ and $T_{\rm int,min} = 7.5\ \sigma$: 5824 on blocks were found in the positive survey, and 1159 were found in the inverted survey, implying that *at least* 80% of the detections in the catalog are real. This overestimates the number of false detections, however, because some negative-temperature features are actually the result of emission in the frequency-switched reference band. Almost all of the "detections" in the inverted survey are localized near the Galactic plane in the second quadrant (cf. the $v = -200$ kms^{-1} velocity slice). A second test of the cataloging algorithm run on simulated spectra containing only Gaussian noise resulted in no detections. This underestimates the number of false detections since systematic instrumental effects can create features that look real. Finally, note that the criteria for detections are not corrected for variations in noise level from spectrum to spectrum or with declination. Thus in some parts of the sky (near the lower declination limit of the survey), false detections are more likely. We estimate that 95% of the features in Table 2 are real.

6. CONCLUSION

This survey provides an accurate picture of H I column densities in the Galaxy and in high-velocity clouds. The total column density in high-velocity material (defined in § 5) is shown in Figures 9*a*, 9*b*, and 9*c*. Figure 11 shows the Magellanic Stream. The data represented here may be used to test models of high velocity clouds such as the infall model of Oort (1969), models of the Magellanic Stream (Kerr & Sullivan 1969) and the Galactic fountain model (Corbelli & Salpeter 1988). Esti-

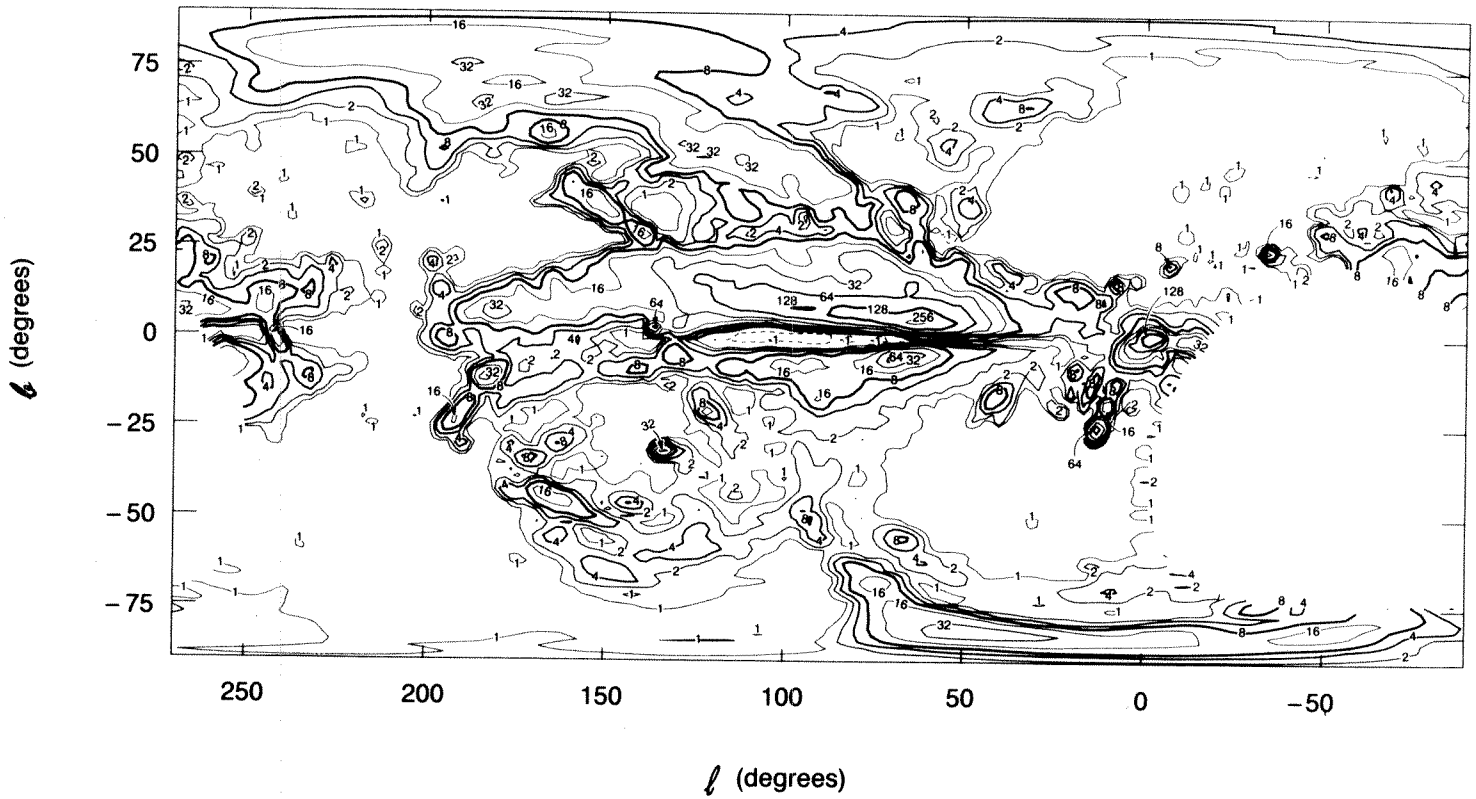

FIG. 9*b*

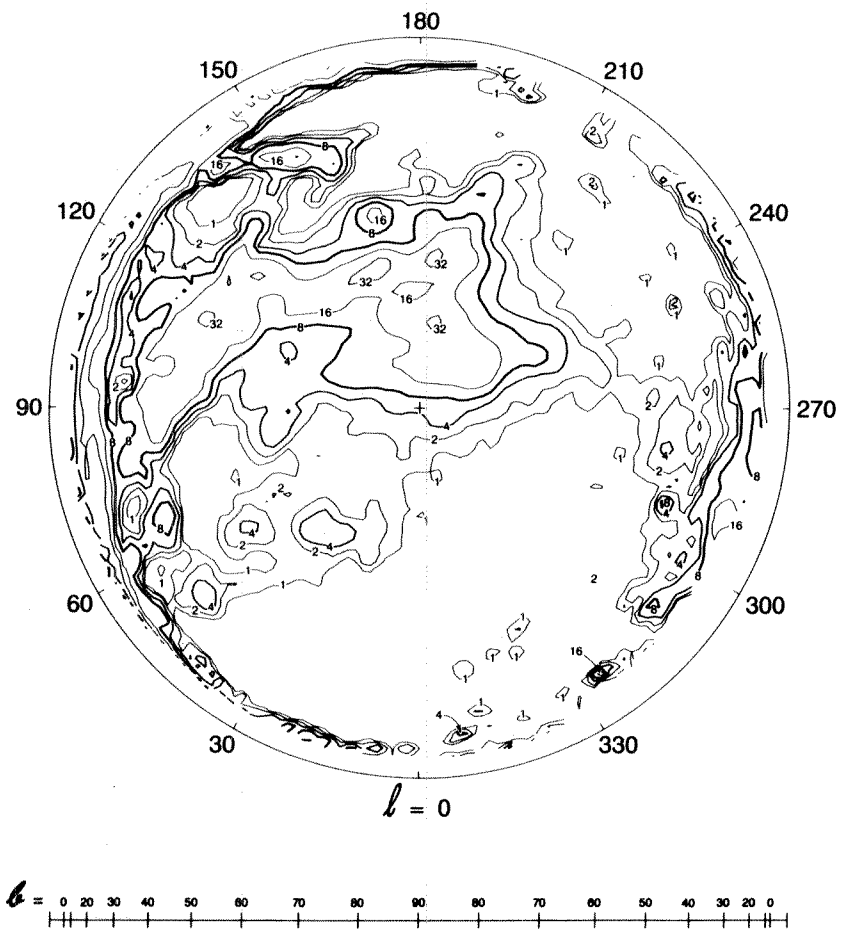

FIG. 9*a*

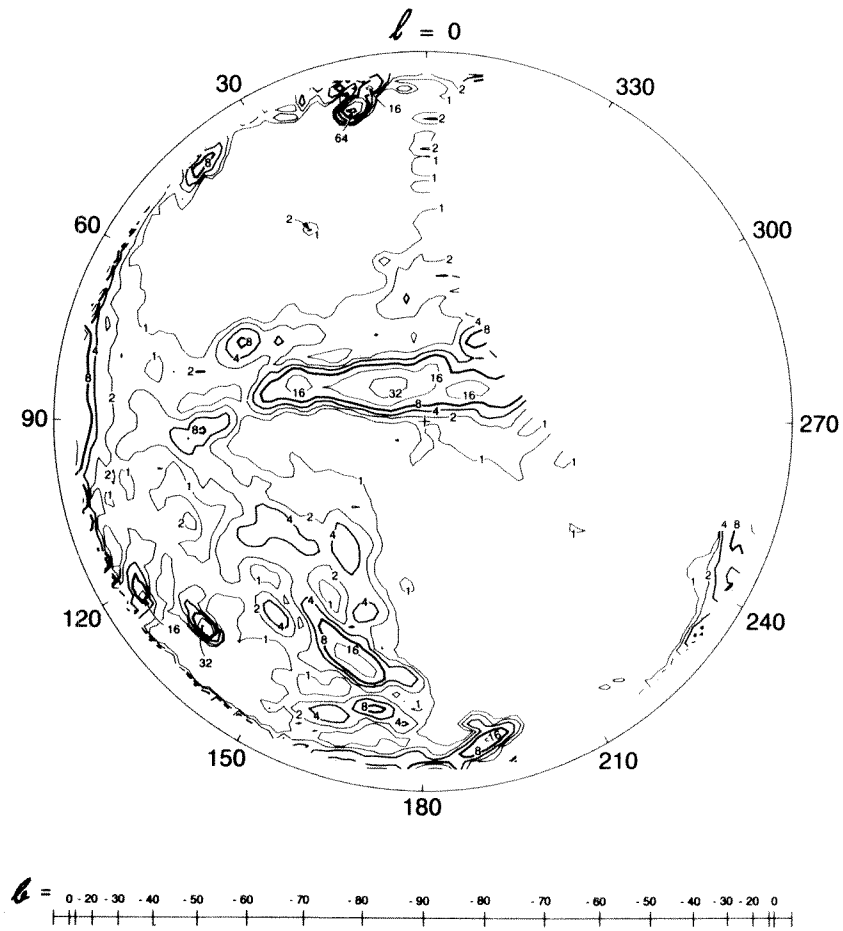

FIG. 9*c*

FIG. 9.—Maps of the column density of high-velocity H I in (*a*) the north, (*b*) the south, and the (*c*) full sky, respectively. Contours are labeled in units of K km s^{-1}

TABLE 2

HIGH-VELOCITY CLOUD CATALOG

No.	Peak α_{1950}	δ_{1950}	Peak l	b	l max	l min	b max	b min	v max	v min	F_{tot}	T_{peak}	# pts
1	0.031	−20.175	64.322	−77.032	74.48	59.69	−73.16	−79.28	−100.2	−211.0	165.21	0.49	11
2	0.052	49.824	115.461	−12.105	115.46	115.46	−12.10	−12.10	−174.1	−195.2	2.55	0.12	1
3	0.065	53.825	116.307	−8.190	116.31	116.31	−8.19	−8.19	−121.3	−168.8	14.85	0.51	1
4	0.072	−12.174	86.291	−71.521	86.29	86.29	−71.52	−71.52	−52.5	−63.1	1.10	0.08	1
5	0.080	−22.176	58.106	−78.698	77.11	44.90	−76.12	−82.66	−79.1	−179.4	173.23	0.60	10
6	0.161	−40.175	332.972	−74.858	332.97	330.40	−74.86	−75.30	73.9	47.5	5.51	0.15	2
7	0.161	−40.175	332.972	−74.858	332.97	332.97	−74.86	−74.86	142.5	126.6	2.08	0.12	1
8	0.161	−40.175	332.972	−74.858	332.97	332.97	−74.86	−74.86	−279.7	−290.2	1.94	0.17	1
9	0.231	−40.175	330.399	−75.303	332.97	330.40	−74.86	−75.30	126.6	95.0	7.10	0.17	2
10	0.231	−40.175	330.399	−75.303	332.97	330.40	−74.86	−75.30	179.4	137.2	7.33	0.14	2
11	0.245	75.829	120.849	13.372	120.85	120.85	13.37	13.37	121.4	116.1	1.22	0.17	1
12	0.270	−36.173	339.378	−78.804	339.38	339.38	−78.80	−78.80	−311.3	−321.9	1.24	0.09	1
13	0.270	−36.173	339.378	−78.804	354.23	331.49	−78.24	−80.63	−95.0	−163.6	34.24	0.22	8
14	0.271	53.825	118.130	−8.466	118.13	118.13	−8.47	−8.47	−163.5	−168.8	1.14	0.13	1
15	0.276	−24.172	55.058	−82.023	359.79	0.63	−79.26	−86.80	−42.2	−158.3	874.74	1.05	57
16	0.300	−40.174	327.668	−75.709	327.67	327.67	−75.71	−75.71	110.8	95.0	1.57	0.10	1
17	0.300	−40.174	327.668	−75.709	327.67	327.67	−75.71	−75.71	179.4	126.6	5.38	0.16	1
18	0.333	17.825	113.340	−44.231	114.91	113.34	−44.23	−44.39	−84.4	−110.8	4.97	0.17	2
19	0.335	41.828	117.256	−20.450	117.26	117.26	−20.45	−20.45	−94.9	−121.3	5.39	0.30	1
20	0.364	33.829	116.584	−28.433	116.58	116.58	−28.43	−28.43	−105.5	−110.8	1.06	0.11	1
21	0.370	−40.174	324.758	−76.075	324.76	324.76	−76.07	−76.07	−290.2	−295.5	1.64	0.21	1
22	0.440	55.830	119.813	−6.631	119.81	119.81	−6.63	−6.63	−153.0	−174.1	1.74	0.08	1
23	0.452	7.827	113.669	−54.377	113.67	113.67	−54.38	−54.38	−79.1	−89.7	1.22	0.08	1
24	0.466	39.828	118.623	−22.593	119.48	117.76	−22.52	−22.66	−84.4	−121.3	30.43	0.44	3
25	0.481	11.826	115.238	−50.470	116.10	115.24	−48.52	−50.47	−68.6	−73.8	1.83	0.10	2
26	0.482	17.826	116.291	−44.513	116.29	116.29	−44.51	−44.51	−89.7	−100.2	1.11	0.08	1
27	0.519	−40.173	318.005	−76.702	318.01	318.01	−76.70	−76.70	−290.2	−300.8	1.59	0.16	1
28	0.570	−30.174	351.546	−85.736	358.15	12.87	−85.74	−88.64	−52.8	−100.3	35.87	0.40	6
29	0.588	−40.173	314.636	−76.917	322.60	314.64	−76.92	−80.63	73.9	63.3	2.94	0.11	3
30	0.593	53.827	121.000	−8.721	121.00	121.00	−8.72	−8.72	−131.9	−147.7	1.87	0.13	1
31	0.604	39.829	120.344	−22.705	121.21	118.62	−22.59	−22.74	−485.4	−511.8	12.46	0.37	4
32	0.628	−36.171	317.634	−80.905	317.63	312.41	−80.90	−81.10	−279.7	−300.8	2.98	0.15	2
33	0.644	41.830	120.938	−20.729	120.94	120.94	−20.73	−20.73	−179.3	−247.9	14.24	0.23	1
34	0.644	41.830	120.938	−20.729	120.94	120.94	−20.73	−20.73	−258.5	−279.6	3.91	0.17	1
35	0.644	41.830	120.938	−20.729	120.94	120.94	−20.73	−20.73	−290.2	−300.7	1.53	0.12	1
36	0.657	3.826	118.400	−58.688	118.40	118.40	−58.69	−58.69	−364.0	−385.2	2.57	0.12	1
37	0.661	−34.175	318.888	−82.936	318.89	318.89	−82.94	−82.94	79.1	58.0	2.07	0.11	1
38	0.680	−32.170	322.989	−84.908	322.99	322.99	−84.91	−84.91	−47.5	−100.3	16.36	0.62	1
39	0.747	41.831	122.172	−20.763	122.17	122.17	−20.76	−20.76	−179.3	−290.2	22.55	0.30	1
40	0.781	59.828	122.734	−2.771	122.73	122.73	−2.77	−2.77	−179.3	−195.2	2.01	0.12	1
41	0.781	−38.169	305.240	−79.222	305.24	300.66	−79.22	−81.22	−279.7	−295.5	3.48	0.14	3
42	0.797	−40.171	304.026	−77.227	304.03	304.03	−77.23	−77.23	73.9	63.3	1.37	0.11	1
43	0.810	−34.173	303.660	−83.226	303.66	303.66	−83.23	−83.23	−89.7	−95.0	1.17	0.12	1
44	0.851	−38.168	300.849	−79.223	300.85	300.85	−79.22	−79.22	137.2	126.6	1.86	0.13	1
45	0.851	−38.168	300.849	−79.223	300.85	300.85	−79.22	−79.22	158.3	147.7	1.68	0.13	1
46	0.851	−38.168	300.849	−79.223	305.24	296.51	−79.15	−79.22	195.2	147.7	13.66	0.20	3
47	0.856	47.833	123.410	−14.765	123.41	122.20	−14.76	−16.77	−94.9	−142.4	26.54	0.41	3
48	0.902	53.830	123.767	−8.762	123.77	123.77	−8.76	−8.76	−142.4	−184.6	4.79	0.12	1
49	0.920	−38.167	296.505	−79.154	300.85	287.52	−77.00	−81.22	126.6	63.3	32.80	0.28	7
50	0.956	5.828	126.777	−56.711	126.78	126.78	−56.71	−56.71	−89.7	−105.5	1.61	0.09	1
51	0.957	−10.174	129.963	−72.660	129.96	129.96	−72.66	−72.66	−68.6	−89.7	1.66	0.07	1
52	0.990	−38.167	292.231	−79.016	292.23	287.52	−78.78	−79.02	126.6	105.5	4.69	0.13	2
53	1.015	−40.169	292.824	−76.995	296.32	292.82	−77.00	−77.13	163.6	126.6	4.59	0.18	2
54	1.015	−40.169	292.824	−76.995	300.42	292.82	−77.00	−77.21	116.1	95.0	4.13	0.20	3
55	1.025	5.829	128.657	−56.634	128.66	128.66	−56.63	−56.63	84.5	84.5	1.59	0.30	1
56	1.043	1.831	129.929	−60.587	132.03	127.81	−60.46	−60.68	−221.6	−248.0	10.83	0.24	3
57	1.069	−38.166	287.515	−78.776	287.52	287.52	−78.78	−78.78	58.0	52.8	1.78	0.17	1
58	1.085	−40.168	289.404	−76.805	289.40	286.10	−76.56	−76.81	−263.8	−269.1	2.28	0.15	2
59	1.089	25.831	127.581	−36.624	128.74	126.25	−36.54	−36.70	−411.5	−437.9	14.00	0.19	5
60	1.124	−36.166	280.083	−80.400	280.08	271.26	−80.01	−81.93	−147.7	−168.9	5.63	0.14	3
61	1.124	−36.166	280.083	−80.400	280.08	275.72	−80.01	−80.40	−95.0	−126.6	5.08	0.14	2
62	1.155	−40.167	286.104	−76.562	286.10	282.96	−76.27	−76.56	121.3	89.7	5.04	0.16	2
63	1.224	−40.166	282.955	−76.270	282.96	276.43	−76.27	−78.16	89.7	52.8	15.23	0.37	4
64	1.224	−40.166	282.955	−76.270	282.96	282.96	−76.27	−76.27	364.1	358.8	1.08	0.11	1
65	1.227	−34.168	266.514	−81.413	266.51	266.51	−81.41	−81.41	−279.7	−290.2	1.06	0.07	1
66	1.278	55.838	126.904	−6.552	128.74	125.16	−6.30	−8.37	−147.7	−184.6	32.88	0.26	6
67	1.278	−38.163	276.431	−77.776	276.43	276.43	−77.78	−77.78	−58.1	−68.6	1.29	0.09	1
68	1.289	29.839	130.284	−32.361	132.39	125.96	−32.09	−34.70	−358.8	−406.2	29.40	0.29	8
69	1.382	5.834	138.111	−55.771	138.11	138.11	−55.77	−55.77	−63.3	−89.7	2.80	0.11	1
70	1.390	69.840	125.981	7.439	130.29	123.86	8.47	7.25	−158.2	−211.0	122.32	0.53	10
71	1.415	−0.165	142.033	−61.435	142.03	142.03	−61.44	−61.44	−79.1	−84.4	1.28	0.14	1
72	1.443	−40.162	274.074	−75.062	277.11	274.07	−75.06	−75.55	68.6	58.0	1.84	0.10	2
73	1.462	31.837	132.498	−30.049	132.50	132.50	−30.05	−30.05	−221.6	−232.1	1.13	0.08	1
74	1.486	−38.159	267.492	−76.341	267.49	267.49	−76.34	−76.34	68.6	52.8	3.04	0.16	1
75	1.494	13.837	137.718	−47.600	137.72	137.52	−45.58	−47.60	−84.4	−100.2	2.90	0.15	2
76	1.497	29.842	133.435	−31.931	133.44	133.44	−31.93	−31.93	−179.4	−221.6	14.83	0.38	1
77	1.497	29.842	133.435	−31.931	133.44	133.44	−31.93	−31.93	−232.1	−232.1	1.51	0.29	1
78	1.497	29.842	133.435	−31.931	135.51	131.34	−31.56	−32.23	−79.1	−221.6	126.71	0.61	5
79	1.497	29.842	133.435	−31.931	135.51	132.39	−29.71	−32.09	−205.7	−284.9	54.51	0.34	7
80	1.509	3.837	142.399	−57.193	142.40	142.40	−57.19	−57.19	−68.6	−84.4	2.20	0.14	1
81	1.512	−40.161	271.596	−74.597	271.60	271.60	−74.60	−74.60	−110.8	−116.1	1.07	0.13	1
82	1.584	25.839	135.759	−35.621	135.76	135.76	−35.62	−35.62	−84.4	−94.9	1.17	0.09	1
83	1.619	−16.163	170.261	−74.169	170.26	170.26	−74.17	−74.17	−95.0	−105.5	1.16	0.09	1
84	1.636	29.845	135.512	−31.561	135.51	135.51	−31.56	−31.56	−179.4	−189.9	1.73	0.13	1
85	1.636	29.845	135.512	−31.561	135.51	135.51	−31.56	−31.56	−211.0	−221.6	1.38	0.10	1
86	1.651	7.842	143.769	−52.732	143.77	143.77	−52.73	−52.73	−100.2	−105.5	1.08	0.11	1
87	1.673	−32.156	239.218	−77.894	239.22	239.22	−77.89	−77.89	58.0	36.9	2.10	0.11	1
88	1.691	9.843	143.646	−50.647	143.65	143.65	−50.65	−50.65	−89.7	−100.2	1.26	0.08	1
89	1.694	47.846	132.055	−13.828	134.89	132.05	−13.31	−15.49	−168.8	−200.5	13.17	0.16	5
90	1.699	−12.156	164.736	−70.347	164.74	164.74	−70.35	−70.35	−52.5	−63.1	1.08	0.08	1
91	1.724	−34.159	246.397	−76.511	254.50	246.40	−75.15	−76.51	−84.4	−105.5	4.17	0.11	3
92	1.771	13.843	143.413	−46.480	147.68	140.60	−44.78	−48.08	−79.1	−126.6	46.51	0.34	8
93	1.790	−40.156	263.301	−72.438	263.30	263.30	−72.44	−72.44	−63.3	−68.6	1.11	0.11	1
94	1.812	−32.153	236.764	−76.218	236.76	236.76	−76.22	−76.22	−100.3	−110.8	1.14	0.09	1

TABLE 2—*Continued*

No.	Peak α_{1950}	δ_{1950}	Peak l	b	l max	l min	b max	b min	v max	v min	F_{tot}	T_{peak}	# pts
95	1.847	37.849	136.225	−23.163	136.23	136.23	−23.16	−23.16	−147.7	−163.5	1.53	0.09	1
96	1.877	57.850	131.405	−3.710	133.78	131.40	−3.02	−3.71	−168.8	−205.7	18.85	0.34	5
97	1.885	51.846	132.956	−9.514	132.96	132.96	−9.51	−9.51	−142.4	−153.0	1.10	0.08	1
98	1.887	31.846	138.557	−28.811	138.56	138.33	−26.78	−28.81	−89.7	−110.8	2.28	0.08	2
99	1.922	55.851	132.258	−5.556	133.10	129.70	−3.71	−7.85	−126.6	−200.5	135.39	0.54	9
100	1.939	−40.153	259.803	−71.126	259.80	259.80	−71.13	−71.13	−58.1	−63.3	1.07	0.11	1
101	1.955	63.852	130.439	2.240	135.61	120.43	6.23	1.32	−163.5	−242.7	767.51	1.60	38
102	1.980	−0.153	157.480	−58.015	157.48	155.76	−58.01	−58.53	−52.7	−84.4	6.94	0.17	2
103	2.048	9.851	151.204	−48.673	151.20	151.20	−48.67	−48.67	−73.8	−89.7	1.62	0.09	1
104	2.082	−34.151	240.193	−72.390	240.19	240.19	−72.39	−72.39	−68.6	−79.2	1.24	0.09	1
105	2.082	−34.151	240.193	−72.390	242.14	240.19	−72.39	−74.02	68.6	58.0	2.75	0.16	3
106	2.091	51.851	134.818	−8.991	134.82	134.82	−8.99	−8.99	−131.9	−147.7	2.12	0.11	1
107	2.099	−2.148	162.400	−58.747	162.40	162.40	−58.75	−58.75	−52.7	−73.9	5.89	0.26	1
108	2.147	7.853	154.579	−49.804	157.90	154.58	−49.80	−51.43	−68.6	−84.4	4.50	0.14	3
109	2.151	15.851	149.571	−42.591	149.57	149.57	−42.59	−42.59	−110.8	−121.3	1.09	0.07	1
110	2.164	31.853	142.359	−27.698	142.36	142.36	−27.70	−27.70	−89.7	−100.2	1.40	0.09	1
111	2.223	47.858	137.316	−12.388	137.32	136.31	−12.39	−14.55	−158.2	−184.6	5.76	0.13	3
112	2.243	1.854	161.581	−54.226	165.57	160.08	−52.94	−56.26	−47.5	−100.2	38.32	0.29	7
113	2.274	23.855	147.433	−34.572	147.43	147.43	−34.57	−34.57	−116.1	−131.9	1.77	0.10	1
114	2.285	7.857	157.333	−48.797	177.60	145.31	−42.54	−54.53	−63.3	−147.7	285.68	0.43	50
115	2.287	−40.144	253.631	−67.771	253.63	253.63	−67.77	−67.77	137.2	126.6	1.10	0.08	1
116	2.372	49.858	138.030	−10.005	138.03	136.92	−10.01	−10.41	−126.6	−163.5	14.67	0.23	4
117	2.375	43.862	140.280	−15.586	140.28	140.28	−15.59	−15.59	−100.2	−110.8	1.15	0.08	1
118	2.406	57.864	135.424	−2.424	135.42	135.42	−2.42	−2.42	−174.1	−179.4	1.34	0.15	1
119	2.425	25.859	148.675	−31.898	148.67	148.67	−31.90	−31.90	−110.8	−121.3	1.06	0.07	1
120	2.442	5.858	161.978	−49.238	161.98	160.65	−49.24	−49.81	−63.3	−89.7	5.21	0.14	2
121	2.457	−2.139	170.220	−55.469	170.22	170.22	−55.47	−55.47	−47.5	−79.1	4.23	0.14	1
122	2.468	59.860	135.145	−0.389	135.95	135.14	−0.05	−0.39	−353.5	−358.8	1.76	0.09	2
123	2.482	23.861	150.541	−33.354	150.54	149.66	−31.49	−33.35	−110.8	−131.9	2.63	0.13	2
124	2.500	21.862	151.911	−35.020	151.91	151.91	−35.02	−35.02	−89.7	−100.2	1.35	0.12	1
125	2.501	3.861	164.868	−50.365	164.87	164.87	−50.36	−50.36	−68.6	−84.4	1.62	0.09	1
126	2.501	3.861	164.868	−50.365	164.87	164.87	−50.36	−50.36	131.9	105.5	11.42	0.88	1
127	2.503	7.863	161.429	−47.067	161.43	161.43	−47.07	−47.07	−68.6	−84.4	5.15	0.28	1
128	2.543	9.864	160.541	−45.074	164.06	158.07	−43.31	−47.07	−300.7	−358.8	72.57	0.49	9
129	2.548	61.865	134.922	1.687	134.92	134.92	1.69	1.69	−232.1	−284.9	5.97	0.13	1
130	2.548	61.865	134.922	1.687	134.92	134.92	1.69	1.69	−469.6	−485.4	1.98	0.11	1
131	2.613	9.866	161.740	−44.501	161.74	161.74	−44.50	−44.50	−79.1	−95.0	2.44	0.16	1
132	2.649	65.867	133.929	5.621	133.93	133.93	5.62	5.62	−179.4	−216.3	4.62	0.15	1
133	2.681	11.867	161.328	−42.283	161.33	161.33	−42.28	−42.28	−348.2	−353.5	1.13	0.11	1
134	2.685	61.869	135.808	2.082	135.81	135.81	2.08	2.08	−327.1	−437.9	17.75	0.23	1
135	2.717	−34.134	235.477	−64.692	235.48	235.48	−64.69	−64.69	73.9	63.3	1.45	0.10	1
136	2.781	49.870	141.692	−8.415	143.26	139.86	−8.34	−10.78	−121.3	−163.5	62.24	0.33	9
137	2.790	59.870	137.357	0.603	137.36	137.36	0.60	0.60	−348.2	−358.8	1.06	0.07	1
138	2.822	61.873	136.681	2.504	136.68	136.68	2.50	2.50	126.7	95.0	9.08	0.33	1
139	2.822	61.873	136.681	2.504	136.68	136.68	2.50	2.50	142.5	137.2	1.61	0.17	1
140	2.822	61.873	136.681	2.504	136.68	136.68	2.50	2.50	−195.2	−221.6	56.83	1.88	1
141	2.822	61.873	136.681	2.504	136.68	136.68	2.50	2.50	−232.1	−321.8	87.71	1.73	1
142	2.822	61.873	136.681	2.504	136.68	136.68	2.50	2.50	−401.0	−411.5	1.66	0.13	1
143	2.822	61.873	136.681	2.504	136.68	136.68	2.50	2.50	−422.1	−474.8	14.81	0.43	1
144	2.854	−40.128	247.702	−61.782	247.70	247.70	−61.78	−61.78	−89.7	−100.3	1.12	0.07	1
145	2.929	7.876	168.603	−43.256	170.72	162.67	−40.68	−47.67	−221.6	−316.6	178.25	0.63	17
146	2.946	31.875	152.309	−23.373	152.31	151.48	−23.37	−23.82	−116.1	−147.7	5.35	0.13	2
147	3.003	−40.123	246.709	−60.137	246.71	246.71	−60.14	−60.14	416.8	411.5	1.51	0.16	1
148	3.069	25.879	157.364	−27.584	157.36	157.36	−27.58	−27.58	−84.4	−105.5	3.77	0.16	1
149	3.111	−36.118	238.385	−59.645	238.38	238.38	−59.64	−59.64	84.4	73.8	1.35	0.11	1
150	3.119	13.880	166.447	−36.842	166.45	166.45	−36.84	−36.84	−343.0	−353.5	1.13	0.08	1
151	3.156	5.880	173.856	−42.489	173.86	173.86	−42.49	−42.49	−73.9	−105.5	4.16	0.14	1
152	3.177	9.884	170.563	−39.335	170.56	169.56	−39.34	−40.01	−269.1	−284.9	3.25	0.09	2
153	3.203	21.885	161.711	−29.778	166.92	160.12	−26.66	−31.31	−68.6	−121.3	55.59	0.41	10
154	3.208	25.883	159.090	−26.514	159.09	159.09	−26.51	−26.51	−84.4	−105.5	3.16	0.18	1
155	3.227	43.889	148.708	−11.394	148.71	148.71	−11.39	−11.39	−116.1	−121.3	1.28	0.15	1
156	3.235	17.885	164.988	−32.668	164.99	164.99	−32.67	−32.67	−84.4	−89.7	1.21	0.15	1
157	3.249	61.888	139.311	3.988	139.31	139.31	3.99	3.99	−342.9	−353.5	1.22	0.08	1
158	3.351	−40.111	245.034	−56.250	245.03	245.03	−56.25	−56.25	416.8	411.5	1.10	0.15	1
159	3.353	3.888	178.554	−41.784	179.49	178.55	−41.02	−41.78	−73.9	−105.5	7.12	0.21	2
160	3.384	11.891	171.700	−35.800	171.70	170.77	−35.80	−36.49	−269.1	−295.5	3.07	0.10	2
161	3.392	55.894	143.489	−0.451	150.01	139.25	2.22	−3.37	−300.7	−321.8	22.87	0.12	18
162	3.407	13.890	170.343	−34.107	172.96	164.26	−32.02	−35.80	−95.0	−158.3	72.16	0.36	14
163	3.454	11.893	172.608	−35.099	173.62	171.23	−33.42	−35.10	−248.0	−311.3	16.80	0.18	3
164	3.454	17.893	167.792	−30.665	167.79	167.79	−30.67	−30.67	89.7	84.4	1.06	0.11	1
165	3.545	53.897	145.713	−1.343	145.71	145.71	−1.34	−1.34	95.0	84.5	1.43	0.13	1
166	3.569	−40.103	244.344	−53.772	244.34	244.34	−53.77	−53.77	−95.0	−100.3	1.08	0.11	1
167	3.569	−40.103	244.344	−53.772	244.34	244.34	−53.77	−53.77	−211.1	−216.4	1.17	0.16	1
168	3.593	67.903	137.711	10.183	137.71	137.71	10.18	10.18	121.4	95.0	6.51	0.28	1
169	3.638	15.899	171.614	−30.354	172.44	171.61	−29.66	−30.35	−100.2	−121.4	2.52	0.10	2
170	3.672	11.901	175.341	−32.835	176.24	174.49	−32.84	−34.95	−242.7	−274.4	5.07	0.09	3
171	3.700	3.901	182.993	−37.867	182.99	181.33	−36.34	−37.87	−253.3	−258.5	1.80	0.11	2
172	3.736	49.903	149.519	−3.486	149.52	149.52	−3.49	−3.49	−147.7	−158.3	1.23	0.09	1
173	3.736	49.903	149.519	−3.486	149.52	149.52	−3.49	−3.49	−274.3	−284.9	1.09	0.08	1
174	3.741	11.904	176.174	−32.098	177.93	175.34	−30.60	−33.45	−79.1	−121.4	13.82	0.17	5
175	3.757	37.908	157.258	−12.725	157.26	156.61	−12.72	−13.24	−110.8	−131.9	3.92	0.09	2
176	3.832	13.907	175.548	−29.752	175.55	175.55	−29.75	−29.75	−306.0	−311.3	1.15	0.14	1
177	3.856	49.908	150.429	−2.752	150.43	150.30	−2.75	−2.86	−274.3	−284.9	1.96	0.09	2
178	3.891	9.910	179.664	−31.804	181.80	179.66	−31.80	−32.77	−253.3	−258.5	1.69	0.09	2
179	3.897	33.914	161.261	−14.660	163.03	161.26	−14.66	−15.82	−95.0	−110.8	2.43	0.10	2
180	3.897	51.910	149.447	−0.965	149.45	147.96	0.40	−0.96	100.3	84.5	2.00	0.09	2
181	3.897	51.910	149.447	−0.965	151.81	149.45	−0.34	−2.22	−422.1	−432.6	3.74	0.11	4
182	3.902	13.909	176.339	−29.012	176.34	174.94	−27.40	−29.75	−89.7	−131.9	9.43	0.13	3
183	3.977	33.917	162.021	−13.995	162.02	162.02	−14.00	−14.00	−110.8	−116.1	1.12	0.13	1
184	3.986	21.914	170.847	−22.601	170.85	169.24	−22.60	−24.06	−126.6	−153.0	3.78	0.10	3
185	4.046	49.916	151.813	−1.559	151.81	151.81	−1.56	−1.56	−274.3	−284.9	1.16	0.08	1
186	4.075	31.917	164.363	−14.612	164.36	164.36	−14.61	−14.61	−116.1	−126.6	1.86	0.17	1
187	4.177	19.922	174.400	−22.039	174.40	174.40	−22.04	−22.04	−300.8	−311.3	1.35	0.09	1
188	4.180	13.921	179.355	−25.981	179.36	179.36	−25.98	−25.98	100.3	100.3	1.08	0.20	1

TABLE 2—*Continued*

No.	Peak α_{1950}	δ_{1950}	Peak l	b	l max	l min	b max	b min	v max	v min	F_{tot}	T_{peak}	# pts
189	4.191	29.925	166.901	−14.993	167.59	165.47	−14.99	−17.81	−84.4	−126.6	15.28	0.25	5
190	4.205	39.925	159.868	−7.744	160.52	159.87	−7.10	−7.74	110.8	84.4	1.92	0.08	2
191	4.249	13.923	180.072	−25.209	180.07	180.07	−25.21	−25.21	−300.8	−311.3	1.17	0.08	1
192	4.265	49.925	153.360	−0.108	153.36	153.36	−0.11	−0.11	−422.1	−432.6	1.33	0.11	1
193	4.321	37.931	162.260	−8.205	162.26	162.26	−8.20	−8.20	105.6	84.4	2.22	0.11	1
194	4.345	3.927	190.012	−30.168	190.69	187.55	−28.88	−31.02	−168.9	−226.9	31.23	0.32	5
195	4.374	1.929	192.220	−30.930	192.22	192.22	−30.93	−30.93	100.2	89.7	1.81	0.18	1
196	4.420	15.930	180.108	−22.015	180.11	180.11	−22.02	−22.02	−95.0	−121.4	2.76	0.12	1
197	4.467	45.936	157.621	−1.469	157.62	157.62	−1.47	−1.47	131.9	121.4	1.80	0.18	1
198	4.472	33.937	166.468	−9.629	166.47	166.47	−9.63	−9.63	89.7	79.2	1.24	0.09	1
199	4.475	25.933	172.585	−14.957	181.44	170.63	−14.54	−21.23	−84.4	−131.9	78.28	0.33	22
200	4.516	25.936	172.959	−14.537	172.96	172.96	−14.54	−14.54	−116.1	−126.6	2.04	0.19	1
201	4.531	51.936	153.671	3.091	153.67	153.67	3.09	3.09	84.5	73.9	1.26	0.09	1
202	4.532	23.936	174.675	−15.677	174.68	174.68	−15.68	−15.68	95.0	84.4	1.08	0.07	1
203	4.532	23.936	174.675	−15.677	175.93	174.68	−14.21	−15.68	−306.0	−311.3	2.87	0.13	3
204	4.533	19.937	177.897	−18.226	179.35	177.24	−18.23	−19.71	−253.3	−258.5	2.90	0.12	3
205	4.542	33.940	167.054	−8.988	168.81	167.05	−8.99	−10.05	−353.5	−364.1	1.89	0.11	2
206	4.593	49.939	155.549	2.183	155.55	153.02	3.09	0.60	−416.8	−432.6	7.54	0.12	7
207	4.606	13.939	183.580	−21.130	183.58	183.58	−21.13	−21.13	−84.4	−95.0	1.11	0.07	1
208	4.640	31.941	169.399	−9.384	169.40	169.40	−9.38	−9.38	89.7	79.2	1.33	0.10	1
209	4.699	59.943	148.574	9.449	149.07	146.16	10.57	9.45	−100.2	−147.7	140.44	1.49	4
210	4.700	39.946	163.786	−3.591	163.79	163.79	−3.59	−3.59	100.3	89.7	1.21	0.10	1
211	4.700	39.946	163.786	−3.591	163.79	163.79	−3.59	−3.59	−121.3	−142.4	1.89	0.08	1
212	4.721	1.944	195.432	−26.561	197.59	195.43	−25.68	−27.25	−63.3	−137.2	22.86	0.31	3
213	4.722	17.945	181.281	−17.370	181.28	179.18	−16.70	−18.16	−253.3	−258.5	2.54	0.10	3
214	4.759	21.947	178.322	−14.507	178.32	178.32	−14.51	−14.51	−95.0	−105.5	1.54	0.16	1
215	4.819	33.952	169.310	−6.360	169.31	165.66	−3.84	−6.36	110.8	84.4	3.44	0.11	4
216	4.849	39.953	164.883	−2.281	164.88	164.88	−2.28	−2.28	−126.6	−142.5	1.78	0.11	1
217	4.872	75.956	136.029	19.965	136.03	136.03	19.96	19.96	126.7	121.4	1.16	0.14	1
218	4.882	9.952	189.567	−20.160	196.73	185.28	−13.86	−26.73	−73.9	−163.6	308.59	0.52	32
219	4.901	25.952	176.314	−10.505	176.31	176.31	−10.51	−10.51	−300.8	−311.3	1.13	0.07	1
220	4.940	11.955	188.325	−18.327	188.33	187.72	−18.33	−19.16	−147.7	−184.7	4.95	0.12	2
221	4.981	7.957	192.201	−20.044	192.20	192.20	−20.04	−20.04	100.2	95.0	2.01	0.22	1
222	4.988	39.959	165.875	−1.031	165.88	165.88	−1.03	−1.03	−142.5	−163.6	2.25	0.11	1
223	5.019	11.958	189.011	−17.361	189.01	189.01	−17.36	−17.36	−84.4	−89.7	1.23	0.12	1
224	5.033	29.962	174.157	−6.690	174.16	174.16	−6.69	−6.69	110.8	95.0	1.51	0.08	1
225	5.033	29.962	174.157	−6.690	174.70	174.16	−5.96	−6.69	−290.2	−306.0	2.00	0.09	2
226	5.038	83.964	128.930	24.565	128.93	128.93	24.57	24.57	−110.8	−131.9	2.01	0.08	1
227	5.051	57.964	151.859	10.373	151.86	150.03	11.29	10.37	−89.7	−142.4	72.91	1.43	2
228	5.057	39.962	166.359	−0.400	166.36	166.36	−0.40	−0.40	−332.4	−348.2	1.58	0.08	1
229	5.057	39.962	166.359	−0.400	168.28	166.36	0.24	−1.82	110.8	84.4	6.33	0.14	4
230	5.104	37.965	168.283	−1.165	172.07	165.73	4.28	−1.33	−321.9	−353.5	24.56	0.12	16
231	5.116	21.963	181.351	−10.519	186.72	176.89	−6.61	−15.67	−105.5	−226.9	626.88	1.00	38
232	5.126	43.966	163.626	2.629	163.63	163.63	2.63	2.63	95.0	84.4	1.40	0.11	1
233	5.148	17.964	184.963	−12.436	185.53	184.96	−11.62	−12.44	−110.8	−147.7	14.66	0.32	2
234	5.158	11.964	190.182	−15.660	190.18	190.18	−15.66	−15.66	−84.4	−95.0	2.09	0.17	1
235	5.275	39.972	167.835	1.628	167.83	167.83	1.63	1.63	137.2	126.7	1.16	0.08	1
236	5.275	39.972	167.835	1.628	169.25	167.83	1.63	0.16	116.1	89.7	3.70	0.14	2
237	5.282	85.973	127.115	25.765	127.12	127.12	25.76	25.76	−116.0	−126.6	1.13	0.08	1
238	5.318	27.973	177.981	−4.813	177.98	177.98	−4.81	−4.81	−321.9	−327.1	1.06	0.12	1
239	5.320	45.974	163.184	5.467	163.18	163.18	5.47	5.47	105.5	84.4	1.93	0.08	1
240	5.344	39.975	168.289	2.284	168.29	167.83	2.28	1.63	131.9	110.8	2.80	0.15	2
241	5.384	33.978	173.501	−0.721	173.50	173.50	−0.72	−0.72	100.3	84.4	1.45	0.07	1
242	5.384	33.978	173.501	−0.721	178.33	170.46	5.13	−4.91	−279.6	−306.0	65.76	0.16	31
243	5.389	29.978	176.850	−2.913	176.85	176.85	−2.91	−2.91	95.0	84.4	1.10	0.07	1
244	5.391	37.978	170.245	1.605	170.24	170.24	1.60	1.60	−279.6	−290.2	1.46	0.10	1
245	5.457	27.980	179.009	−3.285	179.01	179.01	−3.29	−3.29	89.7	79.1	1.19	0.09	1
246	5.466	25.977	180.750	−4.287	180.75	180.75	−4.29	−4.29	−89.7	−100.3	1.55	0.12	1
247	5.466	25.977	180.750	−4.287	180.75	180.75	−4.29	−4.29	−253.3	−258.5	1.13	0.15	1
248	5.507	25.980	181.051	−3.825	182.85	181.05	−3.39	−5.53	−316.6	−327.1	5.98	0.18	4
249	5.542	21.982	184.682	−5.591	184.68	184.68	−5.59	−5.59	−253.3	−258.5	1.18	0.12	1
250	5.561	31.982	176.399	0.039	176.40	176.40	0.04	0.04	95.0	84.4	1.53	0.12	1
251	5.613	3.984	200.866	−14.031	202.89	200.87	−14.03	−14.62	105.5	105.5	1.91	0.21	2
252	5.615	25.984	181.835	−2.597	181.84	181.84	−2.60	−2.60	121.4	110.8	1.25	0.09	1
253	5.677	29.991	178.877	0.228	182.82	177.86	2.40	−2.60	−311.3	−327.1	16.45	0.22	10
254	5.691	39.991	170.449	5.634	170.45	170.45	5.63	5.63	−348.2	−358.8	1.32	0.10	1
255	5.700	31.989	177.337	1.536	177.34	177.34	1.54	1.54	−290.2	−306.0	1.61	0.09	1
256	5.733	−36.009	241.276	−28.143	241.28	241.28	−28.14	−28.14	105.5	100.2	1.17	0.15	1
257	5.746	29.995	179.346	0.995	179.35	179.35	0.99	0.99	95.0	84.4	1.21	0.08	1
258	5.782	17.993	189.877	−4.803	189.88	189.88	−4.80	−4.80	−290.2	−300.8	1.20	0.10	1
259	5.807	37.997	172.866	5.769	174.17	172.45	6.58	4.04	116.1	84.4	6.04	0.14	4
260	5.815	29.998	179.810	1.768	179.81	179.81	1.77	1.77	−95.0	−105.5	1.31	0.09	1
261	5.819	21.995	186.702	−2.304	186.70	186.70	−2.30	−2.30	−95.0	−105.5	1.61	0.12	1
262	5.823	25.994	183.297	−0.203	183.30	183.30	−0.20	−0.20	−316.6	−327.1	1.99	0.15	1
263	5.883	27.999	181.983	1.511	181.98	181.98	1.51	1.51	131.9	121.4	1.08	0.07	1
264	5.883	27.999	181.983	1.511	186.70	181.52	2.31	−3.95	−253.3	−258.5	23.89	0.20	19
265	5.916	−34.004	239.810	−25.429	239.81	239.54	−25.43	−26.26	105.5	94.9	2.30	0.21	2
266	5.918	31.999	178.757	3.924	179.81	178.31	3.92	1.77	116.1	89.7	3.66	0.12	3
267	5.933	26.000	184.048	1.080	184.05	184.05	1.08	1.08	116.1	95.0	2.60	0.16	1
268	5.951	20.001	189.356	−1.726	189.36	187.74	−0.51	−1.73	−279.7	−295.5	1.65	0.08	2
269	5.953	28.002	182.444	2.307	183.79	177.26	7.94	0.60	−316.6	−327.1	19.30	0.17	15
270	5.958	50.000	163.028	13.024	165.20	162.55	13.02	11.87	−95.0	−137.2	86.90	0.94	5
271	5.983	44.006	168.567	10.455	168.57	168.57	10.46	10.46	84.4	73.9	1.21	0.08	1
272	6.001	18.003	191.442	−2.109	191.44	191.44	−2.11	−2.11	−95.0	−121.4	4.87	0.23	1
273	6.019	24.004	186.357	1.088	186.36	186.36	1.09	1.09	−279.7	−290.2	1.10	0.08	1
274	6.041	26.004	184.770	2.346	184.77	184.77	2.35	2.35	110.8	95.0	1.55	0.09	1
275	6.060	32.006	179.641	5.492	181.60	179.64	5.49	4.90	110.8	100.3	2.20	0.12	2
276	6.072	26.006	184.972	2.709	184.97	184.97	2.71	2.71	−316.6	−327.1	1.32	0.12	1
277	6.139	18.009	192.408	−0.383	192.88	190.32	0.49	−1.25	−284.9	−300.8	4.78	0.14	4
278	6.139	80.012	133.877	25.216	136.22	130.00	27.42	21.27	−126.6	−221.6	281.70	0.60	37
279	6.157	24.010	187.281	2.748	187.28	187.28	2.75	2.75	−274.4	−284.9	1.14	0.08	1
280	6.159	20.011	190.792	0.831	190.79	190.79	0.83	0.83	126.6	121.4	1.11	0.12	1
281	6.161	28.012	183.787	4.714	184.97	183.34	4.71	2.71	−253.3	−258.5	3.63	0.14	3
282	6.166	36.013	176.723	8.562	176.72	176.13	8.56	7.45	−279.6	−290.2	1.65	0.08	2

TABLE 2—*Continued*

No.	Peak α_{1950}	δ_{1950}	Peak *l*	*b*	*l* max	*l* min	*b* max	*b* min	*v* max	*v* min	F_{tot}	T_{peak}	# pts
283	6.176	22.012	189.158	2.010	189.16	189.16	2.01	2.01	−284.9	−290.2	1.07	0.11	1
284	6.177	66.012	148.449	21.116	150.82	146.33	23.85	20.33	−79.1	−137.2	177.97	0.96	9
285	6.231	14.013	196.549	−1.151	196.55	196.55	−1.15	−1.15	174.1	158.3	1.63	0.09	1
286	6.237	24.014	187.802	3.708	187.80	187.80	3.71	3.71	−68.6	−100.3	15.07	0.68	1
287	6.278	32.016	180.954	7.944	185.93	155.02	15.79	1.60	−63.3	−153.0	2775.24	1.80	129
288	6.315	22.018	190.072	3.708	190.07	190.07	3.71	3.71	−290.2	−300.8	1.36	0.09	1
289	6.344	−25.981	233.744	−17.462	233.74	233.74	−17.46	−17.46	110.8	100.2	1.17	0.08	1
290	6.352	−17.980	226.174	−14.149	226.17	226.17	−14.15	−14.15	116.0	105.5	1.15	0.08	1
291	6.379	−13.978	222.623	−12.096	222.62	222.62	−12.10	−12.10	126.6	116.0	1.39	0.10	1
292	6.409	−39.979	247.967	−21.604	247.97	245.27	−21.26	−22.82	316.5	300.7	4.86	0.13	4
293	6.409	−39.979	247.967	−21.604	247.97	246.92	−21.60	−24.77	306.0	269.0	11.65	0.18	5
294	6.436	−23.976	232.329	−15.529	232.33	228.80	−13.37	−18.16	147.7	121.3	10.83	0.18	6
295	6.438	10.024	201.502	−0.362	201.50	201.50	−0.36	−0.36	−89.7	−105.6	3.06	0.23	1
296	6.470	−27.977	236.350	−16.671	236.35	236.35	−16.67	−16.67	121.3	110.8	1.46	0.13	1
297	6.478	−39.976	248.236	−20.846	248.24	248.24	−20.85	−20.85	131.9	94.9	6.05	0.23	1
298	6.548	−39.972	248.514	−20.088	248.51	248.51	−20.09	−20.09	121.3	116.0	2.02	0.20	1
299	6.556	−13.971	223.755	−9.780	223.75	223.75	−9.78	−9.78	131.9	116.0	3.50	0.21	1
300	6.571	76.034	138.496	25.647	138.50	136.30	25.98	25.65	126.7	126.7	2.46	0.26	2
301	6.584	−23.969	233.175	−13.664	233.17	233.17	−13.66	−13.66	158.2	131.9	3.85	0.18	1
302	6.584	−23.969	233.175	−13.664	233.17	233.17	−13.66	−13.66	174.1	168.8	1.13	0.11	1
303	6.654	−23.966	233.575	−12.796	233.58	233.58	−12.80	−12.80	163.5	116.0	7.09	0.19	1
304	6.686	−39.966	249.085	−18.590	249.08	249.08	−18.59	−18.59	147.7	100.2	9.31	0.26	1
305	6.720	−29.965	239.584	−14.433	239.58	237.53	−14.01	−15.27	147.7	110.8	12.21	0.23	4
306	6.756	−39.963	249.381	−17.843	250.04	242.91	−15.82	−17.84	153.0	116.0	22.63	0.28	8
307	6.790	−29.962	239.955	−13.610	243.99	239.96	−11.96	−14.65	174.1	110.8	21.57	0.20	8
308	6.792	−23.959	234.386	−11.070	234.80	234.39	−10.21	−11.07	158.2	131.9	5.35	0.18	2
309	6.892	−29.957	240.512	−12.398	240.51	240.51	−12.40	−12.40	168.8	147.7	2.05	0.11	1
310	6.923	12.046	202.978	6.902	202.98	202.98	6.90	6.90	131.9	95.0	7.64	0.23	1
311	6.928	−29.956	240.715	−11.965	241.10	240.71	−11.15	−11.96	195.2	142.4	9.25	0.15	2
312	6.974	−39.953	250.356	−15.514	250.36	250.36	−15.51	−15.51	153.0	142.4	1.13	0.08	1
313	6.998	−29.953	241.103	−11.146	241.55	241.10	−10.22	−11.15	174.1	142.4	4.83	0.13	2
314	7.113	−39.947	251.009	−14.052	251.01	250.68	−14.05	−14.78	284.9	269.0	2.54	0.12	2
315	7.132	−31.943	243.689	−10.451	243.69	243.69	−10.45	−10.45	232.1	216.3	1.42	0.07	1
316	7.154	−35.944	247.488	−11.930	247.49	246.77	−11.93	−13.47	137.1	116.0	7.20	0.28	3
317	7.181	−19.945	233.186	−4.446	233.19	233.19	−4.45	−4.45	158.2	153.0	1.09	0.13	1
318	7.235	−37.939	249.755	−11.913	250.12	249.76	−11.17	−11.91	327.1	316.5	2.38	0.10	2
319	7.235	−37.939	249.755	−11.913	251.35	249.40	−11.91	−15.51	306.0	274.3	9.42	0.17	6
320	7.251	−39.941	251.689	−12.600	251.69	251.35	−12.60	−13.32	137.1	126.6	3.01	0.14	2
321	7.269	32.061	186.197	19.466	186.20	186.20	19.47	19.47	−105.5	−121.4	2.02	0.14	1
322	7.277	76.065	138.738	28.189	143.28	138.56	31.23	26.14	−126.6	−216.3	325.08	0.96	19
323	7.305	−37.936	250.119	−11.170	250.12	249.76	−11.17	−11.91	348.2	337.6	2.96	0.16	2
324	7.319	4.062	212.842	8.548	212.84	212.84	8.55	8.55	121.3	110.8	2.01	0.23	1
325	7.357	−23.934	237.873	−4.142	237.87	237.43	−4.14	−4.98	179.3	163.5	2.10	0.09	2
326	7.419	−31.931	245.353	−7.180	245.35	245.35	−7.18	−7.18	237.4	226.8	1.58	0.13	1
327	7.443	−37.930	250.863	−9.704	250.86	250.86	−9.70	−9.70	163.5	153.0	1.20	0.08	1
328	7.462	−27.932	242.074	−4.801	242.07	242.07	−4.80	−4.80	179.3	163.5	1.68	0.09	1
329	7.506	24.071	195.296	19.459	195.30	195.30	19.46	19.46	−52.8	−95.0	4.59	0.12	1
330	7.555	−25.926	240.917	−2.744	240.92	239.75	−2.74	−4.89	379.9	306.0	35.26	0.44	3
331	7.555	−25.926	240.917	−2.744	240.92	240.92	−2.74	−2.74	205.7	200.5	2.16	0.23	1
332	7.645	24.077	196.045	21.228	196.05	196.05	21.23	21.23	−73.9	−84.4	1.36	0.11	1
333	7.650	−25.922	241.549	−1.621	241.55	239.75	−1.62	−4.89	311.3	216.3	61.02	0.75	4
334	7.650	−25.922	241.549	−1.621	241.55	241.55	−1.62	−1.62	242.7	237.4	1.56	0.15	1
335	7.650	−25.922	241.549	−1.621	241.55	241.55	−1.62	−1.62	369.3	306.0	28.74	0.76	1
336	7.755	−13.918	231.894	5.679	231.89	228.38	8.06	5.41	163.5	131.9	13.70	0.18	6
337	7.764	−25.918	242.321	−0.289	243.90	242.32	2.31	−0.29	369.3	311.3	56.42	0.94	3
338	7.764	−25.918	242.321	−0.289	244.59	242.32	3.41	−0.29	300.7	237.4	61.64	0.98	4
339	7.798	−35.916	251.161	−5.003	255.20	248.29	−5.00	−11.88	189.9	137.1	113.79	0.65	24
340	7.816	−39.917	254.738	−6.844	255.20	254.74	−6.06	−6.84	184.6	158.2	10.03	0.35	2
341	7.868	72.090	143.155	30.805	145.53	142.79	34.00	28.82	−105.5	−189.9	104.78	0.44	13
342	7.868	−35.913	251.591	−4.277	251.59	251.16	−4.28	−5.00	189.9	174.1	3.07	0.15	2
343	7.965	−39.911	255.619	−5.370	256.90	255.62	−3.35	−5.37	216.3	163.5	17.76	0.31	5
344	7.988	−15.912	235.350	7.555	235.35	235.35	7.55	7.55	163.5	153.0	1.10	0.08	1
345	8.053	−7.906	228.873	12.491	228.87	228.87	12.49	12.49	137.1	126.6	1.56	0.11	1
346	8.065	10.095	212.374	21.176	214.50	212.37	21.18	20.69	110.8	89.7	2.96	0.14	2
347	8.152	−11.906	233.152	11.687	233.15	233.15	11.69	11.69	142.4	121.3	6.72	0.40	1
348	8.209	−23.899	243.823	5.907	249.55	240.31	13.43	5.18	195.2	131.9	329.47	0.98	31
349	8.312	−39.897	257.795	−2.027	257.79	257.79	−2.03	−2.03	216.3	205.7	2.03	0.18	1
350	8.320	−13.896	236.219	12.714	236.55	235.66	13.22	11.86	158.2	126.6	10.14	0.18	4
351	8.327	−9.900	232.795	14.933	233.36	232.80	15.81	14.93	137.1	79.1	22.40	0.34	2
352	8.352	10.106	214.360	25.010	214.36	214.36	25.01	25.01	121.3	89.7	3.34	0.12	1
353	8.408	−1.892	226.262	20.111	226.82	225.71	21.01	19.21	137.1	84.4	18.75	0.28	3
354	8.410	12.108	212.752	26.635	212.75	212.75	26.64	26.64	105.5	94.9	1.17	0.08	1
355	8.414	−29.894	250.344	4.772	250.34	250.34	4.77	4.77	174.1	163.5	2.14	0.19	1
356	8.422	10.109	214.849	25.936	214.85	214.85	25.94	25.94	116.1	100.2	1.82	0.09	1
357	8.460	−39.891	258.782	−0.633	258.78	258.78	−0.63	−0.63	−105.6	−116.1	2.01	0.19	1
358	8.479	−7.889	232.274	17.918	236.62	232.27	18.79	16.96	126.6	89.7	15.03	0.25	5
359	8.521	26.111	198.305	33.128	198.31	198.31	33.13	33.13	95.0	84.4	1.27	0.10	1
360	8.528	−19.890	243.011	11.837	243.01	243.01	11.84	11.84	126.6	110.8	4.49	0.28	1
361	8.571	−35.886	256.355	2.814	256.36	256.36	2.81	2.81	184.6	174.1	3.96	0.34	1
362	8.588	4.113	222.021	25.409	222.02	222.02	25.41	25.41	121.3	121.3	1.19	0.23	1
363	8.613	50.114	169.235	37.670	169.24	169.24	37.67	37.67	−126.6	−131.9	1.17	0.13	1
364	8.631	−29.886	252.020	7.048	252.02	252.02	7.05	7.05	179.3	168.8	1.51	0.13	1
365	8.632	−15.887	240.519	15.351	240.52	239.93	15.35	14.53	142.4	105.5	9.72	0.21	2
366	8.677	−13.883	239.200	17.037	239.20	239.20	17.04	17.04	126.6	110.8	2.79	0.19	1
367	8.704	−23.881	247.776	11.461	247.78	247.78	11.46	11.46	174.1	142.4	4.18	0.15	1
368	8.717	−11.885	237.822	18.652	237.82	237.82	18.65	18.65	121.3	110.8	1.40	0.10	1
369	8.736	−19.883	244.769	14.217	247.34	243.93	17.43	13.43	142.4	89.6	29.34	0.31	8
370	8.791	−37.877	259.557	3.654	259.56	259.56	3.65	3.65	179.3	168.8	1.68	0.12	1
371	8.816	−13.878	240.423	18.690	240.42	240.42	18.69	18.69	110.8	105.5	1.29	0.13	1
372	8.820	−33.881	256.677	6.458	265.72	252.03	15.70	5.61	195.2	131.9	161.82	0.55	57
373	8.836	−7.877	235.347	22.367	235.35	235.35	22.37	22.37	105.5	94.9	1.46	0.10	1
374	8.886	−39.876	261.805	3.222	262.32	261.80	3.83	3.22	195.2	184.6	3.70	0.21	2
375	8.912	−23.874	249.566	13.715	251.57	248.96	14.46	11.59	174.1	142.4	11.60	0.16	7
376	8.917	62.127	153.661	38.587	169.25	146.86	49.26	30.15	−110.8	−205.8	933.33	1.52	97

TABLE 2—*Continued*

No.	Peak α_{1950}	δ_{1950}	Peak *l*	*b*	*l* max	*l* min	*b* max	*b* min	*v* max	*v* min	F_{tot}	T_{peak}	# pts
377	8.965	−13.873	241.778	20.441	241.78	241.78	20.44	20.44	105.5	89.6	1.42	0.07	1
378	8.981	−23.872	250.182	14.455	252.19	249.58	17.63	12.95	126.6	105.5	9.57	0.16	6
379	8.999	14.127	214.732	35.306	214.73	214.73	35.31	35.31	131.9	126.6	1.15	0.15	1
380	9.024	−39.872	262.852	4.429	262.85	262.85	4.43	4.43	200.4	189.9	1.31	0.09	1
381	9.087	8.132	221.974	33.865	221.97	221.97	33.87	33.87	126.6	121.3	3.12	0.47	1
382	9.095	40.134	182.363	42.676	182.36	182.36	42.68	42.68	−79.1	−89.7	1.21	0.08	1
383	9.108	−17.868	246.481	19.619	246.48	246.48	19.62	19.62	116.0	89.6	2.85	0.11	1
384	9.130	−23.867	251.534	16.019	251.53	251.53	16.02	16.02	147.7	142.4	1.42	0.18	1
385	9.163	−39.867	263.929	5.606	263.93	263.93	5.61	5.61	195.2	184.6	1.25	0.10	1
386	9.167	−25.866	253.448	15.094	253.45	253.45	15.09	15.09	110.7	100.2	1.18	0.09	1
387	9.182	−1.865	232.974	29.999	233.64	232.97	30.86	30.00	110.8	94.9	2.84	0.10	2
388	9.195	12.135	218.446	37.076	218.45	218.45	37.08	37.08	110.8	79.1	3.50	0.12	1
389	9.197	26.135	201.377	41.903	201.38	201.19	41.90	41.37	−68.6	−89.7	9.38	0.29	2
390	9.205	−35.865	261.334	8.711	263.21	261.33	10.61	8.71	158.2	100.2	46.75	0.61	4
391	9.314	6.136	226.079	35.874	226.08	226.08	35.87	35.87	100.2	89.7	1.19	0.08	1
392	9.336	−15.864	247.062	23.422	247.06	247.06	23.42	23.42	105.5	94.9	1.14	0.08	1
393	9.345	10.140	221.939	38.183	221.94	221.94	38.18	38.18	126.6	121.3	3.60	0.60	1
394	9.381	−29.862	258.474	14.468	258.69	256.26	15.79	14.47	126.6	110.7	5.07	0.15	4
395	9.395	−17.859	249.312	22.769	249.31	249.31	22.77	22.77	131.9	89.6	4.96	0.15	1
396	9.400	−1.859	235.111	32.716	235.11	234.42	32.72	31.86	110.8	84.4	2.65	0.08	2
397	9.419	0.140	233.321	34.072	235.11	233.32	34.07	32.72	142.4	126.6	2.76	0.10	2
398	9.431	34.144	191.120	46.290	191.12	191.12	46.29	46.29	−89.7	−100.3	1.28	0.09	1
399	9.450	−39.859	266.265	7.962	266.27	265.69	7.96	7.41	211.0	195.2	3.29	0.14	2
400	9.459	−25.857	256.227	17.996	259.34	256.23	18.00	15.32	147.7	131.9	3.04	0.14	3
401	9.500	−11.860	245.374	27.832	245.37	245.37	27.83	27.83	94.9	84.4	1.43	0.10	1
402	9.534	−3.856	238.434	33.183	239.18	237.70	34.02	32.34	174.1	142.4	7.57	0.15	3
403	9.534	−17.855	250.751	24.247	250.75	250.75	24.25	24.25	105.5	94.9	1.26	0.10	1
404	9.588	66.146	146.722	41.235	150.08	142.21	43.46	39.72	−89.7	−137.2	34.73	0.25	11
405	9.589	−39.855	267.445	9.056	267.44	264.45	11.78	9.06	158.2	79.1	68.59	0.75	4
406	9.589	−39.855	267.445	9.056	267.44	267.44	9.06	9.06	158.2	142.4	5.05	0.41	1
407	9.639	−11.856	246.880	29.383	246.88	246.88	29.38	29.38	100.2	89.6	1.25	0.10	1
408	9.644	30.150	197.461	48.502	197.65	194.22	49.39	47.33	−63.3	−100.3	21.18	0.32	5
409	9.658	−39.853	268.043	9.588	269.27	267.18	11.51	9.59	153.0	94.9	48.63	0.61	4
410	9.667	−25.852	258.325	19.984	258.33	257.61	19.98	19.33	147.7	131.9	2.02	0.11	2
411	9.693	−15.854	250.846	27.280	255.19	248.91	28.38	22.72	126.6	89.6	8.90	0.13	5
412	9.700	−35.851	265.717	12.914	265.72	265.72	12.91	12.91	179.3	153.0	3.19	0.17	1
413	9.727	−39.851	268.652	10.114	269.27	268.65	10.63	10.11	105.5	79.1	16.11	0.44	2
414	9.731	−27.852	260.441	19.115	260.44	259.74	19.12	18.49	116.0	73.8	33.90	0.63	2
415	9.747	−31.848	263.420	16.294	264.21	263.42	16.96	16.29	189.9	158.2	3.89	0.10	2
416	9.764	−23.849	257.858	22.338	258.61	253.66	24.74	21.68	126.6	84.4	26.67	0.22	9
417	9.778	−11.853	248.446	30.906	248.45	248.45	30.91	30.91	100.2	89.6	1.13	0.08	1
418	9.783	30.154	197.843	50.285	197.84	197.84	50.29	50.29	−84.4	−105.5	5.09	0.27	1
419	9.794	−21.849	256.692	24.078	256.69	256.69	24.08	24.08	121.3	110.8	1.20	0.09	1
420	9.796	−39.849	269.269	10.632	271.26	269.27	12.21	10.63	174.1	131.9	12.71	0.30	5
421	9.820	32.152	194.794	50.970	194.79	191.64	54.17	50.97	−68.6	−110.8	19.25	0.21	5
422	9.822	−17.847	253.900	27.214	253.90	253.90	27.21	27.21	153.0	137.1	1.44	0.08	1
423	9.848	−13.847	250.944	30.285	250.94	250.94	30.29	30.29	121.3	110.8	1.16	0.08	1
424	9.899	−29.848	263.591	19.093	263.59	263.59	19.09	19.09	110.7	105.5	1.07	0.13	1
425	9.918	−35.845	267.792	14.634	267.79	266.79	16.42	14.63	147.7	137.1	1.94	0.11	2
426	9.922	30.157	198.202	52.072	198.20	198.20	52.07	52.07	−84.4	−105.5	4.28	0.17	1
427	9.945	−39.846	270.620	11.714	271.26	269.27	12.21	10.63	269.0	247.9	9.81	0.16	4
428	9.955	−25.844	261.403	22.615	262.18	261.40	23.23	22.61	369.3	342.9	3.80	0.13	3
429	9.960	−3.845	243.279	38.213	243.28	243.28	38.21	38.21	153.0	142.4	1.15	0.08	1
430	9.968	2.155	237.176	41.987	238.01	237.18	42.83	41.99	131.9	116.0	1.93	0.08	2
431	−0.008	−36.174	350.016	−76.327	353.81	350.02	−74.93	−76.33	73.9	47.5	4.29	0.10	3
432	−0.011	−24.173	46.327	−78.368	46.33	44.90	−77.46	−78.37	−63.3	−137.2	21.07	0.35	2
433	−0.018	−16.179	74.476	−73.863	74.48	74.48	−73.86	−73.86	−131.9	−137.2	1.14	0.13	1
434	−0.025	−32.173	6.411	−78.057	6.41	6.41	−78.06	−78.06	73.9	47.5	2.70	0.11	1
435	10.025	−25.843	262.178	23.227	262.18	262.18	23.23	23.23	379.8	364.0	1.62	0.10	1
436	10.050	−23.842	261.048	24.976	261.05	260.15	24.98	24.26	105.5	89.6	1.97	0.12	2
437	10.064	0.156	240.489	41.937	240.49	239.64	41.94	41.11	121.3	89.7	4.00	0.13	2
438	10.091	36.160	188.310	54.435	188.31	188.31	54.43	54.43	−100.3	−126.6	2.93	0.14	1
439	10.106	2.158	238.853	43.662	239.73	238.85	44.49	43.66	121.3	105.5	2.94	0.11	2
440	10.114	68.162	142.207	42.699	142.21	142.21	42.70	42.70	−100.2	−110.8	1.61	0.11	1
441	10.125	−35.841	269.856	16.194	270.56	269.86	16.69	16.19	142.4	137.1	1.92	0.12	2
442	10.128	−5.840	247.313	38.794	249.15	247.31	40.31	38.79	137.1	105.5	7.88	0.18	3
443	10.152	−19.842	259.341	28.938	261.19	258.50	30.28	26.78	137.1	84.4	15.62	0.19	5
444	10.157	40.162	181.295	54.825	181.30	181.30	54.83	54.83	−79.1	−84.4	1.07	0.10	1
445	10.157	−33.843	268.925	18.022	268.92	268.92	18.02	18.02	116.0	105.5	1.45	0.12	1
446	10.184	−29.841	266.657	21.425	270.36	263.59	27.34	13.10	253.2	168.8	256.23	0.49	42
447	10.220	−21.839	261.631	28.019	261.63	261.63	28.02	28.02	100.2	89.6	1.36	0.10	1
448	10.246	−25.838	264.717	25.103	265.56	263.76	25.69	24.42	184.6	147.7	8.63	0.16	3
449	10.259	−23.837	263.501	26.788	264.35	262.67	27.37	26.20	168.8	142.4	7.11	0.18	3
450	10.312	50.162	164.079	53.534	164.08	164.08	53.53	53.53	−100.2	−110.8	1.35	0.10	1
451	10.316	32.163	195.393	57.263	195.39	195.39	57.26	57.26	−89.7	−95.0	1.27	0.17	1
452	10.319	64.166	145.498	46.162	145.50	145.50	46.16	46.16	−131.9	−142.4	1.13	0.08	1
453	10.352	38.167	184.237	57.356	184.80	173.65	59.78	54.04	−73.9	−131.9	100.83	0.35	18
454	10.370	−19.838	262.077	30.893	262.08	262.08	30.89	30.89	94.9	84.4	1.80	0.15	1
455	10.384	−29.837	268.922	22.964	268.92	268.92	22.96	22.96	100.2	84.4	2.39	0.14	1
456	10.391	−31.834	270.232	21.375	270.23	270.23	21.38	21.38	126.6	116.0	1.32	0.10	1
457	10.397	−23.835	265.203	27.944	265.20	265.20	27.94	27.94	116.0	105.5	1.38	0.11	1
458	10.406	48.168	166.571	55.178	169.79	162.37	57.06	53.53	−110.8	−163.6	73.28	0.68	11
459	10.412	−35.835	272.841	18.204	272.84	272.84	18.20	18.20	131.9	131.9	1.39	0.26	1
460	10.416	50.164	163.350	54.436	163.35	163.35	54.44	54.44	−84.4	−105.5	3.05	0.16	1
461	10.440	−39.835	275.392	15.020	275.39	275.39	15.02	15.02	142.4	137.1	1.07	0.13	1
462	10.457	−25.834	267.264	26.799	269.02	266.40	27.87	26.25	105.5	79.1	9.76	0.19	5
463	10.458	64.169	144.647	46.855	144.65	144.65	46.86	46.86	−131.9	−158.3	3.05	0.12	1
464	10.460	−31.832	271.019	21.870	271.02	271.02	21.87	21.87	89.6	79.1	3.60	0.25	1
465	10.498	−21.834	265.131	30.377	265.13	265.13	30.38	30.38	184.6	174.1	1.13	0.08	1
466	10.501	22.167	214.658	58.140	214.66	214.66	58.14	58.14	−68.6	−73.9	1.09	0.14	1
467	10.526	−17.832	262.694	33.828	262.69	262.69	33.83	33.83	94.9	79.1	1.74	0.10	1
468	10.529	−31.831	271.813	22.353	273.44	265.04	26.02	22.35	158.2	94.9	46.74	0.20	14
469	10.543	50.166	162.372	55.518	162.37	162.37	55.52	55.52	−105.5	−110.8	1.24	0.12	1
470	10.585	40.170	179.463	59.622	179.46	179.05	60.39	59.62	−89.7	−131.9	7.07	0.16	2

TABLE 2—*Continued*

No.	Peak α_{1950}	δ_{1950}	Peak *l*	*b*	*l* max	*l* min	*b* max	*b* min	*v* max	*v* min	F_{tot}	T_{peak}	# pts
471	10.652	−33.834	274.364	21.464	276.77	265.42	26.41	15.32	147.7	68.5	160.75	0.41	28
472	10.654	40.171	179.051	60.390	179.05	178.53	61.27	60.39	−84.4	−105.5	2.54	0.12	2
473	10.660	50.168	161.377	56.495	161.38	160.64	57.16	56.50	−100.2	−116.1	2.51	0.07	2
474	10.701	−37.828	277.053	18.313	279.82	273.57	21.01	17.46	142.4	100.2	24.42	0.20	14
475	10.724	−33.828	275.201	21.927	275.20	275.20	21.93	21.93	126.6	116.0	2.58	0.21	1
476	10.742	2.170	247.876	50.975	250.39	247.88	52.58	50.97	110.8	79.1	6.35	0.13	3
477	10.747	−25.829	270.959	28.956	272.81	270.96	29.91	28.96	189.9	163.5	12.15	0.20	3
478	10.785	−21.829	269.017	32.630	269.99	268.05	33.14	32.10	84.4	63.3	4.30	0.11	3
479	10.813	−17.828	266.787	36.206	269.99	265.62	36.75	33.14	158.2	116.0	18.88	0.15	8
480	10.865	−39.829	279.819	17.457	279.82	279.82	17.46	17.46	116.0	84.4	5.10	0.24	1
481	10.930	4.172	248.677	54.398	248.68	248.68	54.40	54.40	100.2	79.1	2.11	0.14	1
482	10.932	−33.825	277.661	23.166	277.66	276.94	25.08	23.17	147.7	131.9	3.40	0.15	2
483	10.947	36.175	185.668	64.704	186.25	184.99	65.93	63.47	−68.6	−105.5	106.19	1.70	3
484	10.989	−37.825	280.241	19.893	282.85	280.24	20.25	18.50	142.4	79.1	17.72	0.23	4
485	11.071	−33.823	279.349	23.933	279.35	278.59	23.93	23.59	153.0	142.4	1.78	0.12	2
486	11.078	−33.828	279.440	23.967	279.44	279.44	23.97	23.97	142.4	121.3	3.02	0.17	1
487	11.107	−29.827	277.905	27.742	277.90	277.90	27.74	27.74	110.8	100.2	1.56	0.11	1
488	11.108	−7.824	264.142	46.915	264.14	264.14	46.92	46.92	89.7	79.1	1.20	0.08	1
489	11.196	38.179	178.901	66.995	178.90	178.12	67.76	67.00	−73.9	−116.1	29.35	0.69	2
490	11.271	14.176	239.797	64.689	239.80	239.80	64.69	64.69	79.1	52.7	2.46	0.10	1
491	11.281	−39.824	284.414	19.436	285.32	284.41	19.76	19.44	116.0	105.5	2.87	0.16	2
492	11.287	−27.825	279.397	30.545	280.38	279.40	30.91	30.54	116.0	100.2	3.01	0.12	2
493	11.296	44.180	164.476	65.180	171.73	161.10	66.83	62.91	−89.7	−142.5	115.19	1.10	9
494	11.335	−37.821	284.267	21.533	285.32	284.27	21.82	19.76	179.3	163.5	4.14	0.14	3
495	11.342	−29.824	281.071	28.990	281.07	281.07	28.99	28.99	147.7	142.4	1.09	0.13	1
496	11.358	−33.820	282.960	25.359	282.96	282.96	25.36	25.36	153.0	142.4	1.12	0.08	1
497	11.374	−13.822	273.294	43.743	274.81	272.42	43.74	41.15	89.7	73.8	5.88	0.13	4
498	11.381	−31.821	282.450	27.328	283.05	282.45	27.33	25.39	137.1	131.9	2.94	0.18	2
499	11.402	−35.822	284.314	23.688	284.31	284.31	23.69	23.69	189.9	179.3	1.62	0.13	1
500	11.410	14.177	242.676	66.320	242.68	242.68	66.32	66.32	73.8	58.0	1.52	0.08	1
501	11.415	−29.824	282.083	29.347	282.08	282.08	29.35	29.35	174.1	163.5	1.36	0.11	1
502	11.427	−33.820	283.850	25.668	283.85	283.85	25.67	25.67	89.6	79.1	2.78	0.23	1
503	11.435	−33.825	283.952	25.697	283.95	283.95	25.70	25.70	−116.1	−121.4	1.07	0.14	1
504	11.447	−17.821	276.907	40.590	276.91	276.91	40.59	40.59	100.2	73.8	2.85	0.12	1
505	11.494	−27.823	282.374	31.588	283.39	282.37	31.91	31.59	174.1	153.0	4.15	0.13	2
506	11.499	−39.822	286.918	20.301	286.92	286.92	20.30	20.30	263.8	258.5	1.38	0.15	1
507	11.523	−1.821	267.291	55.318	267.29	267.29	55.32	55.32	73.8	58.0	1.75	0.10	1
508	11.550	28.180	205.905	73.192	212.63	205.91	73.19	72.74	79.1	63.3	2.05	0.09	2
509	11.568	−39.822	287.727	20.551	287.73	287.73	20.55	20.55	100.2	94.9	1.06	0.12	1
510	11.583	46.180	156.004	66.200	162.87	153.76	67.79	64.62	−79.1	−137.2	123.68	0.80	7
511	11.622	−37.819	287.734	22.653	291.97	286.05	27.50	20.30	274.3	195.2	285.21	1.09	31
512	11.629	62.180	136.809	53.273	136.81	136.81	53.27	53.27	−110.8	−131.9	1.96	0.09	1
513	11.643	−27.822	284.562	32.251	284.56	284.56	32.25	32.25	110.8	79.1	5.78	0.21	1
514	11.644	−33.819	286.705	26.552	286.72	286.21	28.51	26.55	105.5	79.1	12.04	0.38	3
515	11.652	−13.821	278.448	45.429	286.88	278.13	48.62	40.46	116.0	73.8	25.27	0.17	16
516	11.665	−23.820	283.345	36.135	283.34	283.34	36.14	36.14	163.5	153.0	1.32	0.10	1
517	11.691	−37.819	288.583	22.888	289.36	287.73	22.89	21.01	195.2	163.5	2.65	0.12	3
518	11.706	−39.821	289.361	21.012	289.36	289.36	21.01	21.01	211.0	205.7	1.69	0.19	1
519	11.713	−27.822	285.602	32.536	285.60	284.56	32.54	32.25	153.0	131.9	2.14	0.10	2
520	11.714	−33.818	287.629	26.804	287.78	287.63	26.84	26.80	105.5	79.1	11.49	0.35	2
521	11.782	−27.822	286.648	32.804	286.65	286.65	32.80	32.80	105.5	73.8	4.60	0.19	1
522	11.783	4.178	267.774	62.469	267.77	267.77	62.47	62.47	131.9	131.9	1.62	0.31	1
523	11.784	48.183	148.950	65.983	148.95	146.81	66.57	65.98	−79.1	−110.8	28.09	0.73	2
524	11.794	−33.823	288.708	27.072	288.71	288.71	27.07	27.07	216.3	205.7	1.93	0.16	1
525	11.806	32.179	189.366	76.015	197.83	169.44	78.80	75.67	−31.7	−84.4	548.41	2.95	13
526	11.807	−31.819	288.290	29.049	288.29	287.13	31.12	29.05	131.9	89.6	9.98	0.14	3
527	11.814	2.179	270.700	60.957	270.70	270.70	60.96	60.96	79.1	68.6	1.19	0.08	1
528	11.833	24.179	223.329	76.341	223.33	223.33	76.34	76.34	58.0	42.2	1.53	0.09	1
529	11.848	−29.822	288.277	31.116	288.28	288.28	31.12	31.12	89.6	84.4	1.18	0.14	1
530	11.897	−35.820	290.642	25.456	304.90	272.73	31.59	17.82	153.0	47.4	942.26	0.68	198
531	11.899	−37.819	291.173	23.517	291.17	291.17	23.52	23.52	126.6	94.9	9.94	0.49	1
532	11.920	−27.822	288.759	33.291	288.76	288.76	33.29	33.29	105.5	89.6	3.21	0.21	1
533	11.922	−33.818	290.442	27.472	290.44	290.44	27.47	27.47	163.5	153.0	1.36	0.09	1
534	11.991	−33.818	291.392	27.666	291.39	291.39	27.67	27.67	121.3	116.0	1.48	0.19	1
535	11.993	−39.821	292.810	21.802	292.81	292.81	21.80	21.80	116.0	105.5	2.48	0.22	1
536	12.010	36.181	169.441	76.495	169.44	169.44	76.50	76.50	63.3	52.8	1.18	0.09	1
537	12.059	−27.822	290.907	33.711	290.91	290.91	33.71	33.71	121.3	105.5	2.39	0.16	1
538	12.075	58.183	134.142	58.247	135.60	128.96	58.89	56.92	−31.6	−147.7	160.56	1.19	6
539	12.080	52.178	138.478	63.877	138.48	138.48	63.88	63.88	−95.0	−110.8	5.03	0.34	1
540	12.115	46.181	144.121	69.458	144.12	140.96	69.98	69.46	−95.0	−116.1	4.78	0.16	2
541	12.139	44.182	146.284	71.339	146.28	146.28	71.34	71.34	−52.8	−79.1	15.49	0.86	1
542	12.139	−27.822	292.152	33.922	293.24	290.83	34.09	31.65	121.3	63.3	16.77	0.20	4
543	12.142	50.178	139.019	65.948	139.02	136.42	66.34	65.95	−84.4	−121.3	25.28	0.62	2
544	12.160	−23.820	291.559	37.905	291.56	290.38	37.91	37.71	121.3	110.8	2.29	0.10	2
545	12.175	−29.822	293.143	32.041	293.14	293.14	32.04	32.04	131.9	126.6	1.21	0.14	1
546	12.177	−37.819	294.707	24.164	294.71	294.71	24.16	24.16	116.0	110.8	3.14	0.33	1
547	12.186	−37.819	294.821	24.181	294.82	294.71	24.18	24.16	131.9	126.6	2.39	0.19	2
548	12.186	−37.819	294.821	24.181	294.82	294.82	24.18	24.18	147.7	137.1	1.82	0.13	1
549	12.201	−39.821	295.350	22.231	295.35	295.35	22.23	22.23	321.8	311.3	1.83	0.17	1
550	12.202	−19.823	291.311	41.941	291.31	290.03	41.94	41.74	−95.0	−105.6	2.74	0.15	2
551	12.202	−19.823	291.311	41.941	291.31	291.31	41.94	41.94	137.1	131.9	1.86	0.20	1
552	12.202	−19.823	291.311	41.941	291.31	291.31	41.94	41.94	158.2	147.7	2.78	0.22	1
553	12.202	−19.823	291.311	41.941	291.31	291.31	41.94	41.94	211.0	168.8	4.29	0.13	1
554	12.202	−19.823	291.311	41.941	291.31	291.31	41.94	41.94	−116.1	−126.7	2.04	0.15	1
555	12.202	−19.823	291.311	41.941	291.31	291.31	41.94	41.94	−137.2	−147.8	2.20	0.15	1
556	12.202	−19.823	291.311	41.941	291.81	291.31	41.94	39.98	121.3	79.1	11.42	0.27	2
557	12.202	−21.821	291.811	39.979	291.81	290.58	39.98	39.79	89.7	73.8	2.32	0.12	2
558	12.208	−27.822	293.244	34.087	294.34	293.14	34.09	32.04	116.0	100.2	4.17	0.12	3
559	12.284	58.183	131.116	58.712	131.12	131.12	58.71	58.71	−100.2	−116.1	1.85	0.12	1
560	12.289	76.182	125.500	41.064	126.15	124.18	41.19	40.97	−200.5	−211.0	4.89	0.16	4
561	12.310	74.182	125.830	43.051	125.83	125.83	43.05	43.05	−121.3	−131.9	1.14	0.08	1
562	12.343	26.178	222.288	83.542	222.29	222.29	83.54	83.54	−290.2	−300.8	1.47	0.11	1
563	12.350	−39.822	297.183	22.462	297.18	297.18	22.46	22.46	137.1	131.9	1.18	0.16	1
564	12.378	−23.821	295.314	38.387	295.31	292.92	38.39	38.10	94.9	84.4	2.73	0.10	3

TABLE 2—*Continued*

No.	Peak α_{1950}	δ_{1950}	Peak l	b	l max	l min	b max	b min	v max	v min	F_{tot}	T_{peak}	# pts
565	12.416	−27.823	296.550	34.477	296.55	296.55	34.48	34.48	105.5	79.1	3.26	0.13	1
566	12.419	−39.822	298.042	22.549	298.04	297.38	24.50	22.55	131.9	105.5	6.89	0.20	2
567	12.427	−33.824	297.477	28.525	297.48	297.48	28.53	28.53	100.2	84.4	1.92	0.14	1
568	12.500	−31.820	298.318	30.608	298.32	298.32	30.61	30.61	126.6	116.0	1.55	0.13	1
569	12.500	−31.820	298.318	30.608	298.32	298.32	30.61	30.61	147.7	137.1	1.74	0.14	1
570	12.505	58.182	127.794	59.044	127.79	127.79	59.04	59.04	−100.2	−110.8	1.38	0.12	1
571	12.511	−25.822	297.853	36.595	297.85	297.85	36.60	36.60	105.5	94.9	1.15	0.08	1
572	12.570	−31.821	299.337	30.674	299.34	299.34	30.67	30.67	174.1	100.2	8.14	0.14	1
573	12.627	−39.824	300.628	22.724	300.63	300.63	22.72	22.72	279.6	274.3	1.11	0.14	1
574	12.649	−25.823	300.177	36.722	301.52	300.18	36.76	36.72	105.5	94.9	3.26	0.14	2
575	12.649	−31.821	300.507	30.730	300.51	300.51	30.73	30.73	100.2	73.8	6.30	0.27	1
576	12.649	−31.821	300.507	30.730	300.51	300.51	30.73	30.73	153.0	110.8	8.53	0.23	1
577	12.649	−31.821	300.507	30.730	300.51	300.51	30.73	30.73	174.1	163.5	1.92	0.13	1
578	12.690	54.176	125.471	63.188	131.57	119.15	66.87	63.10	−79.1	−110.8	60.59	0.56	11
579	12.734	−23.823	301.553	38.763	301.55	301.55	38.76	38.76	89.7	79.1	2.33	0.22	1
580	12.846	−19.827	303.561	42.771	303.56	303.56	42.77	42.77	89.7	79.1	1.19	0.10	1
581	12.853	−33.828	303.517	28.770	303.52	303.52	28.77	28.77	126.6	116.0	1.34	0.11	1
582	12.873	−23.824	303.989	38.769	303.99	303.99	38.77	38.77	73.8	68.5	1.36	0.13	1
583	13.050	−27.828	306.763	34.670	314.44	301.21	37.99	30.67	126.6	63.3	44.55	0.20	20
584	13.069	40.175	110.172	76.846	110.17	110.17	76.85	76.85	−47.5	−79.1	15.49	0.71	1
585	13.134	−31.826	307.695	30.600	307.69	307.69	30.60	30.60	121.3	105.5	1.93	0.13	1
586	13.150	−23.828	308.850	38.545	308.85	308.85	38.55	38.55	110.8	100.2	1.26	0.10	1
587	13.243	−35.829	308.796	26.483	313.91	308.80	26.48	23.69	142.4	100.2	24.75	0.22	9
588	13.272	−19.832	311.697	42.307	311.70	311.70	42.31	42.31	84.4	73.8	1.23	0.09	1
589	13.342	−31.830	310.749	30.297	313.91	305.48	32.61	26.13	131.9	47.4	222.48	0.33	42
590	13.348	−33.834	310.510	28.302	310.51	310.51	28.30	28.30	110.8	105.5	1.43	0.18	1
591	13.489	−29.835	313.311	31.958	314.67	312.91	31.96	29.99	137.2	73.8	8.81	0.15	3
592	13.549	−19.837	316.865	41.580	316.86	316.86	41.58	41.58	89.7	73.8	1.54	0.09	1
593	13.589	−35.835	313.426	25.827	313.43	313.43	25.83	25.83	89.7	79.1	1.24	0.10	1
594	13.616	−39.837	312.899	21.841	312.90	312.05	21.99	21.84	100.2	73.8	3.21	0.11	2
595	13.631	44.166	95.844	70.572	95.84	95.84	70.57	70.57	68.6	52.8	1.42	0.08	1
596	13.641	−25.836	316.690	35.448	316.69	316.69	35.45	35.45	84.4	73.8	1.32	0.10	1
597	13.708	−31.836	316.029	29.411	316.03	316.03	29.41	29.41	100.2	89.7	1.15	0.08	1
598	13.713	46.164	97.011	68.434	97.01	97.01	68.43	68.43	89.7	79.2	1.31	0.09	1
599	13.738	−35.838	315.385	25.432	315.38	315.38	25.43	25.43	147.7	121.3	2.90	0.13	1
600	13.807	−35.840	316.285	25.226	316.29	316.29	25.23	25.23	−163.6	−174.2	1.43	0.14	1
601	13.833	68.163	114.556	48.227	114.56	114.56	48.23	48.23	−31.6	−100.2	54.39	1.55	1
602	13.834	−39.841	315.523	21.274	315.52	315.52	21.27	21.27	94.9	73.8	2.76	0.14	1
603	13.903	−39.843	316.352	21.065	316.35	315.52	21.27	21.06	−147.8	−153.1	1.86	0.11	2
604	13.903	−39.843	316.352	21.065	316.35	315.52	21.27	21.06	−179.4	−179.4	1.89	0.19	2
605	13.903	−39.843	316.352	21.065	316.35	316.35	21.06	21.06	126.6	110.8	1.86	0.14	1
606	13.910	42.159	85.067	70.086	85.07	85.07	70.09	70.09	73.9	52.8	3.16	0.16	1
607	13.910	42.159	85.067	70.086	90.41	85.07	70.91	69.11	89.7	79.2	3.40	0.13	3
608	13.926	−31.841	319.097	28.676	319.10	319.10	28.68	28.68	−89.7	−100.3	1.09	0.07	1
609	13.980	−9.846	329.813	49.096	329.81	329.81	49.10	49.10	−79.2	−95.0	1.51	0.08	1
610	14.041	−27.847	322.175	32.011	322.17	322.17	32.01	32.01	94.9	84.4	1.30	0.10	1
611	14.042	−39.846	317.986	20.611	317.99	317.17	20.84	20.61	364.0	353.5	2.00	0.13	2
612	14.042	−39.846	317.986	20.611	317.99	317.99	20.61	20.61	147.7	137.2	1.14	0.09	1
613	14.050	−33.849	320.095	26.289	320.10	320.10	26.29	26.29	105.5	68.6	5.32	0.15	1
614	14.050	−33.849	320.095	26.289	320.10	320.10	26.29	26.29	142.4	116.0	3.05	0.12	1
615	14.050	−33.849	320.095	26.289	320.10	320.10	26.29	26.29	163.5	153.0	1.10	0.07	1
616	14.064	−31.844	321.004	28.132	321.00	321.00	28.13	28.13	121.3	110.8	1.39	0.10	1
617	14.096	54.153	100.512	59.774	100.51	100.51	59.77	59.77	−411.5	−416.8	1.37	0.17	1
618	14.119	−33.850	321.005	26.009	321.01	321.01	26.01	26.01	189.9	179.4	1.36	0.12	1
619	14.131	42.154	80.682	68.194	80.68	80.68	68.19	68.19	89.7	79.2	1.74	0.13	1
620	14.136	−25.847	324.426	33.445	324.43	324.43	33.45	33.45	110.8	100.2	1.08	0.07	1
621	14.181	−39.850	319.604	20.104	319.60	319.60	20.10	20.10	−174.2	−184.7	1.84	0.18	1
622	14.183	−19.851	327.975	38.752	327.98	327.98	38.75	38.75	−100.3	−110.8	1.08	0.07	1
623	14.188	−9.851	333.985	47.751	333.98	333.98	47.75	47.75	−58.1	−79.2	2.56	0.12	1
624	14.188	−9.851	333.985	47.751	333.98	333.98	47.75	47.75	−89.7	−126.7	3.84	0.12	1
625	14.250	−39.851	320.399	19.834	320.40	320.40	19.83	19.83	105.5	89.7	1.72	0.11	1
626	14.289	−23.851	327.658	34.496	327.66	325.37	35.29	34.50	−89.7	−116.1	6.36	0.15	3
627	14.302	−35.852	322.557	23.350	322.56	318.80	24.26	20.36	116.0	79.1	12.97	0.16	7
628	14.317	70.150	112.343	45.346	112.34	112.34	45.35	45.35	−110.8	−163.5	7.70	0.19	1
629	14.339	16.146	9.712	66.049	9.71	9.71	66.05	66.05	−58.0	−68.6	1.33	0.09	1
630	14.339	42.149	77.359	66.274	77.36	77.36	66.27	66.27	89.7	73.9	2.52	0.16	1
631	14.358	56.149	99.435	56.824	100.69	99.44	57.36	56.82	84.5	68.6	2.48	0.09	2
632	14.362	46.148	84.846	63.802	84.85	84.85	63.80	63.80	89.7	73.9	2.48	0.13	1
633	14.365	−37.852	322.512	21.212	322.51	322.51	21.21	21.21	105.5	84.4	2.05	0.09	1
634	14.365	−37.852	322.512	21.212	322.51	322.51	21.21	21.21	168.8	158.3	1.26	0.11	1
635	14.401	−31.853	325.506	26.570	325.51	325.51	26.57	26.57	−95.0	−105.6	1.20	0.09	1
636	14.434	−37.854	323.323	20.896	324.13	323.32	20.90	20.57	89.7	68.6	4.04	0.15	2
637	14.436	52.143	93.357	59.313	96.38	87.12	61.89	58.05	84.5	58.1	6.62	0.12	4
638	14.441	−35.855	324.251	22.701	324.25	324.25	22.70	22.70	−174.2	−179.4	1.07	0.13	1
639	14.442	76.148	115.605	39.823	118.08	113.95	40.63	39.04	−116.0	−142.4	16.56	0.13	8
640	14.467	−33.854	325.452	24.403	325.45	325.45	24.40	24.40	153.0	89.7	160.34	12.21	1
641	14.468	−39.857	322.871	18.900	322.87	322.87	18.90	18.90	205.7	189.9	1.58	0.08	1
642	14.471	22.144	25.348	66.904	25.35	25.35	66.90	66.90	−63.3	−79.1	2.71	0.20	1
643	14.476	−33.860	325.557	24.354	325.56	325.56	24.35	24.35	84.4	79.1	1.06	0.13	1
644	14.487	44.146	79.409	63.850	79.41	79.41	63.85	63.85	89.7	79.2	1.77	0.15	1
645	14.503	66.143	107.974	48.206	107.97	107.97	48.21	48.21	−168.8	−189.9	2.26	0.11	1
646	14.528	−11.862	338.765	43.515	338.77	338.77	43.52	43.52	−58.1	−84.4	3.15	0.11	1
647	14.546	42.143	74.687	64.256	74.69	74.69	64.26	64.26	89.7	73.9	2.92	0.18	1
648	14.615	−27.862	330.290	28.972	330.29	330.29	28.97	28.97	295.5	284.9	1.39	0.11	1
649	14.641	18.139	18.624	63.191	19.53	17.67	64.08	62.29	−58.0	−84.4	10.52	0.24	3
650	14.661	−5.861	345.945	47.329	345.95	345.95	47.33	47.33	189.9	174.1	3.26	0.28	1
651	14.672	24.137	31.879	64.779	46.59	30.73	67.76	58.97	−52.7	−95.0	126.74	0.48	29
652	14.674	46.140	80.894	61.130	80.89	80.89	61.13	61.13	89.7	63.3	2.89	0.11	1
653	14.683	−9.865	342.936	43.906	344.08	342.94	43.91	43.31	−73.9	−95.0	4.37	0.15	2
654	14.695	44.140	76.998	61.903	77.00	77.00	61.90	61.90	89.7	68.6	2.28	0.11	1
655	14.754	−27.866	332.126	28.097	332.13	332.13	28.10	28.10	110.8	89.7	2.23	0.10	1
656	14.754	−27.866	332.126	28.097	332.13	332.13	28.10	28.10	290.2	279.6	1.23	0.09	1
657	14.758	−31.863	330.029	24.569	330.03	330.03	24.57	24.57	−95.0	−100.3	1.08	0.14	1
658	14.775	−35.865	328.189	20.938	328.19	327.65	21.20	20.94	406.3	395.7	2.30	0.14	2

TABLE 2—*Continued*

No.	Peak α_{1950}	δ_{1950}	Peak l	b	l max	l min	b max	b min	v max	v min	F_{tot}	T_{peak}	# pts
659	14.867	−35.868	329.237	20.406	329.24	329.24	20.41	20.41	−105.6	−116.1	1.54	0.11	1
660	14.867	−35.868	329.237	20.406	329.24	329.24	20.41	20.41	−147.8	−153.0	1.12	0.11	1
661	14.867	−35.868	329.237	20.406	329.24	329.24	20.41	20.41	−195.3	−200.5	1.24	0.17	1
662	14.870	42.133	71.534	60.953	71.53	71.53	60.95	60.95	73.9	63.3	1.22	0.08	1
663	14.889	30.134	46.214	62.703	46.21	46.21	62.70	62.70	−52.7	−89.7	4.38	0.15	1
664	14.894	−39.870	327.496	16.746	327.50	327.50	16.75	16.75	−205.8	−211.1	1.39	0.17	1
665	14.902	−33.872	330.690	21.933	330.69	330.69	21.93	21.93	121.3	105.5	1.45	0.08	1
666	15.035	−19.876	340.858	32.795	340.86	340.86	32.79	32.79	−100.3	−110.8	1.22	0.10	1
667	15.045	60.124	97.625	50.187	98.43	97.62	50.77	50.19	−73.8	−84.4	1.79	0.18	2
668	15.115	−31.875	334.284	22.244	334.28	334.28	22.24	22.24	−79.2	−95.0	1.94	0.10	1
669	15.142	72.126	109.465	41.417	109.47	109.47	41.42	41.42	−121.3	−153.0	2.72	0.09	1
670	15.169	58.125	94.235	50.672	94.23	94.23	50.67	50.67	−68.6	−79.1	1.14	0.08	1
671	15.179	−9.881	350.583	39.326	350.58	350.58	39.33	39.33	−84.4	−95.0	1.23	0.10	1
672	15.217	−15.883	346.255	34.388	347.18	346.26	34.39	33.75	−89.7	−110.8	2.61	0.09	2
673	15.298	20.118	29.096	55.303	29.10	29.10	55.30	55.30	−68.6	−79.1	1.09	0.08	1
674	15.319	−39.884	331.831	14.188	331.83	331.83	14.19	14.19	295.5	284.9	1.10	0.07	1
675	15.327	42.118	68.660	56.096	68.66	68.66	56.10	56.10	−63.3	−73.8	1.29	0.09	1
676	15.328	−33.887	335.460	19.077	335.46	335.46	19.08	19.08	105.5	100.2	1.30	0.18	1
677	15.340	−35.884	334.385	17.355	334.38	334.38	17.35	17.35	−95.0	−100.3	1.14	0.15	1
678	15.380	62.116	97.733	47.050	97.73	97.73	47.05	47.05	−158.3	−179.4	3.40	0.19	1
679	15.390	34.117	54.187	56.356	64.40	50.50	57.73	53.42	−52.7	−89.7	56.24	0.28	14
680	15.412	−17.886	347.276	31.057	347.28	347.28	31.06	31.06	−89.7	−100.3	1.14	0.08	1
681	15.414	−25.887	341.566	24.843	341.57	341.57	24.84	24.84	−89.7	−100.3	1.59	0.12	1
682	15.599	−19.896	348.044	27.797	348.04	347.22	28.45	27.80	−63.3	−105.5	6.73	0.15	2
683	15.617	−13.895	353.000	31.996	353.00	353.00	32.00	32.00	−68.6	−89.7	2.23	0.09	1
684	15.626	−23.894	345.408	24.552	345.41	341.49	25.17	22.34	−79.2	−121.4	6.28	0.12	4
685	15.641	66.105	100.951	43.349	100.95	100.95	43.35	43.35	−110.8	−126.6	2.10	0.10	1
686	15.675	−33.894	339.083	16.463	339.08	338.37	17.01	16.46	−73.9	−105.6	4.81	0.13	2
687	15.696	−35.897	337.985	14.743	338.66	337.98	14.74	14.21	−121.4	−126.7	2.39	0.16	2
688	15.705	−23.897	346.301	23.830	346.30	346.30	23.83	23.83	−110.8	−121.4	1.48	0.11	1
689	15.727	−39.900	335.704	11.393	335.70	335.70	11.39	11.39	131.9	121.3	1.23	0.09	1
690	15.747	56.104	87.969	47.598	87.97	87.97	47.60	47.60	−84.4	−100.2	2.79	0.16	1
691	15.748	−19.901	349.769	26.372	349.77	348.86	27.14	26.37	−95.0	−110.8	2.08	0.08	2
692	15.780	66.100	100.311	42.651	100.31	100.31	42.65	42.65	−100.2	−110.8	1.08	0.07	1
693	15.797	−39.902	336.333	10.888	336.33	336.33	10.89	10.89	−174.2	−179.4	1.12	0.12	1
694	15.797	−39.902	336.333	10.888	337.49	336.33	12.55	10.89	121.3	110.8	3.16	0.19	2
695	15.840	−25.903	346.319	21.109	346.32	346.32	21.11	21.11	−253.3	−258.6	1.17	0.14	1
696	15.881	28.097	45.098	49.565	45.35	45.10	49.57	48.66	−68.6	−84.4	1.79	0.11	2
697	15.948	−21.908	350.448	22.976	350.45	350.45	22.98	22.98	−105.5	−116.1	1.28	0.08	1
698	15.989	−37.907	339.393	10.935	339.39	339.39	10.94	10.94	105.5	84.4	2.13	0.12	1
699	16.089	28.089	45.854	46.852	45.85	45.85	46.85	46.85	−68.6	−84.4	1.71	0.11	1
700	16.101	−27.915	347.519	17.243	348.19	347.52	17.24	16.59	226.9	211.0	2.44	0.10	2
701	16.124	32.085	51.740	47.047	51.74	51.59	47.92	47.05	−73.8	−79.1	1.92	0.12	2
702	16.138	−37.913	340.702	9.740	340.70	340.70	9.74	9.74	105.5	84.4	2.46	0.12	1
703	16.160	−29.918	346.611	15.285	346.61	346.61	15.29	15.29	−253.3	−263.8	1.25	0.11	1
704	16.166	−21.917	352.720	20.791	352.72	352.72	20.79	20.79	274.4	200.5	12.46	0.20	1
705	16.166	−21.917	352.720	20.791	353.42	352.72	20.79	20.08	137.2	121.4	1.74	0.09	2
706	16.166	−21.917	352.720	20.791	354.10	352.72	20.79	19.36	216.3	137.2	11.80	0.20	3
707	16.236	−21.920	353.418	20.080	353.42	353.42	20.08	20.08	−263.8	−279.7	1.66	0.10	1
708	16.236	−21.920	353.418	20.080	353.42	353.42	20.08	20.08	−290.2	−300.8	1.60	0.16	1
709	16.261	36.082	57.746	45.726	57.78	57.75	45.73	45.41	−63.3	−79.1	2.39	0.10	2
710	16.305	−21.923	354.104	19.362	354.10	353.42	20.08	19.36	168.8	110.8	7.90	0.15	2
711	16.309	−27.924	349.513	15.262	349.51	349.51	15.26	15.26	221.6	211.0	1.18	0.08	1
712	16.375	−21.926	354.780	18.638	355.48	354.78	18.64	17.87	−89.7	−100.0	1.66	0.09	2
713	16.383	56.078	85.467	42.578	143.74	79.22	59.97	35.38	−63.3	−200.5	4445.35	0.99	403
714	16.396	6.072	20.538	34.853	20.54	20.54	34.85	34.85	−364.1	−374.6	1.21	0.08	1
715	16.579	−39.935	342.872	4.641	342.87	342.87	4.64	4.64	110.8	100.2	1.18	0.09	1
716	16.593	−21.935	356.832	16.316	356.83	356.83	16.32	16.32	−110.8	−121.4	1.07	0.07	1
717	16.618	−35.935	346.176	6.964	346.18	346.18	6.96	6.96	−126.7	−142.5	2.38	0.17	1
718	16.633	−37.934	344.791	5.503	344.79	344.79	5.50	5.50	110.8	105.5	1.06	0.10	1
719	16.667	−27.939	352.731	11.708	352.73	352.73	11.71	11.71	−105.5	−116.1	1.63	0.11	1
720	16.687	−35.938	346.731	6.326	346.73	346.73	6.33	6.33	105.5	89.7	2.27	0.16	1
721	16.701	42.063	66.320	40.924	66.32	66.32	40.92	40.92	−89.7	−94.9	1.18	0.12	1
722	16.718	−39.941	343.925	3.439	343.93	343.93	3.44	3.44	131.9	121.3	1.26	0.10	1
723	16.731	−21.941	358.083	14.811	358.08	357.46	15.57	14.81	−79.2	−100.3	2.30	0.10	2
724	16.736	70.063	101.837	36.123	102.16	101.84	36.78	36.12	−116.0	−147.7	4.34	0.08	2
725	16.739	−31.939	350.231	8.416	350.23	349.66	9.09	8.42	−110.8	−121.4	2.36	0.12	2
726	16.788	−39.944	344.440	2.828	344.44	344.44	2.83	2.83	168.8	153.0	2.12	0.12	1
727	16.788	−39.944	344.440	2.828	344.44	344.44	2.83	2.83	242.7	226.9	1.76	0.10	1
728	16.788	−39.944	344.440	2.828	344.44	344.44	2.83	2.83	316.6	306.0	1.18	0.08	1
729	16.800	38.060	61.206	39.484	61.21	58.68	39.48	39.01	−68.6	−84.4	2.14	0.11	2
730	16.804	42.058	66.385	39.770	74.28	61.45	42.08	30.50	−68.5	−163.5	237.44	0.44	46
731	16.804	−33.941	349.198	6.514	349.20	349.20	6.51	6.51	−126.7	−137.2	1.36	0.11	1
732	16.809	−17.943	2.067	16.379	2.07	2.07	16.38	16.38	89.7	84.4	1.19	0.13	1
733	16.809	−17.943	2.067	16.379	2.07	2.07	16.38	16.38	116.1	105.5	1.38	0.11	1
734	16.809	−17.943	2.067	16.379	2.07	2.07	16.38	16.38	−100.3	−105.5	1.94	0.18	1
735	16.809	−17.943	2.067	16.379	2.07	2.07	16.38	16.38	−116.1	−131.9	3.32	0.19	1
736	16.809	−17.943	2.067	16.379	2.07	2.07	16.38	16.38	−142.5	−168.8	3.72	0.15	1
737	16.809	−17.943	2.067	16.379	2.07	2.07	16.38	16.38	−179.4	−211.1	3.82	0.12	1
738	16.809	−17.943	2.067	16.379	2.07	2.07	16.38	16.38	−221.6	−242.7	2.46	0.12	1
739	16.851	72.058	103.910	34.918	103.91	103.91	34.92	34.92	−105.5	−142.4	3.59	0.10	1
740	16.926	−39.950	345.446	1.589	345.45	345.45	1.59	1.59	284.9	274.4	2.18	0.19	1
741	16.944	−27.951	355.059	8.834	355.06	353.04	8.83	7.33	−105.5	−131.9	4.18	0.13	3
742	16.944	−27.951	355.059	8.834	355.06	355.06	8.83	8.83	−163.6	−174.1	1.28	0.09	1
743	16.948	62.052	91.793	37.017	91.79	91.57	37.02	36.06	−89.6	−100.2	2.08	0.13	2
744	17.006	−39.953	346.008	0.870	346.01	345.45	1.59	0.87	179.4	163.5	10.47	0.46	2
745	17.013	−21.952	0.505	11.689	0.51	0.51	11.69	11.69	−84.2	−94.7	1.23	0.08	1
746	17.013	−27.955	355.620	8.100	356.35	355.62	8.10	7.12	−95.0	−105.5	2.35	0.10	2
747	17.022	−9.956	10.782	18.442	10.78	10.18	19.30	18.44	−295.5	−306.0	2.27	0.11	2
748	17.023	−13.954	7.317	16.196	7.32	7.32	16.20	16.20	−121.4	−137.2	2.32	0.13	1
749	17.023	−13.954	7.317	16.196	7.32	7.32	16.20	16.20	−163.6	−189.9	3.52	0.15	1
750	17.023	−13.954	7.317	16.196	7.32	7.32	16.20	16.20	−226.9	−248.0	1.92	0.09	1
751	17.023	−13.954	7.317	16.196	7.32	7.32	16.20	16.20	−290.2	−306.0	2.02	0.12	1
752	17.023	−13.954	7.317	16.196	7.42	7.32	16.20	16.05	−84.4	−126.6	8.30	0.16	3

TABLE 2—*Continued*

No.	Peak α_{1950}	δ_{1950}	Peak l	b	l max	l min	b max	b min	v max	v min	F_{tot}	T_{peak}	# pts
753	17.028	70.050	101.263	34.703	101.26	99.03	35.59	34.70	−126.6	−137.1	1.87	0.09	2
754	17.049	−37.953	347.905	1.686	347.90	347.90	1.69	1.69	364.1	348.2	1.57	0.08	1
755	17.075	−39.956	346.489	0.237	346.49	344.95	3.62	0.24	174.1	116.1	34.20	0.61	8
756	17.075	−39.956	346.489	0.237	346.49	345.45	1.59	0.24	343.0	284.9	17.79	0.24	3
757	17.075	−39.956	346.489	0.237	346.49	346.49	0.24	0.24	274.4	248.0	10.03	0.44	1
758	17.075	−39.956	346.489	0.237	347.43	345.45	1.59	−1.05	216.3	179.4	44.80	0.53	5
759	17.076	58.048	86.666	36.669	86.67	86.67	36.67	36.67	−147.7	−158.2	1.16	0.08	1
760	17.086	62.045	91.574	36.063	91.57	91.40	36.06	35.10	−105.5	−131.9	3.26	0.10	2
761	17.091	−33.954	351.404	3.694	351.40	351.40	3.69	3.69	110.8	100.2	1.11	0.08	1
762	17.104	−13.957	8.006	15.215	8.01	8.01	15.21	15.21	137.2	89.7	7.18	0.23	1
763	17.104	−13.957	8.006	15.215	8.01	8.01	15.21	15.21	163.6	158.3	1.11	0.13	1
764	17.104	−13.957	8.006	15.215	8.01	8.01	15.21	15.21	−121.4	−147.7	11.20	0.40	1
765	17.104	−13.957	8.006	15.215	8.01	8.01	15.21	15.21	−158.3	−168.8	4.07	0.27	1
766	17.104	−13.957	8.006	15.215	8.01	8.01	15.21	15.21	−179.4	−200.5	6.95	0.32	1
767	17.104	−13.957	8.006	15.215	8.01	8.01	15.21	15.21	−211.1	−248.0	8.07	0.27	1
768	17.104	−13.957	8.006	15.215	8.01	8.01	15.21	15.21	−269.1	−290.2	3.85	0.22	1
769	17.104	−13.957	8.006	15.215	8.49	8.01	15.21	14.52	−290.2	−311.3	3.36	0.19	2
770	17.113	−35.957	349.958	2.279	349.96	349.96	2.28	2.28	147.7	126.6	3.88	0.20	1
771	17.113	−35.957	349.958	2.279	349.96	349.96	2.28	2.28	189.9	174.1	2.28	0.13	1
772	17.113	−35.957	349.958	2.279	349.96	349.96	2.28	2.28	216.3	200.5	1.83	0.13	1
773	17.113	−35.957	349.958	2.279	349.96	349.96	2.28	2.28	248.0	232.2	1.96	0.14	1
774	17.129	−37.956	348.465	0.936	348.46	348.46	0.94	0.94	121.3	110.8	1.55	0.12	1
775	17.131	−25.958	358.189	8.015	358.19	358.19	8.02	8.02	−253.3	−263.8	1.24	0.09	1
776	17.144	−39.960	346.965	−0.404	346.96	346.96	−0.40	−0.40	337.7	311.3	5.72	0.26	1
777	17.144	−39.960	346.965	−0.404	347.43	346.96	−0.40	−1.05	179.4	163.6	7.55	0.43	2
778	17.153	50.040	76.667	36.393	76.71	74.16	38.51	36.39	−52.7	−131.9	39.53	0.36	4
779	17.161	−21.958	1.726	10.005	1.73	1.73	10.01	10.01	−100.0	−110.6	1.92	0.14	1
780	17.162	−27.961	356.796	6.506	356.80	356.80	6.51	6.51	−137.2	−158.3	4.43	0.22	1
781	17.179	−29.962	355.293	5.160	355.29	355.26	5.20	5.16	116.1	95.0	3.44	0.14	2
782	17.185	54.039	81.620	36.054	81.62	81.62	36.05	36.05	−110.8	−158.2	6.41	0.17	1
783	17.198	−37.959	348.948	0.273	348.95	345.45	1.59	−1.05	300.7	195.2	76.28	0.66	9
784	17.198	−37.959	348.948	0.273	349.42	346.49	0.27	−1.05	226.9	131.9	102.77	0.84	5
785	17.198	−37.959	348.948	0.273	351.97	347.43	0.27	−1.07	348.2	253.3	49.01	0.54	11
786	17.201	−25.961	358.736	7.252	358.74	358.74	7.25	7.25	100.3	89.7	1.39	0.11	1
787	17.214	−39.963	347.433	−1.050	347.43	347.43	−1.05	−1.05	126.6	110.8	4.85	0.29	1
788	17.221	30.041	52.672	32.827	52.67	52.67	32.83	32.83	−437.9	−443.2	1.06	0.12	1
789	17.227	38.041	62.077	34.494	62.08	62.08	34.49	34.49	−147.7	−158.2	1.18	0.08	1
790	17.230	−9.965	12.521	15.857	13.08	12.52	15.86	14.99	−300.8	−306.0	2.03	0.11	2
791	17.243	−13.963	9.153	13.531	9.15	9.15	13.53	13.53	142.5	131.9	1.20	0.08	1
792	17.248	−29.965	355.817	4.424	355.82	355.82	4.42	4.42	−142.5	−158.3	1.42	0.07	1
793	17.254	−7.963	14.484	16.620	14.48	14.48	16.62	16.62	−348.2	−358.8	1.30	0.12	1
794	17.254	−7.963	14.484	16.620	14.48	14.48	16.62	16.62	−369.3	−379.9	1.24	0.08	1
795	17.267	−37.963	349.422	−0.393	349.42	349.42	−0.39	−0.39	316.6	295.5	2.63	0.14	1
796	17.267	−37.963	349.422	−0.393	349.42	349.42	−0.39	−0.39	332.4	327.1	1.33	0.13	1
797	17.300	82.038	114.499	30.219	114.50	114.20	30.22	29.36	−84.4	−105.5	15.99	0.31	4
798	17.305	−17.966	6.236	10.586	6.24	6.24	10.59	10.59	200.5	190.0	1.33	0.10	1
799	17.316	52.033	79.145	34.888	79.15	79.15	34.89	34.89	−116.0	−163.5	5.44	0.19	1
800	17.321	−35.966	351.427	0.225	351.43	349.89	0.23	−1.07	316.6	311.3	3.06	0.16	2
801	17.321	−35.966	351.427	0.225	351.43	351.43	0.23	0.23	284.9	284.9	1.14	0.22	1
802	17.321	−35.966	351.427	0.225	351.43	351.43	0.23	0.23	300.7	295.5	2.07	0.20	1
803	17.321	−35.966	351.427	0.225	351.43	351.43	0.23	0.23	343.0	332.4	1.07	0.08	1
804	17.321	−35.966	351.427	0.225	351.97	351.43	0.23	−0.57	242.7	179.4	25.24	0.41	2
805	17.323	−13.967	9.798	12.556	9.80	9.80	12.56	12.56	−89.7	−95.0	1.45	0.19	1
806	17.330	−23.966	1.396	6.945	1.40	1.40	6.94	6.94	−100.3	−121.4	3.60	0.15	1
807	17.337	−37.966	349.891	−1.067	349.89	348.35	−1.07	−2.36	248.0	226.9	5.10	0.29	2
808	17.337	−37.966	349.891	−1.067	349.89	349.42	−0.39	−1.07	211.0	163.6	18.94	0.31	2
809	17.337	−37.966	349.891	−1.067	349.89	349.42	−0.39	−1.07	242.7	221.6	8.79	0.29	2
810	17.339	−25.967	359.804	5.714	359.80	359.80	5.71	5.71	−116.1	−126.6	1.38	0.11	1
811	17.343	56.035	84.017	34.637	84.02	84.02	34.64	34.64	−105.5	−153.0	5.05	0.15	1
812	17.348	−11.968	11.730	13.321	11.73	11.73	13.32	13.32	−84.2	−105.3	2.42	0.13	1
813	17.365	38.034	62.425	32.881	62.42	62.42	32.88	32.88	−68.5	−94.9	3.09	0.11	1
814	17.370	−13.969	10.176	11.976	10.18	10.18	11.98	11.98	−163.6	−179.4	1.71	0.09	1
815	17.370	−13.969	10.176	11.976	10.35	10.18	11.98	11.70	−126.6	−142.5	1.81	0.12	2
816	17.388	68.034	98.399	33.241	101.26	98.40	34.70	33.24	−100.2	−142.4	12.93	0.14	6
817	17.392	−13.970	10.352	11.702	10.35	10.35	11.70	11.70	−84.4	−95.0	2.31	0.19	1
818	17.399	−23.969	1.928	6.153	4.43	1.93	7.61	5.99	121.6	105.8	3.72	0.10	4
819	17.400	58.034	86.420	34.106	86.42	86.42	34.11	34.11	−105.5	−121.3	1.83	0.10	1
820	17.400	−35.970	351.970	−0.571	351.97	349.42	0.23	−1.07	179.4	142.5	32.48	0.46	4
821	17.400	−35.970	351.970	−0.571	351.97	351.97	−0.57	−0.57	147.7	121.4	14.78	0.56	1
822	17.400	−35.970	351.970	−0.571	351.97	351.97	−0.57	−0.57	205.8	205.8	1.65	0.31	1
823	17.400	−35.970	351.970	−0.571	351.97	351.97	−0.57	−0.57	226.9	216.3	4.42	0.33	1
824	17.400	−35.970	351.970	−0.571	351.97	351.97	−0.57	−0.57	242.7	237.4	2.36	0.26	1
825	17.415	26.029	49.048	29.215	49.05	49.05	29.21	29.21	−89.7	−105.5	1.40	0.07	1
826	17.422	−39.972	348.792	−3.018	348.79	347.89	−1.70	−3.02	116.1	100.2	3.87	0.12	3
827	17.422	−39.972	348.792	−3.018	348.79	348.79	−3.02	−3.02	137.2	116.1	2.20	0.13	1
828	17.427	−11.972	12.362	12.331	12.36	12.36	12.33	12.33	−94.7	−110.6	2.47	0.19	1
829	17.430	24.028	46.961	28.378	47.32	46.96	28.38	27.48	−142.4	−158.3	1.82	0.10	2
830	17.439	−13.972	10.723	11.123	10.72	10.72	11.12	11.12	116.1	95.0	2.46	0.13	1
831	17.440	30.031	53.555	30.096	53.56	53.56	30.10	30.10	−84.4	−94.9	1.63	0.12	1
832	17.442	−19.974	5.619	7.854	5.62	5.08	8.67	7.85	−306.0	−316.6	2.02	0.10	2
833	17.453	−31.971	355.652	1.122	355.65	355.65	1.12	1.12	221.6	189.9	61.69	1.86	1
834	17.453	−31.971	355.652	1.122	355.65	355.65	1.12	1.12	311.3	232.2	77.35	1.43	1
835	17.453	−31.971	355.652	1.122	355.65	355.65	1.12	1.12	332.4	321.9	3.60	0.29	1
836	17.457	56.030	83.997	33.680	84.00	84.00	33.68	33.68	−100.2	−163.5	6.11	0.13	1
837	17.462	−13.974	10.899	10.845	10.90	10.90	10.85	10.85	−121.4	−126.6	2.21	0.25	1
838	17.462	−13.974	10.899	10.845	10.90	10.90	10.85	10.85	−147.7	−158.3	3.05	0.22	1
839	17.462	−13.974	10.899	10.845	10.90	10.90	10.85	10.85	−168.8	−200.5	5.19	0.21	1
840	17.462	−13.974	10.899	10.845	10.90	10.90	10.85	10.85	−211.1	−232.2	2.67	0.17	1
841	17.462	−13.974	10.899	10.845	10.90	10.90	10.85	10.85	−242.7	−269.1	3.07	0.13	1
842	17.462	−13.974	10.899	10.845	10.90	10.90	10.85	10.85	−290.2	−316.6	3.39	0.17	1
843	17.466	−29.975	357.411	2.081	357.41	357.41	2.08	2.08	168.8	163.6	1.42	0.16	1
844	17.476	2.025	25.307	18.744	25.31	25.31	18.74	18.74	−390.4	−406.3	2.09	0.13	1
845	17.483	60.025	88.784	33.397	91.57	86.39	37.35	31.75	−116.0	−205.7	112.88	0.33	15
846	17.501	0.023	23.647	17.455	23.65	23.65	17.45	17.45	−116.1	−126.6	1.53	0.13	1

TABLE 2—*Continued*

No.	Peak α_{1950}	δ_{1950}	Peak l	b	l max	l min	b max	b min	v max	v min	F_{tot}	T_{peak}	# pts
847	17.501	−39.976	349.293	−3.781	349.29	348.79	−3.02	−3.78	279.6	269.1	1.63	0.09	2
848	17.501	−39.976	349.293	−3.781	349.29	349.29	−3.78	−3.78	327.1	316.6	1.45	0.11	1
849	17.508	28.026	51.656	28.652	51.66	51.66	28.65	28.65	−89.7	−116.0	3.52	0.13	1
850	17.508	−21.974	4.434	5.989	4.43	3.37	7.61	5.99	−94.7	−126.4	7.17	0.15	4
851	17.514	38.028	62.831	31.159	62.83	62.83	31.16	31.16	−110.8	−131.9	2.75	0.13	1
852	17.516	62.026	91.160	33.062	91.16	91.16	33.06	33.06	−94.9	−100.2	1.09	0.14	1
853	17.522	−31.974	356.136	0.382	356.14	356.14	0.38	0.38	205.8	205.8	3.69	0.70	1
854	17.522	−31.974	356.136	0.382	356.14	356.14	0.38	0.38	263.8	216.3	29.02	0.69	1
855	17.522	−31.974	356.136	0.382	356.14	356.14	0.38	0.38	295.5	274.4	9.81	0.48	1
856	17.522	−31.974	356.136	0.382	356.14	356.14	0.38	0.38	332.4	306.0	5.07	0.24	1
857	17.522	−31.974	356.136	0.382	356.61	356.14	0.38	−0.36	−290.2	−295.5	2.42	0.22	2
858	17.524	−3.976	20.186	15.202	20.19	20.19	15.20	15.20	−89.7	−95.0	2.03	0.19	1
859	17.524	−3.976	20.186	15.202	20.19	20.19	15.20	15.20	110.8	95.0	2.38	0.12	1
860	17.524	−3.976	20.186	15.202	20.19	20.19	15.20	15.20	−105.5	−116.1	1.92	0.17	1
861	17.525	68.028	98.266	32.475	100.64	98.27	32.48	32.35	−100.2	−137.1	5.72	0.14	2
862	17.532	−27.978	359.555	2.456	359.56	359.56	2.46	2.46	200.5	184.7	2.56	0.16	1
863	17.538	−23.976	2.967	4.560	2.97	2.97	4.56	4.56	−253.3	−263.8	1.24	0.09	1
864	17.539	−35.976	352.895	−1.976	352.90	352.90	−1.98	−1.98	105.5	84.4	3.20	0.17	1
865	17.555	10.023	33.461	21.330	33.46	33.46	21.33	21.33	−105.5	−116.1	1.34	0.09	1
866	17.555	42.024	67.529	31.464	67.53	67.53	31.46	31.46	−464.3	−469.6	1.18	0.16	1
867	17.569	24.021	47.675	26.584	47.67	47.67	26.58	26.58	−105.5	−116.0	1.07	0.07	1
868	17.570	−39.979	349.722	−4.451	349.72	349.72	−4.45	−4.45	95.0	84.4	1.08	0.07	1
869	17.578	30.025	54.138	28.369	54.14	54.14	28.37	28.37	−406.2	−432.6	2.48	0.09	1
870	17.582	34.024	58.547	29.419	58.55	58.55	29.42	29.42	−168.8	−179.4	1.24	0.08	1
871	17.583	38.024	63.032	30.357	63.03	63.03	30.36	30.36	−189.9	−205.7	2.03	0.14	1
872	17.587	−9.981	15.346	11.360	25.82	11.44	17.82	9.99	−58.0	−137.2	186.91	0.56	19
873	17.587	−33.977	354.894	−1.385	354.89	354.89	−1.39	−1.39	126.6	84.4	25.43	0.89	1
874	17.588	−13.979	11.879	9.274	11.88	11.88	9.27	9.27	−353.5	−364.1	1.68	0.12	1
875	17.602	−29.981	358.370	0.595	359.96	1.40	6.94	−5.31	205.8	68.6	1792.14	5.94	27
876	17.608	−35.980	353.348	−2.688	353.35	353.35	−2.69	−2.69	163.6	153.0	1.29	0.11	1
877	17.623	66.020	95.836	32.098	95.84	95.84	32.10	32.10	−89.6	−105.5	1.56	0.08	1
878	17.627	52.018	79.299	32.019	79.30	79.30	32.02	32.02	−147.7	−163.5	2.40	0.14	1
879	17.640	−39.982	350.146	−5.128	350.15	350.15	−5.13	−5.13	−179.4	−190.0	1.35	0.10	1
880	17.653	38.021	63.241	29.556	63.24	63.24	29.56	29.56	−100.2	−126.6	3.99	0.17	1
881	17.656	−33.980	355.353	−2.117	356.25	355.35	−2.12	−3.59	147.7	121.4	4.50	0.17	4
882	17.658	−27.984	0.447	1.047	0.45	0.45	1.05	1.05	−174.1	−190.0	14.92	0.79	1
883	17.658	−27.984	0.447	1.047	0.45	0.45	1.05	1.05	−200.5	−237.4	15.56	0.63	1
884	17.661	−17.982	8.989	6.283	8.99	8.99	6.28	6.28	131.9	116.1	2.06	0.12	1
885	17.661	−31.981	357.080	−1.107	357.08	357.08	−1.11	−1.11	174.1	163.6	1.83	0.13	1
886	17.664	56.021	84.033	31.940	84.09	84.00	32.81	31.07	−126.6	−179.3	8.11	0.13	3
887	17.670	−7.983	17.744	11.304	17.74	17.74	11.30	11.30	−79.1	−131.9	16.90	0.36	1
888	17.679	68.021	98.155	31.619	98.16	98.16	31.62	31.62	−110.8	−131.9	2.27	0.09	1
889	17.683	−29.985	358.922	−0.289	358.92	358.92	−0.29	−0.29	232.2	221.6	1.10	0.07	1
890	17.684	2.015	26.839	15.989	26.84	26.84	15.99	15.99	110.8	105.6	1.09	0.12	1
891	17.684	50.016	77.020	31.285	81.58	74.64	34.23	30.29	−52.7	−163.5	114.71	0.35	9
892	17.693	10.017	34.402	19.478	34.40	34.40	19.48	19.48	−110.8	−131.9	1.93	0.08	1
893	17.697	−25.984	2.419	1.666	4.05	2.42	2.83	1.67	−116.1	−131.9	2.94	0.16	2
894	17.709	0.013	25.194	14.710	25.19	25.19	14.71	14.71	−116.1	−121.3	1.29	0.13	1
895	17.709	−39.985	350.562	−5.810	350.56	350.56	−5.81	−5.81	290.2	279.6	1.50	0.13	1
896	17.709	−39.985	350.562	−5.810	350.56	350.56	−5.81	−5.81	−237.5	−242.7	1.16	0.12	1
897	17.716	54.015	81.713	31.377	81.71	81.71	31.38	31.38	−110.8	−121.3	1.33	0.10	1
898	17.727	−13.986	12.926	7.543	14.50	12.93	8.84	7.54	−84.4	−105.5	5.31	0.19	2
899	17.727	−27.987	0.929	0.264	0.93	0.93	0.26	0.26	−158.3	−205.8	15.21	0.49	1
900	17.731	16.013	40.464	21.482	40.46	40.46	21.48	21.48	−84.4	−94.9	1.82	0.14	1
901	17.732	−3.986	21.756	12.487	21.76	21.76	12.49	12.49	−131.9	−142.4	1.29	0.09	1
902	17.747	−35.986	354.229	−4.121	354.23	354.23	−4.12	−4.12	−174.1	−184.7	1.70	0.14	1
903	17.756	−29.988	359.417	−1.099	359.42	359.42	−1.10	−1.10	110.8	110.8	12.69	2.40	1
904	17.756	−29.988	359.417	−1.099	359.42	359.42	−1.10	−1.10	184.7	121.4	87.01	2.41	1
905	17.756	−29.988	359.417	−1.099	359.42	359.42	−1.10	−1.10	200.5	195.2	1.85	0.24	1
906	17.756	−29.988	359.417	−1.099	359.42	359.42	−1.10	−1.10	−321.9	−327.1	1.15	0.13	1
907	17.763	10.014	34.868	18.556	34.87	34.87	18.56	18.56	−89.7	−121.3	2.98	0.09	1
908	17.775	20.013	44.701	22.463	44.70	44.70	22.46	22.46	−116.0	−142.4	2.95	0.14	1
909	17.778	−39.989	350.970	−6.493	350.97	350.56	−5.81	−6.49	−153.0	−158.3	1.76	0.10	2
910	17.778	−39.989	350.970	−6.493	352.61	350.97	−5.31	−6.49	−126.6	−142.5	2.20	0.09	2
911	17.796	−13.989	13.442	6.671	13.44	13.02	7.39	6.67	−95.0	−116.1	5.03	0.20	2
912	17.797	−27.991	1.405	−0.523	1.40	1.40	−0.52	−0.52	−184.7	−195.2	1.96	0.18	1
913	17.797	−27.991	1.405	−0.523	3.39	1.40	0.05	−1.31	−168.8	−195.2	8.27	0.26	3
914	17.800	−17.989	10.013	4.584	10.01	10.01	4.58	4.58	174.1	163.6	1.07	0.07	1
915	17.801	−3.989	22.268	11.581	22.27	22.27	11.58	11.58	116.1	110.8	1.06	0.14	1
916	17.803	4.010	29.531	15.338	29.53	29.53	15.34	15.34	110.8	110.8	1.28	0.24	1
917	17.804	80.014	111.906	29.575	111.91	111.83	29.58	29.18	−126.6	−147.7	2.98	0.10	2
918	17.817	−35.989	354.661	−4.846	355.15	354.66	−4.85	−5.68	−121.4	−168.9	10.71	0.22	2
919	17.819	−13.990	13.607	6.388	13.61	13.44	6.67	6.39	−358.8	−374.6	2.76	0.13	2
920	17.832	10.010	35.333	17.630	43.82	27.42	22.40	14.38	−79.1	−147.7	80.16	0.21	26
921	17.836	−25.990	3.392	0.053	3.39	3.39	0.05	0.05	−142.5	−147.7	2.01	0.24	1
922	17.836	−25.990	3.392	0.053	3.39	3.39	0.05	0.05	−158.3	−163.6	1.51	0.16	1
923	17.847	52.008	79.531	29.994	79.53	79.53	29.99	29.99	−131.9	−168.8	3.67	0.13	1
924	17.866	−13.992	13.952	5.797	13.95	13.95	5.80	5.80	−110.8	−116.1	1.20	0.15	1
925	17.869	−31.990	358.447	−3.378	358.45	358.45	−3.38	−3.38	126.6	110.8	2.47	0.18	1
926	17.872	56.011	84.159	30.203	84.16	84.16	30.20	30.20	−105.5	−116.0	1.23	0.10	1
927	17.896	−35.993	355.147	−5.683	355.15	355.15	−5.68	−5.68	147.7	100.2	5.81	0.16	1
928	17.896	−35.993	355.147	−5.683	355.15	355.15	−5.68	−5.68	−110.8	−116.1	1.31	0.13	1
929	17.902	2.005	28.408	13.089	28.41	28.41	13.09	13.09	137.2	121.4	1.89	0.14	1
930	17.904	−29.995	0.401	−2.761	0.85	0.40	−2.76	−3.55	−142.5	−200.5	32.24	0.57	2
931	17.906	−25.993	3.867	−0.758	3.87	3.87	−0.76	−0.76	−195.2	−242.7	26.92	0.67	1
932	17.906	−25.993	3.867	−0.758	4.80	0.40	1.67	−2.76	−248.0	−274.4	26.99	0.49	11
933	17.906	−25.993	3.867	−0.758	5.52	3.87	0.38	−0.76	−279.6	−295.5	3.85	0.20	2
934	17.915	66.006	95.741	30.323	95.74	95.74	30.32	30.32	−116.0	−126.6	1.16	0.08	1
935	17.925	−15.994	12.647	4.048	12.65	11.08	4.05	1.89	−364.1	−379.9	3.54	0.12	3
936	17.927	0.003	26.776	11.820	26.78	26.78	11.82	11.82	−84.4	−100.2	1.67	0.10	1
937	17.928	70.008	100.371	30.165	100.37	100.37	30.16	30.16	−100.2	−110.8	1.34	0.09	1
938	17.935	−21.994	7.521	0.917	7.52	7.52	0.92	0.92	−258.3	−290.0	3.51	0.15	1
939	17.938	−19.997	9.269	1.885	9.27	9.27	1.88	1.88	−316.6	−327.1	1.45	0.11	1
940	17.940	−3.996	23.283	9.758	23.28	23.28	9.76	9.76	−95.0	−110.8	1.78	0.12	1

TABLE 2—*Continued*

No.	Peak α_{1950}	δ_{1950}	Peak l	b	l max	l min	b max	b min	v max	v min	F_{tot}	T_{peak}	# pts
941	17.948	−31.994	358.951	−4.250	358.95	358.95	−4.25	−4.25	147.7	131.9	2.36	0.17	1
942	17.948	−31.994	358.951	−4.250	358.95	358.95	−4.25	−4.25	179.4	158.3	2.18	0.10	1
943	17.948	−31.994	358.951	−4.250	358.95	358.95	−4.25	−4.25	−158.3	−179.4	2.57	0.15	1
944	17.948	−31.994	358.951	−4.250	358.95	358.95	−4.25	−4.25	−253.3	−258.5	1.20	0.15	1
945	17.948	−31.994	358.951	−4.250	359.81	357.12	−4.25	−5.83	−89.7	−158.3	31.15	0.36	6
946	17.949	−17.996	11.083	2.748	11.08	11.08	2.75	2.75	−95.0	−100.2	1.73	0.20	1
947	17.961	48.007	75.198	28.294	75.20	75.20	28.29	28.29	−131.9	−137.1	1.13	0.13	1
948	17.976	−25.997	4.337	−1.573	4.34	4.34	−1.57	−1.57	−168.8	−179.4	1.88	0.15	1
949	17.983	36.005	62.196	25.212	62.20	62.20	25.21	25.21	−100.2	−110.8	1.17	0.08	1
950	17.984	12.003	38.223	16.468	38.22	38.22	16.47	16.47	−121.3	−137.2	2.60	0.14	1
951	17.987	−21.998	7.879	0.289	12.54	6.93	1.02	−2.09	−110.8	−137.2	11.08	0.19	9
952	17.988	56.006	84.266	29.232	84.27	84.16	30.20	29.23	−116.0	−147.7	5.13	0.13	2
953	17.995	24.002	49.915	21.116	50.29	49.92	21.12	20.23	−73.8	−131.9	21.40	0.34	2
954	17.995	24.002	49.915	21.116	53.99	47.64	24.16	21.03	−116.0	−158.2	24.85	0.19	9
955	17.995	50.001	77.495	28.315	77.50	77.50	28.31	28.31	−105.5	−126.6	1.97	0.09	1
956	18.003	−33.996	357.542	−5.834	357.54	357.54	−5.83	−5.83	−137.2	−153.0	2.26	0.14	1
957	18.005	−28.000	2.790	−2.906	359.39	0.40	−2.76	−5.02	−63.3	−174.1	256.92	1.33	6
958	18.027	54.000	82.042	28.649	82.04	82.04	28.65	28.65	−110.8	−142.4	3.39	0.12	1
959	18.034	−23.998	6.462	−1.263	6.46	5.52	0.38	−1.26	−290.2	−311.3	3.32	0.10	3
960	18.035	−35.999	355.973	−7.152	355.97	353.84	−7.15	−8.17	−279.7	−300.8	5.37	0.18	3
961	18.035	−35.999	355.973	−7.152	355.97	355.97	−7.15	−7.15	121.4	110.8	1.42	0.12	1
962	18.035	−35.999	355.973	−7.152	355.97	355.97	−7.15	−7.15	258.5	253.3	1.10	0.11	1
963	18.038	−12.000	16.946	4.590	17.51	16.95	4.59	3.57	−105.3	−126.4	4.54	0.11	3
964	18.054	51.999	79.836	28.099	79.84	79.84	28.10	28.10	−153.0	−163.5	1.14	0.08	1
965	18.064	−16.000	13.633	2.309	13.63	13.63	2.31	2.31	−95.0	−110.8	2.75	0.20	1
966	18.065	23.998	50.289	20.231	50.29	50.29	20.23	20.23	−142.4	−158.2	2.68	0.21	1
967	18.066	−40.002	352.592	−9.380	353.33	352.59	−9.38	−10.80	126.6	84.4	9.12	0.25	2
968	18.076	−20.003	10.231	0.189	10.23	10.23	0.19	0.19	−290.2	−300.8	1.70	0.13	1
969	18.076	−20.003	10.231	0.189	10.23	10.23	0.19	0.19	−311.3	−337.7	3.93	0.18	1
970	18.080	3.997	31.474	11.640	31.47	30.99	12.56	11.64	126.7	116.1	1.83	0.11	2
971	18.084	−28.004	3.304	−3.824	3.30	3.30	−3.82	−3.82	237.4	195.2	5.43	0.16	1
972	18.087	36.000	62.595	24.012	65.19	59.87	32.07	20.24	−94.9	−200.5	184.24	0.59	25
973	18.087	−32.000	359.814	−5.794	359.81	1.73	−5.13	−5.79	147.7	126.6	3.89	0.14	2
974	18.087	−32.000	359.814	−5.794	359.81	359.39	−5.02	−5.79	168.8	137.2	4.24	0.12	2
975	18.087	−32.000	359.814	−5.794	359.81	359.39	−5.02	−5.79	195.2	174.1	3.08	0.11	2
976	18.087	−32.000	359.814	−5.794	359.81	359.81	−5.79	−5.79	116.1	100.3	3.10	0.21	1
977	18.104	39.999	66.869	24.964	69.27	63.68	27.96	24.09	−84.4	−142.4	27.92	0.16	9
978	18.104	−36.003	356.376	−7.894	356.38	356.38	−7.89	−7.89	105.5	95.0	1.61	0.13	1
979	18.104	−36.003	356.376	−7.894	356.77	356.38	−7.89	−8.64	−279.7	−300.8	6.55	0.20	2
980	18.112	49.996	77.720	27.210	77.72	77.72	27.21	27.21	−137.1	−142.4	1.11	0.14	1
981	18.120	−38.002	354.681	−8.998	354.68	354.68	−9.00	−9.00	95.0	89.7	1.06	0.13	1
982	18.139	57.999	86.692	28.249	86.69	86.69	28.25	28.25	−73.8	−100.2	5.90	0.27	1
983	18.143	29.998	56.684	21.404	56.68	56.68	21.40	21.40	−63.3	−126.6	8.73	0.16	1
984	18.145	81.999	114.028	28.511	114.03	113.99	28.51	28.19	−105.5	−121.3	2.30	0.08	2
985	18.152	21.995	48.813	18.354	48.81	46.77	18.35	17.82	−121.3	−131.9	2.63	0.11	2
986	18.157	−18.005	12.537	0.160	16.01	11.25	3.91	−2.51	−358.8	−379.9	16.25	0.20	9
987	18.158	51.994	80.018	27.156	80.02	80.02	27.16	27.16	−100.2	−153.0	6.16	0.15	1
988	18.188	−12.007	18.004	2.672	18.00	18.00	2.67	2.67	−121.1	−136.9	1.60	0.09	1
989	18.188	−12.007	18.004	2.672	18.10	18.00	2.67	2.50	−274.1	−300.5	3.44	0.13	2
990	18.219	69.995	100.347	28.671	100.35	100.35	28.67	28.67	−94.9	−116.0	2.22	0.10	1
991	18.219	69.995	100.347	28.671	100.35	100.35	28.67	28.67	−306.0	−316.5	4.53	0.43	1
992	18.220	61.993	91.272	28.108	93.58	91.18	29.07	27.85	−105.5	−126.6	4.76	0.11	3
993	18.222	27.993	55.072	19.727	55.07	48.81	21.57	18.34	−73.8	−147.7	48.39	0.31	8
994	18.247	53.990	82.385	26.734	82.38	82.38	26.73	26.73	−137.1	−147.7	1.47	0.13	1
995	18.257	−12.010	18.487	1.780	18.49	18.49	1.78	1.78	−136.9	−152.8	1.56	0.09	1
996	18.257	−12.010	18.487	1.780	18.58	18.49	1.78	1.61	−115.8	−126.4	2.75	0.17	2
997	18.270	−12.010	18.580	1.608	18.58	18.58	1.61	1.61	−131.7	−136.9	1.17	0.15	1
998	18.274	51.988	80.246	26.101	80.25	80.25	26.10	26.10	−73.8	−131.9	12.64	0.27	1
999	18.274	−40.012	353.692	−11.512	353.69	353.33	−10.80	−11.51	131.9	121.4	2.15	0.12	2
1000	18.279	−28.013	4.533	−6.098	4.53	4.53	−6.10	−6.10	131.9	116.1	2.43	0.19	1
1001	18.286	33.992	61.374	21.055	61.37	61.07	21.87	21.06	−94.9	−116.0	4.32	0.15	2
1002	18.292	−28.014	4.614	−6.251	4.61	4.61	−6.25	−6.25	−89.7	−121.4	4.50	0.21	1
1003	18.295	−20.013	11.708	−2.511	11.71	11.71	−2.51	−2.51	−95.0	−110.8	2.40	0.16	1
1004	18.312	−36.012	357.545	−10.139	357.55	357.55	−10.14	−10.14	−284.9	−290.2	1.11	0.11	1
1005	18.321	−24.012	8.351	−4.726	10.26	7.90	−3.21	−5.57	−195.2	−226.9	15.70	0.22	5
1006	18.326	−12.013	18.969	0.882	18.97	18.58	1.61	0.88	−290.0	−300.5	2.02	0.08	2
1007	18.343	−40.015	354.046	−12.231	354.05	353.69	−11.51	−12.23	158.3	142.5	3.06	0.13	2
1008	18.343	−40.015	354.046	−12.231	354.39	353.33	−10.80	−12.95	131.9	89.7	12.93	0.19	4
1009	18.361	−14.015	17.447	−0.515	17.45	17.45	−0.51	−0.51	−142.5	−158.3	1.72	0.10	1
1010	18.365	−18.015	13.946	−2.453	13.95	13.95	−2.45	−2.45	−110.8	−121.3	1.25	0.09	1
1011	18.366	−4.015	26.308	4.132	26.31	26.31	4.13	4.13	−116.1	−126.6	1.08	0.07	1
1012	18.384	67.988	98.137	27.665	98.14	98.14	27.67	27.67	−89.6	−126.6	5.03	0.15	1
1013	18.398	1.982	31.869	6.488	33.93	31.87	6.88	5.56	−126.6	−137.2	3.05	0.10	3
1014	18.401	−30.018	3.478	−8.439	3.89	3.48	−8.44	−9.26	126.6	105.5	3.49	0.12	2
1015	18.402	55.986	84.854	25.799	84.85	84.85	25.80	25.80	−158.2	−168.8	1.19	0.09	1
1016	18.421	−16.016	16.085	−2.216	16.09	14.47	−2.22	−3.46	−84.4	−100.2	2.23	0.18	2
1017	18.421	−16.016	16.085	−2.216	17.01	14.47	−1.33	−3.99	−364.1	−374.6	5.30	0.12	5
1018	18.431	−28.020	5.458	−7.885	5.46	5.46	−7.88	−7.88	−116.1	−131.9	1.84	0.12	1
1019	18.444	−32.017	1.917	−9.824	1.92	1.92	−9.82	−9.82	142.5	137.2	1.10	0.12	1
1020	18.450	75.985	107.179	27.847	107.18	107.18	27.85	27.85	−100.2	−110.8	1.84	0.13	1
1021	18.463	−6.019	25.215	1.910	25.21	25.21	1.91	1.91	−100.2	−116.1	1.97	0.14	1
1022	18.475	−26.020	7.524	−7.501	7.52	7.52	−7.50	−7.50	153.0	126.6	2.62	0.10	1
1023	18.489	−12.020	20.081	−1.222	20.08	20.08	−1.22	−1.22	−147.5	−152.8	1.66	0.21	1
1024	18.489	−12.020	20.081	−1.222	20.08	20.08	−1.22	−1.22	−379.7	−390.2	1.27	0.09	1
1025	18.492	−40.022	354.781	−13.781	354.78	354.78	−13.78	−13.78	−284.9	−290.2	1.23	0.15	1
1026	18.503	−20.023	13.071	−5.109	13.07	13.07	−5.11	−5.11	−353.5	−369.3	2.04	0.15	1
1027	18.524	−2.022	29.180	2.962	29.18	29.18	2.96	2.96	−116.1	−126.6	1.45	0.13	1
1028	18.535	−12.023	20.394	−1.822	20.39	20.39	−1.82	−1.82	−105.3	−115.8	1.60	0.13	1
1029	18.552	−22.025	11.595	−6.634	11.60	11.60	−6.63	−6.63	205.8	190.0	1.87	0.12	1
1030	18.561	−40.025	355.114	−14.511	355.11	355.11	−14.51	−14.51	100.2	89.7	1.49	0.11	1
1031	18.580	−28.027	6.340	−9.653	6.34	6.34	−9.65	−9.65	269.1	258.6	1.12	0.08	1
1032	18.593	−8.025	24.333	−0.727	26.24	24.33	−0.06	−0.73	−401.0	−416.8	3.09	0.15	2
1033	18.599	−24.024	10.089	−8.114	10.09	10.09	−8.11	−8.11	131.9	121.4	1.77	0.17	1
1034	18.611	−30.028	4.689	−10.892	4.69	2.69	−10.07	−12.22	−321.9	−327.1	3.96	0.16	4

TABLE 2—*Continued*

No.	Peak α_{1950}	δ_{1950}	Peak *l*	*b*	*l* max	*l* min	*b* max	*b* min	*v* max	*v* min	F_{tot}	T_{peak}	# pts
1035	18.611	−30.028	4.689	−10.892	4.69	4.69	−10.89	−10.89	−269.1	−274.4	1.24	0.17	1
1036	18.629	−16.026	17.465	−4.881	17.92	17.01	−3.99	−5.77	−216.3	−232.2	3.13	0.10	3
1037	18.631	−40.028	355.440	−15.244	355.44	355.44	−15.24	−15.24	116.1	105.5	1.35	0.09	1
1038	18.631	−40.028	355.440	−15.244	355.44	355.44	−15.24	−15.24	−274.4	−290.2	2.21	0.12	1
1039	18.656	3.970	35.419	3.969	35.42	35.42	3.97	3.97	−126.6	−137.2	1.40	0.10	1
1040	18.695	−28.032	7.009	−11.035	7.01	7.01	−11.04	−11.04	284.9	269.1	2.17	0.13	1
1041	18.700	−8.029	25.070	−2.151	25.07	25.07	−2.15	−2.15	−94.7	−100.0	1.38	0.17	1
1042	18.700	−8.029	25.070	−2.151	25.07	25.07	−2.15	−2.15	−115.8	−126.4	1.08	0.08	1
1043	18.700	−40.031	355.758	−15.977	355.76	355.76	−15.98	−15.98	105.5	89.7	1.42	0.07	1
1044	18.751	−6.032	27.188	−1.898	27.19	27.19	−1.90	−1.90	−89.7	−110.8	2.68	0.12	1
1045	18.767	19.967	50.566	9.675	52.51	48.61	10.30	7.92	−36.9	−126.6	636.13	3.25	5
1046	18.775	−28.036	7.460	−11.990	7.53	7.46	−11.99	−12.15	284.9	221.6	23.39	0.44	2
1047	18.788	−28.036	7.534	−12.147	7.53	7.53	−12.15	−12.15	−89.7	−147.7	14.59	0.27	1
1048	18.788	−28.036	7.534	−12.147	7.53	7.53	−12.15	−12.15	131.9	100.3	4.42	0.18	1
1049	18.788	−28.036	7.534	−12.147	7.53	7.53	−12.15	−12.15	248.0	232.2	2.12	0.15	1
1050	18.788	−28.036	7.534	−12.147	7.53	7.53	−12.15	−12.15	−158.3	−184.7	6.48	0.24	1
1051	18.788	−28.036	7.534	−12.147	7.53	7.53	−12.15	−12.15	−195.2	−248.0	10.96	0.22	1
1052	18.788	−28.036	7.534	−12.147	7.53	7.53	−12.15	−12.15	−258.5	−284.9	5.17	0.19	1
1053	18.788	−28.036	7.534	−12.147	7.53	7.53	−12.15	−12.15	−306.0	−316.6	2.15	0.19	1
1054	18.824	1.963	34.795	0.802	34.80	34.80	0.80	0.80	−342.9	−348.2	1.21	0.13	1
1055	18.839	−22.038	13.372	−10.230	13.37	13.37	−10.23	−10.23	−116.1	−174.1	7.18	0.17	1
1056	18.839	−22.038	13.372	−10.230	13.37	13.37	−10.23	−10.23	−195.2	−205.8	2.04	0.14	1
1057	18.839	−22.038	13.372	−10.230	13.37	13.37	−10.23	−10.23	−216.3	−226.9	2.06	0.15	1
1058	18.839	−22.038	13.372	−10.230	13.37	13.37	−10.23	−10.23	−237.4	−248.0	2.20	0.16	1
1059	18.839	−22.038	13.372	−10.230	13.37	13.37	−10.23	−10.23	−269.1	−321.9	6.35	0.16	1
1060	18.839	−40.037	356.378	−17.459	356.38	356.38	−17.46	−17.46	110.8	95.0	2.37	0.17	1
1061	18.839	−40.037	356.378	−17.459	356.38	356.38	−17.46	−17.46	126.6	121.4	1.21	0.12	1
1062	18.852	7.963	40.321	3.186	40.32	40.32	3.19	3.19	−126.6	−137.2	1.12	0.08	1
1063	18.857	−28.039	7.922	−12.985	7.92	7.92	−12.99	−12.99	284.9	200.5	27.15	0.45	1
1064	18.909	−22.041	13.790	−11.103	13.79	13.79	−11.10	−11.10	−358.8	−369.3	1.70	0.13	1
1065	18.914	−28.042	8.233	−13.664	8.23	8.23	−13.66	−13.66	190.0	142.5	6.07	0.16	1
1066	18.916	−16.039	19.325	−8.593	19.33	17.16	−8.59	−9.78	147.8	116.1	23.13	0.54	3
1067	18.931	−4.041	30.195	−3.377	30.74	28.60	−3.38	−4.66	−89.7	−105.5	3.20	0.11	3
1068	18.959	−6.042	28.603	−4.662	28.60	28.60	−4.66	−4.66	−311.3	−321.8	1.08	0.07	1
1069	18.978	−22.044	14.204	−11.976	14.62	14.20	−11.98	−12.85	−168.8	−221.6	5.52	0.16	2
1070	18.983	−28.045	8.613	−14.507	8.69	8.61	−14.51	−14.67	126.6	95.0	6.05	0.17	2
1071	18.996	−28.046	8.686	−14.669	8.69	8.61	−14.51	−14.67	158.3	137.2	4.19	0.11	2
1072	18.996	−28.046	8.686	−14.669	8.69	8.69	−14.67	−14.67	179.4	168.9	1.17	0.08	1
1073	18.996	−28.046	8.686	−14.669	8.69	8.69	−14.67	−14.67	200.5	190.0	1.28	0.08	1
1074	19.038	−6.045	29.141	−5.719	29.14	29.14	−5.72	−5.72	−290.2	−300.7	1.12	0.08	1
1075	19.045	11.954	45.178	2.494	45.18	45.18	2.49	2.49	−401.0	−406.2	1.12	0.13	1
1076	19.048	−22.047	14.616	−12.854	14.62	14.62	−12.85	−12.85	258.6	248.0	1.63	0.12	1
1077	19.048	−22.047	14.616	−12.854	15.02	14.62	−12.85	−13.73	−200.5	−269.1	9.19	0.16	2
1078	19.057	−40.047	357.296	−19.808	357.30	357.30	−19.81	−19.81	−95.0	−105.5	1.46	0.14	1
1079	19.057	−40.047	357.296	−19.808	357.30	357.30	−19.81	−19.81	−316.6	−327.1	1.23	0.08	1
1080	19.070	37.956	68.927	13.692	69.63	66.92	13.69	12.20	−131.9	−163.5	32.78	0.45	4
1081	19.088	79.955	111.815	26.241	111.81	111.81	26.24	26.24	−94.9	−126.6	4.20	0.14	1
1082	19.111	−38.047	359.521	−19.721	359.52	359.18	−18.84	−19.72	−168.8	−184.7	2.37	0.09	2
1083	19.117	−22.050	15.024	−13.734	15.02	15.02	−13.73	−13.73	190.0	179.4	2.88	0.21	1
1084	19.117	−22.050	15.024	−13.734	15.02	15.02	−13.73	−13.73	221.6	200.5	3.81	0.17	1
1085	19.122	−28.051	9.358	−16.196	9.36	8.99	−15.35	−16.20	−100.2	−131.9	3.69	0.11	3
1086	19.122	−28.051	9.358	−16.196	9.36	9.11	−15.63	−16.20	−84.4	−95.0	2.21	0.15	2
1087	19.165	−36.051	1.748	−19.645	1.75	1.75	−19.64	−19.64	95.0	84.4	1.29	0.09	1
1088	19.178	−34.055	3.790	−19.098	3.79	3.79	−19.10	−19.10	−253.3	−295.5	8.58	0.28	1
1089	19.178	−34.055	3.790	−19.098	3.79	3.79	−19.10	−19.10	−306.0	−327.1	7.45	0.31	1
1090	19.193	−12.052	24.749	−10.454	25.11	24.75	−10.45	−11.19	132.2	121.6	2.27	0.11	2
1091	19.197	−22.054	15.488	−14.744	15.49	15.49	−14.74	−14.74	216.4	163.6	8.32	0.21	1
1092	19.197	−22.054	15.488	−14.744	15.49	15.49	−14.74	−14.74	−105.5	−116.1	2.27	0.17	1
1093	19.197	−22.054	15.488	−14.744	15.49	15.49	−14.74	−14.74	−137.2	−158.3	2.28	0.11	1
1094	19.214	57.951	88.842	19.950	88.84	88.84	19.95	19.95	−79.1	−100.2	5.12	0.24	1
1095	19.215	−28.055	9.847	−17.332	9.85	9.85	−17.33	−17.33	−100.2	−126.6	2.70	0.12	1
1096	19.215	−28.055	9.847	−17.332	9.85	9.85	−17.33	−17.33	−137.2	−158.3	2.31	0.10	1
1097	19.215	−28.055	9.847	−17.332	9.85	9.85	−17.33	−17.33	−343.0	−353.5	1.43	0.10	1
1098	19.217	−32.052	5.955	−18.844	5.95	4.11	−18.84	−19.91	−300.8	−316.6	1.86	0.11	2
1099	19.228	−2.054	34.013	−6.417	34.01	34.01	−6.42	−6.42	−89.7	−100.2	1.11	0.08	1
1100	19.248	−34.058	4.108	−19.908	4.11	4.11	−19.91	−19.91	131.9	110.8	2.14	0.10	1
1101	19.265	−40.056	358.111	−22.075	358.11	358.11	−22.07	−22.07	−316.6	−321.9	1.45	0.17	1
1102	19.271	−28.058	10.139	−18.021	10.14	9.85	−17.33	−18.02	284.9	274.4	3.07	0.18	2
1103	19.271	−28.058	10.139	−18.021	10.21	9.85	−17.33	−18.18	263.8	153.0	39.16	0.36	3
1104	19.284	−28.058	10.207	−18.182	10.21	9.85	−17.33	−18.18	−168.8	−242.7	42.78	0.55	4
1105	19.284	−28.058	10.207	−18.182	10.21	10.14	−18.02	−18.18	−63.3	−163.6	21.60	0.48	2
1106	19.284	−28.058	10.207	−18.182	10.21	10.21	−18.18	−18.18	−58.0	−84.4	14.02	0.46	1
1107	19.284	−28.058	10.207	−18.182	10.21	10.21	−18.18	−18.18	−95.0	−110.8	9.41	0.48	1
1108	19.284	−28.058	10.207	−18.182	10.21	10.21	−18.18	−18.18	−121.4	−142.5	11.96	0.47	1
1109	19.284	−28.058	10.207	−18.182	10.50	10.21	−18.18	−18.88	−168.8	−242.7	15.86	0.45	2
1110	19.310	17.942	52.271	1.894	52.27	52.27	1.89	1.89	−395.7	−406.2	1.08	0.07	1
1111	19.335	−22.060	16.287	−16.511	16.29	16.29	−16.51	−16.51	163.6	142.5	2.72	0.15	1
1112	19.335	−40.059	358.370	−22.836	358.37	0.37	−22.05	−22.84	−89.7	−105.5	1.80	0.10	2
1113	19.340	−28.061	10.497	−18.876	10.50	10.50	−18.88	−18.88	179.4	131.9	8.07	0.21	1
1114	19.340	−28.061	10.497	−18.876	10.50	10.50	−18.88	−18.88	200.5	190.0	1.95	0.15	1
1115	19.340	−28.061	10.497	−18.876	10.50	10.50	−18.88	−18.88	−221.6	−258.5	6.06	0.19	1
1116	19.350	21.941	56.066	3.287	145.76	52.82	28.17	3.29	−36.9	−179.3	49834.58	16.88	1044
1117	19.357	−18.060	20.217	−15.168	20.22	20.22	−15.17	−15.17	158.3	131.9	4.75	0.22	1
1118	19.357	−18.060	20.217	−15.168	20.22	20.22	−15.17	−15.17	184.7	168.9	2.50	0.13	1
1119	19.357	−18.060	20.217	−15.168	20.22	20.22	−15.17	−15.17	−126.6	−137.2	1.12	0.08	1
1120	19.405	−22.063	16.684	−17.399	16.68	16.68	−17.40	−17.40	147.8	116.1	3.74	0.16	1
1121	19.410	−28.064	10.850	−19.733	10.85	10.85	−19.73	−19.73	131.9	121.4	1.92	0.12	1
1122	19.412	−16.061	22.442	−15.059	22.44	22.01	−14.15	−15.06	116.1	100.3	2.23	0.08	2
1123	19.413	23.937	58.237	3.475	58.24	58.24	3.48	3.48	−142.4	−153.0	1.23	0.11	1
1124	19.423	−28.065	10.916	−19.895	10.92	10.85	−19.73	−19.89	174.1	126.6	9.27	0.16	2
1125	19.423	−28.065	10.916	−19.895	10.92	10.92	−19.89	−19.89	190.0	184.7	1.16	0.11	1
1126	19.423	−28.065	10.916	−19.895	10.92	10.92	−19.89	−19.89	−189.9	−211.1	2.71	0.12	1
1127	19.423	−28.065	10.916	−19.895	10.92	10.92	−19.89	−19.89	−221.6	−232.2	2.08	0.15	1
1128	19.423	−28.065	10.916	−19.895	10.92	10.92	−19.89	−19.89	−242.7	−258.5	2.08	0.12	1

TABLE 2—*Continued*

No.	Peak α_{1950}	δ_{1950}	Peak l	b	l max	l min	b max	b min	v max	v min	F_{tot}	T_{peak}	# pts
1129	19.445	−8.063	30.075	−12.036	30.08	30.08	−12.04	−12.04	−84.4	−94.9	1.31	0.11	1
1130	19.492	−28.068	11.265	−20.754	11.27	11.20	−20.59	−20.75	168.9	95.0	14.55	0.19	2
1131	19.492	−28.068	11.265	−20.754	11.27	11.27	−20.75	−20.75	190.0	179.4	1.34	0.10	1
1132	19.548	−28.070	11.544	−21.450	11.54	11.27	−20.75	−21.45	−300.8	−311.3	1.64	0.09	2
1133	19.572	−28.071	11.659	−21.740	11.66	11.66	−21.74	−21.74	116.1	105.5	1.36	0.11	1
1134	19.594	31.930	66.418	5.231	67.35	64.90	6.01	3.07	−158.2	−184.6	9.93	0.18	6
1135	19.618	−28.073	11.886	−22.314	11.89	11.89	−22.31	−22.31	158.3	147.7	1.41	0.10	1
1136	19.618	−28.073	11.886	−22.314	11.89	11.89	−22.31	−22.31	−290.2	−327.1	6.38	0.21	1
1137	19.618	−28.073	11.886	−22.314	11.89	11.89	−22.31	−22.31	−337.7	−353.5	2.15	0.16	1
1138	19.622	−40.072	359.366	−26.009	359.37	359.37	−26.01	−26.01	100.3	84.4	1.76	0.09	1
1139	19.640	−14.072	25.761	−17.227	25.76	25.76	−17.23	−17.23	−73.8	−95.0	5.26	0.24	1
1140	19.651	79.930	112.162	24.801	112.16	112.16	24.80	24.80	121.4	121.4	1.52	0.29	1
1141	19.687	−28.076	12.223	−23.176	12.22	12.22	−23.18	−23.18	−89.7	−131.9	4.09	0.17	1
1142	19.687	−28.076	12.223	−23.176	12.22	12.22	−23.18	−23.18	158.3	100.3	24.29	0.42	1
1143	19.687	−28.076	12.223	−23.176	12.22	12.22	−23.18	−23.18	216.3	205.8	4.11	0.30	1
1144	19.687	−28.076	12.223	−23.176	12.22	12.22	−23.18	−23.18	279.7	226.9	11.12	0.26	1
1145	19.687	−28.076	12.223	−23.176	12.22	12.22	−23.18	−23.18	−300.8	−311.3	2.33	0.18	1
1146	19.687	−28.076	12.223	−23.176	12.34	12.22	−23.18	−23.47	242.7	158.3	27.58	0.38	2
1147	19.692	−40.075	359.589	−26.781	359.59	359.37	−26.01	−26.78	−316.6	−327.1	2.48	0.15	2
1148	19.711	−28.077	12.337	−23.470	12.34	12.22	−23.18	−23.47	−306.0	−374.6	15.60	0.26	2
1149	19.711	−28.077	12.337	−23.470	12.34	12.34	−23.47	−23.47	121.4	95.0	7.73	0.26	1
1150	19.711	−28.077	12.337	−23.470	12.34	12.34	−23.47	−23.47	147.8	131.9	5.11	0.25	1
1151	19.714	−18.075	22.364	−19.831	22.36	22.36	−19.83	−19.83	−116.1	−147.7	3.31	0.11	1
1152	19.714	−18.075	22.364	−19.831	24.59	22.36	−18.70	−21.65	−216.3	−258.5	16.05	0.18	5
1153	19.733	−30.077	10.376	−24.406	10.38	10.38	−24.41	−24.41	110.8	100.3	1.18	0.08	1
1154	19.750	65.924	98.184	19.422	98.18	97.84	20.20	19.42	−89.6	−100.2	6.09	0.22	2
1155	19.767	−28.079	12.605	−24.168	12.60	12.60	−24.17	−24.17	−73.9	−126.6	27.29	0.53	1
1156	19.767	−28.079	12.605	−24.168	12.60	12.60	−24.17	−24.17	248.0	100.3	75.97	0.79	1
1157	19.767	−28.079	12.605	−24.168	12.60	12.60	−24.17	−24.17	−137.2	−205.8	27.02	0.44	1
1158	19.767	−28.079	12.605	−24.168	12.60	12.60	−24.17	−24.17	−216.3	−248.0	8.30	0.35	1
1159	19.780	−28.080	12.668	−24.335	12.67	12.67	−24.33	−24.33	253.3	131.9	52.96	0.67	1
1160	19.818	11.921	50.615	−7.470	50.61	50.61	−7.47	−7.47	−94.9	−100.2	1.15	0.15	1
1161	19.831	−40.080	0.013	−28.329	0.01	0.01	−28.33	−28.33	174.1	163.6	1.16	0.09	1
1162	19.836	−28.082	12.935	−25.037	12.94	12.94	−25.04	−25.04	232.2	205.8	4.98	0.23	1
1163	19.836	−28.082	12.935	−25.037	12.94	12.94	−25.04	−25.04	−237.4	−290.2	12.64	0.39	1
1164	19.849	−28.083	12.998	−25.204	13.00	12.94	−25.04	−25.20	−100.2	−168.8	34.80	0.50	2
1165	19.849	−28.083	12.998	−25.204	13.32	12.67	−24.33	−26.08	−147.7	−237.4	62.23	0.43	6
1166	19.849	−28.083	12.998	−25.204	13.32	13.00	−25.20	−26.08	−121.3	−158.3	27.98	0.47	4
1167	19.849	−28.083	12.998	−25.204	13.58	13.00	−25.20	−26.78	248.0	84.4	138.94	0.79	4
1168	19.882	41.920	76.860	7.216	78.83	74.63	10.89	7.04	−58.0	−142.4	912.12	5.59	7
1169	19.900	77.927	110.357	23.456	110.36	110.36	23.46	23.46	−84.4	−94.9	3.80	0.28	1
1170	19.906	−28.085	13.262	−25.908	13.26	13.26	−25.91	−25.91	221.6	105.5	24.74	0.35	1
1171	19.906	−28.085	13.262	−25.908	13.26	13.26	−25.91	−25.91	−290.2	−295.5	1.42	0.17	1
1172	19.919	−28.085	13.324	−26.076	13.32	12.94	−25.04	−26.08	−200.5	−279.6	37.40	0.42	4
1173	19.919	−28.085	13.324	−26.076	13.32	13.32	−26.08	−26.08	−79.1	−121.3	20.95	0.46	1
1174	19.919	−28.085	13.324	−26.076	13.32	13.32	−26.08	−26.08	−163.6	−168.8	4.32	0.42	1
1175	19.919	−28.085	13.324	−26.076	13.32	13.32	−26.08	−26.08	−232.2	−284.9	14.54	0.37	1
1176	19.975	−28.088	13.584	−26.778	13.58	13.58	−26.78	−26.78	216.4	179.4	5.01	0.19	1
1177	19.988	−28.088	13.645	−26.946	13.65	13.65	−26.95	−26.95	137.2	58.1	11.78	0.18	1
1178	19.988	−28.088	13.645	−26.946	13.65	13.65	−26.95	−26.95	174.1	147.8	3.41	0.14	1
1179	19.988	−28.088	13.645	−26.946	13.65	13.65	−26.95	−26.95	−211.0	−232.2	2.11	0.11	1
1180	19.988	−28.088	13.645	−26.946	13.65	13.65	−26.95	−26.95	−258.5	−274.4	1.71	0.10	1
1181	19.988	−28.088	13.645	−26.946	13.65	13.65	−26.95	−26.95	−284.9	−295.5	1.21	0.09	1
1182	20.033	9.912	50.485	−11.216	50.48	50.48	−11.22	−11.22	−84.4	−94.9	2.30	0.18	1
1183	20.044	−28.090	13.903	−27.652	13.90	13.90	−27.65	−27.65	−89.7	−116.1	2.59	0.12	1
1184	20.049	−40.089	0.621	−30.782	0.80	0.62	−30.78	−31.56	−306.0	−321.9	3.24	0.16	2
1185	20.063	3.909	45.394	−14.626	45.39	43.82	−14.63	−16.00	−63.3	−94.9	3.72	0.11	2
1186	20.068	−28.091	14.010	−27.947	14.01	14.01	−27.95	−27.95	147.8	89.7	9.00	0.20	1
1187	20.068	−28.091	14.010	−27.947	14.01	14.01	−27.95	−27.95	190.0	174.1	1.93	0.10	1
1188	20.096	47.913	83.217	8.394	83.22	82.61	9.39	8.39	−79.1	−153.0	328.54	5.13	2
1189	20.114	−28.093	14.220	−28.529	14.22	14.22	−28.53	−28.53	248.0	232.2	1.87	0.09	1
1190	20.137	−28.094	14.326	−28.824	14.33	14.33	−28.82	−28.82	−63.3	−110.8	4.74	0.10	1
1191	20.137	−28.094	14.326	−28.824	14.33	14.33	−28.82	−28.82	−126.6	−137.2	1.28	0.10	1
1192	20.157	−36.092	5.491	−31.178	5.49	5.49	−31.18	−31.18	84.4	84.4	1.22	0.23	1
1193	20.205	41.907	78.777	4.158	78.78	78.78	4.16	4.16	−116.0	−153.0	83.91	6.76	1
1194	20.242	−38.094	3.435	−32.589	3.43	3.43	−32.59	−32.59	−311.3	−316.6	1.11	0.14	1
1195	20.258	−22.098	21.394	−28.434	21.39	21.39	−28.43	−28.43	−385.2	−395.7	1.10	0.07	1
1196	20.269	7.903	50.574	−15.258	51.13	50.57	−15.26	−16.14	−79.1	−89.7	2.35	0.11	2
1197	20.280	−4.098	39.664	−21.334	39.66	39.66	−21.33	−21.33	126.7	121.4	1.13	0.12	1
1198	20.281	3.901	47.085	−17.461	47.09	47.09	−17.46	−17.46	−73.8	−84.4	1.23	0.09	1
1199	20.371	39.901	78.192	1.468	78.19	78.19	1.47	1.47	−411.5	−422.1	1.07	0.07	1
1200	20.402	−28.104	15.496	−32.174	15.50	15.50	−32.17	−32.17	258.6	237.5	2.24	0.10	1
1201	20.418	−4.103	40.710	−23.168	40.71	40.71	−23.17	−23.17	126.7	73.9	8.43	0.18	1
1202	20.448	11.896	55.533	−15.364	55.53	55.53	−15.36	−15.36	−184.6	−195.2	2.18	0.24	1
1203	20.480	−34.108	8.816	−34.616	8.82	8.82	−34.62	−34.62	84.4	73.9	1.11	0.08	1
1204	20.485	37.898	77.352	−0.788	77.35	77.35	−0.79	−0.79	−490.7	−501.2	1.71	0.15	1
1205	20.488	7.895	52.349	−18.020	52.35	52.35	−18.02	−18.02	−79.1	−110.8	2.96	0.09	1
1206	20.489	3.893	48.758	−20.141	48.76	47.16	−20.14	−21.55	−79.1	−94.9	2.02	0.09	2
1207	20.519	17.893	61.255	−12.869	61.26	61.26	−12.87	−12.87	−89.6	−105.5	2.36	0.16	1
1208	20.545	−40.108	1.710	−36.399	1.83	1.58	−35.61	−37.19	−306.0	−327.1	5.33	0.19	3
1209	20.599	−38.108	4.284	−36.750	4.28	4.11	−35.82	−36.75	−121.4	−142.5	3.44	0.11	2
1210	20.599	−38.108	4.284	−36.750	6.70	4.28	−36.25	−36.75	−116.1	−121.4	1.65	0.10	2
1211	20.695	13.886	59.357	−17.248	59.36	59.36	−17.25	−17.25	−73.8	−94.9	2.55	0.13	1
1212	20.765	7.885	54.721	−21.485	54.72	53.11	−21.49	−22.86	−79.1	−94.9	2.44	0.10	2
1213	20.823	−40.118	2.124	−39.570	4.79	2.03	−38.78	−40.37	−311.3	−327.1	4.89	0.18	4
1214	20.829	−28.120	17.294	−37.629	17.29	17.29	−37.63	−37.63	89.7	79.2	1.30	0.09	1
1215	20.865	17.881	64.248	−16.885	64.25	64.25	−16.88	−16.88	−89.6	−100.2	1.42	0.12	1
1216	20.967	−28.124	17.855	−39.411	17.85	17.85	−39.41	−39.41	−63.3	−95.0	2.80	0.11	1
1217	20.972	−40.123	2.281	−41.277	2.28	2.28	−41.28	−41.28	−105.5	−110.8	1.06	0.10	1
1218	20.992	15.875	63.728	−19.545	63.73	63.73	−19.54	−19.54	−100.2	−110.8	1.17	0.08	1
1219	21.011	−36.123	7.641	−41.375	7.64	7.64	−41.37	−41.37	−295.5	−300.8	1.17	0.13	1
1220	21.042	−40.125	2.337	−42.071	2.34	2.34	−42.07	−42.07	−121.4	−131.9	1.48	0.12	1
1221	21.042	−40.125	2.337	−42.071	2.38	2.34	−42.07	−42.87	−306.0	−321.9	2.06	0.09	2
1222	21.045	79.877	113.927	21.535	113.93	113.93	21.53	21.53	121.4	121.4	1.20	0.23	1

TABLE 2—*Continued*

No.	Peak α_{1950}	δ_{1950}	Peak l	b	l max	l min	b max	b min	v max	v min	F_{tot}	T_{peak}	# pts
1223	21.101	53.873	93.748	4.413	93.75	93.75	4.41	4.41	−179.3	−195.2	1.71	0.11	1
1224	21.181	−40.130	2.415	−43.666	2.42	2.38	−42.87	−43.67	−105.5	−126.6	3.18	0.15	2
1225	21.181	−40.130	2.415	−43.666	2.42	2.42	−43.67	−43.67	−121.4	−137.2	2.74	0.15	1
1226	21.204	53.870	94.371	3.747	94.37	94.37	3.75	3.75	−184.6	−205.7	2.10	0.10	1
1227	21.214	5.867	57.060	−28.131	57.06	57.06	−28.13	−28.13	−73.8	−84.4	1.23	0.10	1
1228	21.261	7.869	59.356	−27.520	59.36	59.36	−27.52	−27.52	−68.5	−94.9	2.74	0.11	1
1229	21.320	−40.134	2.445	−45.258	2.44	2.44	−45.26	−45.26	−284.9	−295.5	1.06	0.08	1
1230	21.369	−36.134	8.176	−45.695	8.18	8.18	−45.70	−45.70	−348.2	−353.5	1.09	0.14	1
1231	21.451	19.863	71.498	−22.023	71.50	71.50	−22.02	−22.02	−342.9	−348.2	1.08	0.14	1
1232	21.451	19.863	71.498	−22.023	72.32	71.50	−22.02	−22.85	−311.3	−337.6	4.65	0.14	2
1233	21.537	13.859	67.477	−26.940	69.36	67.48	−25.82	−26.94	−73.8	−94.9	2.90	0.11	2
1234	21.577	−24.139	25.897	−46.393	25.90	25.90	−46.39	−46.39	−95.0	−105.5	1.50	0.11	1
1235	21.604	27.860	79.156	−17.951	79.16	79.16	−17.95	−17.95	−105.5	−116.0	1.58	0.13	1
1236	21.608	−40.142	2.333	−48.561	2.33	2.33	−48.56	−48.56	−100.3	−105.5	1.23	0.15	1
1237	21.608	−40.142	2.333	−48.561	2.38	2.33	−47.76	−48.56	−306.0	−321.9	3.00	0.19	2
1238	21.612	33.862	83.528	−13.667	84.18	83.53	−13.67	−14.25	−94.9	−126.6	18.94	0.37	2
1239	21.652	57.861	99.859	4.038	99.86	99.86	4.04	4.04	−495.9	−506.5	1.15	0.09	1
1240	21.681	23.856	76.984	−21.548	76.98	76.98	−21.55	−21.55	−84.4	−89.6	1.23	0.13	1
1241	21.726	−24.143	26.666	−48.362	26.67	26.67	−48.36	−48.36	−84.4	−105.5	1.82	0.07	1
1242	21.744	−0.147	56.744	−38.092	56.74	56.74	−38.09	−38.09	89.7	84.5	1.21	0.13	1
1243	21.889	23.851	79.228	−23.505	79.23	79.23	−23.51	−23.51	−89.6	−94.9	1.17	0.13	1
1244	21.955	−22.151	30.946	−50.867	30.95	30.51	−49.94	−50.87	−126.6	−142.4	3.41	0.15	2
1245	21.955	−22.151	30.946	−50.867	31.39	30.51	−49.94	−51.79	−89.7	−116.1	6.03	0.15	3
1246	22.144	43.849	94.879	−9.849	94.88	94.88	−9.85	−9.85	−110.7	−147.7	12.79	0.46	1
1247	22.182	7.845	69.875	−38.000	69.88	69.88	−38.00	−38.00	−68.5	−79.1	1.13	0.08	1
1248	22.243	−40.157	1.024	−55.800	1.02	0.48	−55.80	−57.36	−306.0	−321.9	4.78	0.26	3
1249	22.246	33.847	89.872	−18.677	89.87	89.87	−18.68	−18.68	−94.9	−121.3	8.92	0.40	1
1250	22.385	37.844	93.707	−16.343	93.71	93.71	−16.34	−16.34	−116.0	−126.6	1.85	0.17	1
1251	22.418	47.844	99.532	−8.109	103.32	96.72	−7.55	−11.54	−121.3	−168.8	134.43	0.74	12
1252	22.586	79.838	117.102	18.802	117.10	117.10	18.80	18.80	121.4	121.4	1.36	0.26	1
1253	22.671	−40.165	358.961	−60.574	359.77	2.65	−59.03	−61.68	−311.3	−327.1	5.74	0.19	5
1254	22.693	−32.163	15.403	−62.044	15.40	15.34	−62.04	−62.93	121.4	110.8	10.29	1.32	2
1255	22.695	39.837	98.021	−16.528	98.02	98.02	−16.53	−16.53	−105.5	−110.7	1.36	0.13	1
1256	22.740	−40.166	358.499	−61.340	358.50	358.50	−61.34	−61.34	253.3	242.7	1.14	0.07	1
1257	22.744	−34.168	11.009	−62.562	11.01	11.01	−62.56	−62.56	−332.4	−337.7	1.18	0.16	1
1258	22.780	−36.165	6.570	−62.728	6.57	2.24	−62.48	−62.73	116.1	110.8	1.77	0.16	2
1259	22.788	9.834	80.388	−42.502	80.39	80.39	−42.50	−42.50	−68.5	−89.7	2.03	0.09	1
1260	22.794	−38.164	2.245	−62.476	358.00	1.79	−60.88	−63.27	68.6	47.5	6.00	0.12	5
1261	22.850	63.837	110.428	4.147	110.43	108.87	4.56	2.69	−184.6	−200.4	3.28	0.10	3
1262	22.927	−6.168	66.067	−55.721	67.49	63.15	−54.94	−57.70	−52.7	−94.9	60.97	0.67	5
1263	22.959	−40.169	356.761	−63.714	356.76	356.76	−63.71	−63.71	−100.3	−110.8	1.10	0.07	1
1264	22.959	−40.169	356.761	−63.714	357.45	356.10	−62.85	−64.46	−311.3	−316.6	2.73	0.17	3
1265	22.969	45.834	103.609	−12.562	104.62	102.49	−12.03	−13.01	−137.1	−158.2	4.12	0.09	3
1266	22.995	11.831	85.334	−42.656	86.67	85.33	−42.66	−43.29	−353.5	−374.6	3.33	0.09	2
1267	22.999	−36.168	5.357	−65.321	5.36	5.36	−65.32	−65.32	79.1	58.0	2.17	0.09	1
1268	23.003	−38.167	0.745	−64.847	0.74	0.74	−64.85	−64.85	121.4	105.5	7.32	0.84	1
1269	23.024	−12.168	58.832	−60.575	58.83	58.83	−60.58	−60.58	−68.3	−78.9	1.56	0.10	1
1270	23.028	−40.170	356.103	−64.458	356.76	356.10	−63.71	−64.46	68.6	52.8	2.49	0.13	2
1271	23.031	3.829	79.215	−49.467	79.21	77.79	−48.82	−51.30	−311.3	−337.7	4.28	0.12	3
1272	23.051	−32.167	14.818	−66.581	14.82	14.82	−66.58	−66.58	73.9	63.3	1.36	0.10	1
1273	23.056	−8.170	65.628	−58.486	65.63	65.63	−58.49	−58.49	−84.4	−89.7	1.24	0.15	1
1274	23.074	11.830	86.668	−43.293	86.67	86.67	−43.29	−43.29	−342.9	−353.5	1.33	0.09	1
1275	23.148	−12.169	61.069	−62.058	63.63	60.05	−60.39	−62.87	−63.3	−89.4	15.50	0.24	5
1276	23.163	−28.173	25.161	−68.077	25.16	25.16	−68.08	−68.08	−58.0	−63.3	1.16	0.12	1
1277	23.167	−40.171	354.613	−65.923	354.61	354.61	−65.92	−65.92	−290.2	−300.8	1.53	0.11	1
1278	23.169	3.828	81.797	−50.715	81.80	79.10	−50.10	−51.95	−306.0	−342.9	7.40	0.11	3
1279	23.169	3.828	81.797	−50.715	81.80	81.80	−50.71	−50.71	−306.0	−316.6	1.31	0.10	1
1280	23.222	−38.169	358.646	−67.281	359.38	358.65	−66.51	−67.28	95.0	63.3	5.13	0.16	2
1281	23.237	−40.172	353.770	−66.646	354.61	353.77	−65.92	−66.65	−311.3	−327.1	3.99	0.24	2
1282	23.329	−32.170	13.737	−70.092	19.69	6.78	−69.56	−71.96	79.2	42.2	16.97	0.18	9
1283	23.351	11.827	91.577	−45.355	91.58	91.58	−45.35	−45.35	−342.9	−353.5	1.57	0.14	1
1284	23.356	−36.172	2.232	−69.480	356.96	2.23	−68.79	−69.54	73.9	52.8	5.66	0.13	3
1285	23.373	47.831	108.313	−12.290	109.32	108.31	−12.29	−12.63	−121.3	−153.0	7.30	0.21	2
1286	23.395	−4.173	78.017	−59.128	78.02	78.02	−59.13	−59.13	−253.2	−269.1	1.49	0.08	1
1287	23.477	39.828	106.668	−20.215	106.67	106.67	−20.21	−20.21	−105.5	−116.0	1.12	0.08	1
1288	23.525	−40.174	349.440	−69.529	349.44	349.44	−69.53	−69.53	68.6	58.0	1.15	0.09	1
1289	23.553	5.823	91.297	−52.061	95.21	82.31	−45.83	−58.31	−279.6	−369.3	103.87	0.28	27
1290	23.573	−6.173	79.737	−62.345	81.53	79.74	−60.49	−62.34	−232.1	−274.3	7.40	0.21	2
1291	23.595	−40.174	348.162	−70.191	349.44	348.16	−69.53	−70.19	126.6	116.1	1.81	0.18	2
1292	23.598	−34.176	5.127	−72.935	5.13	4.14	−72.94	−73.75	63.3	52.8	1.82	0.11	2
1293	23.610	49.825	111.212	−11.114	111.21	110.24	−10.82	−11.11	−147.7	−158.2	2.14	0.10	2
1294	23.614	−4.175	83.270	−61.092	83.27	83.27	−61.09	−61.09	−221.6	−232.1	1.63	0.15	1
1295	23.635	−30.175	18.657	−74.233	18.70	18.66	−74.12	−74.23	73.9	63.3	2.30	0.12	2
1296	23.649	−38.172	352.283	−71.806	352.28	352.28	−71.81	−71.81	89.7	79.1	1.21	0.10	1
1297	23.664	−40.174	346.772	−70.840	348.16	345.27	−70.19	−71.47	−300.8	−321.9	5.32	0.18	3
1298	23.669	7.826	95.206	−51.029	95.21	95.21	−51.03	−51.03	−342.9	−369.3	3.60	0.16	1
1299	23.689	−2.174	87.401	−60.023	87.40	87.40	−60.02	−60.02	−284.9	−300.7	1.59	0.09	1
1300	23.714	25.825	104.893	−34.443	104.89	103.66	−34.10	−34.44	−84.4	−105.5	2.46	0.08	2
1301	23.720	19.826	102.595	−40.159	102.60	102.60	−40.16	−40.16	−395.7	−411.5	1.65	0.09	1
1302	23.728	−12.173	74.664	−68.420	86.94	67.83	−61.09	−71.48	−142.4	−274.3	400.76	0.63	42
1303	23.771	51.825	113.245	−9.586	114.19	113.25	−9.59	−9.81	−121.3	−168.8	18.87	0.31	2
1304	23.788	−38.172	349.299	−73.177	349.30	349.30	−73.18	−73.18	−311.3	−321.9	1.90	0.15	1
1305	23.814	−10.177	80.702	−67.706	80.70	80.70	−67.71	−67.71	−226.9	−242.7	2.44	0.16	1
1306	23.816	49.825	113.178	−11.630	114.30	111.36	−11.38	−13.77	−153.0	−195.2	14.66	0.17	6
1307	23.831	5.822	97.517	−53.833	97.52	93.86	−53.42	−55.98	−332.4	−385.1	11.38	0.11	7
1308	23.843	−16.179	69.665	−72.425	74.48	63.69	−70.12	−73.86	−126.6	−226.9	63.06	0.30	10
1309	23.878	−28.177	26.155	−77.528	26.15	26.11	−77.53	−78.44	−79.1	−89.7	1.96	0.09	2
1310	23.892	−20.175	59.691	−75.409	59.69	59.69	−75.41	−75.41	−179.4	−189.9	2.01	0.15	1
1311	23.947	−12.174	81.679	−70.474	81.68	81.68	−70.47	−70.47	−200.3	−231.9	3.42	0.14	1
1312	23.967	−26.174	36.246	−78.565	36.25	26.11	−78.44	−78.57	−58.0	−89.7	4.79	0.12	2

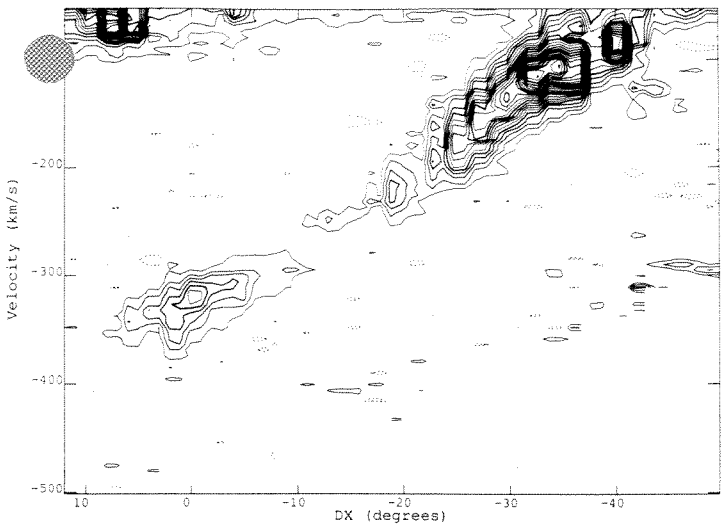

FIG. 11.—A position-velocity plot of the Magellanic Stream, where abscissa is position along a great circle between $(l, b) = (94.2, -39.6)$ and $(-50.2, -76.1)$. Contours are shown at −0.03 K (*dashed*), 0.03 K, 0.06 K, 0.09 K, 0.12 K, 0.15 K, 0.18 K, 0.21 K, 0.24 K, 0.27 K, 0.3 K, 0.33 K, 0.36 K, 0.4 K, 0.8 K, 1.6 K, 3.2 K, 6.4 K, 12.8 K, and 25.6 K.

mates of the infall rate are particularly interesting given their implications for Galactic structure but until distances are known for a significant fraction of the high-velocity clouds, direct estimates probably cannot improve on that of Oort (1969). A review of the observational and theoretical status of high-velocity clouds can be found in van Woerden et al. (1985).

The total column density at all velocities is shown in Figures 12*a*, 12*b*, and 12*c*. This may be used to estimate the reddening to extragalactic objects and can be compared to the diffuse background at a variety of wavelengths. The projection is orthographic, and the contours are spaced evenly in logarithmic intervals. The contour at 100 K kms^{-1} corresponds to a column density of 1.82×10^{20} cm^{-2}. The contours are spaced at powers of 1.4 times this column density. Caution is recommended in the use of column densities at low latitudes ($b < 5°$), where the saturation problem in the filter bank (cf. § 2) causes inaccuracies.

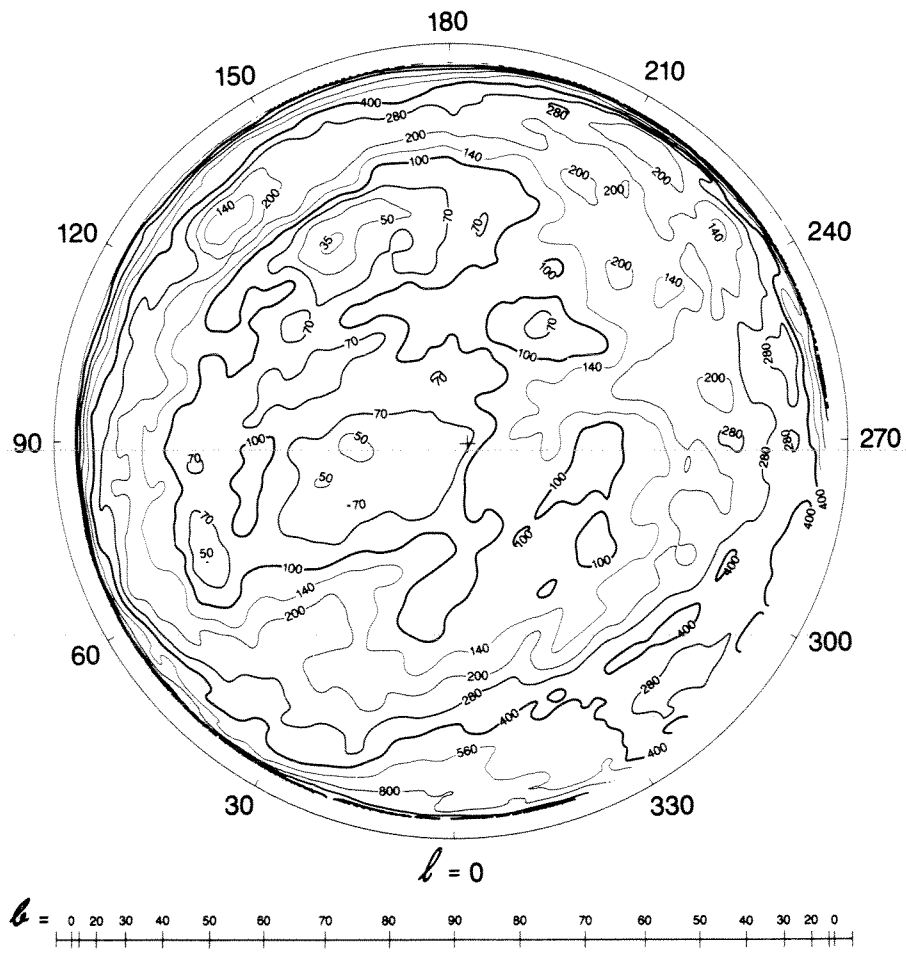

FIG. 12*a*

FIG. 12.—Contour maps of the total column density of H I in (*a*) the north, (*b*) the full sky, and (*c*) the south, respectively. Contours are labeled in units of K kms^{-1}.

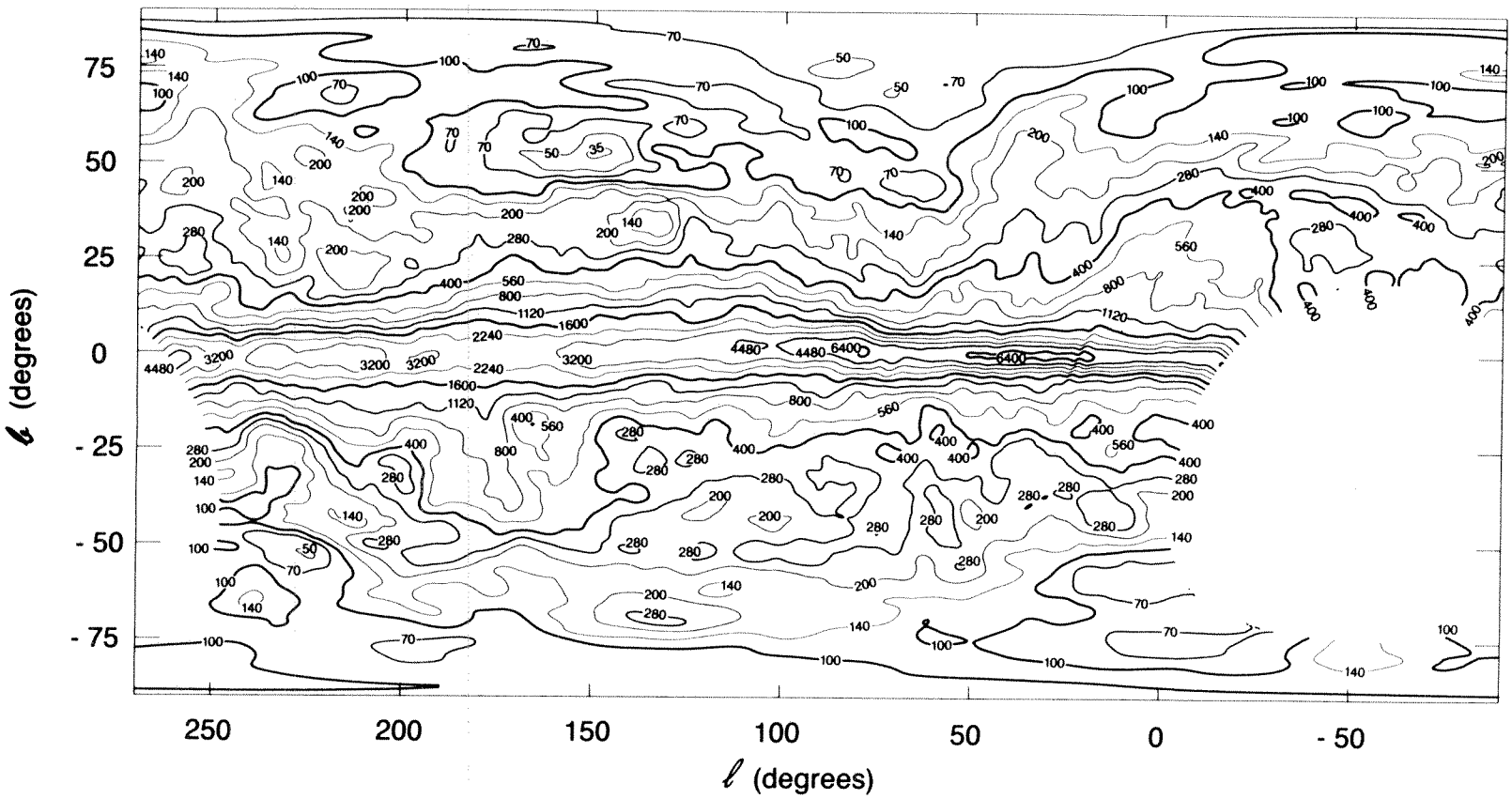

FIG. 12*b*

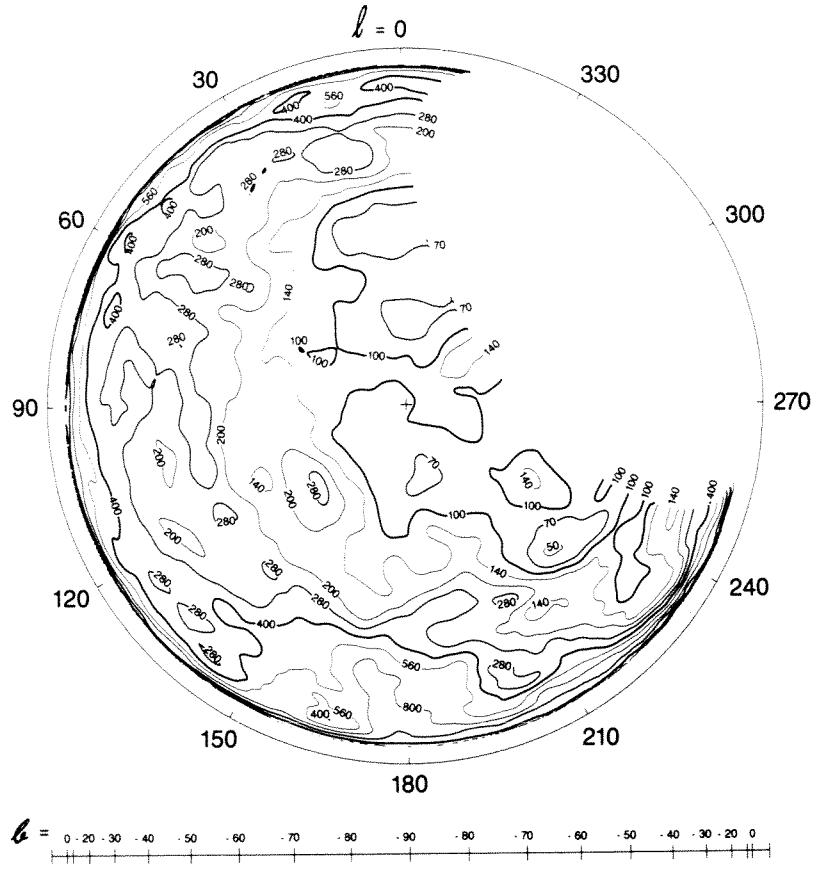

FIG. 12*c*

We thank the NRAO for help with the plates, particularly Paul van den Bout, who gave us permission and Arnold Rots, who helped us with the Dicomed and its software. This work was supported in part by NSF grant 443836-21705 to CH.

APPENDIX A
DATA TAPE VARIABLES

As of this writing, there is still no FITS spectral line format into which the individual spectra of the survey could be translated, and this has considerably delayed the dissemination of the data. Two types of data tape containing individual spectra are in circulation: COMB format for UNIX system users and a data tape written by VMS FORTRAN. Both consist of alternating records of header data and floating point representations of baseline corrected calibrated spectra. The COMB headers consist of the standard COMB header, plus some auxiliary variables which have been included in the interest of completeness. These are on the FORTRAN tape as well. The auxiliary variables are listed in Table 3. The first column lists the variable names. The variables I_n are 16 bit integers, while variables R_m are floating point. In COMB I_n is stored in integer dummy header variable `.isdum(n)`, and the value R_m is stored in real dummy header variable `.rsdm(m)`. The variable I_{15} indicates the direction of frequency switching: a 1 indicates the reference band is higher frequency than the signal, while 2 indicates the opposite (less desirable) condition. The baseline coefficients allow the original temperature of channel n, $T_{0,n}$, to be recovered from the values on tape, T_n, via

$$T_{0,n} = T_n + R_1 + R_2 n_z + R_3 n_z^2 + R_4 + R_5 n + R_6 n^2 , \tag{1}$$

where

$$n_z = n - n_{\rm lsr} ,$$

TABLE 3

DATA TAPE VARIABLES

Variable	Description	Units
I_1, I_2, I_3	Hour angle of observation	Hour, Minute, Second
I_4, I_5	Azimuth of observation	$a = I_4 + 10^{-3} I_5$
I_6, I_7	Elevation of observation	$e = I_6 + 10^{-3} I_7$
I_8	$T_{\rm coldload} \times 10$	
I_9, I_{10}, I_{11} ...	Sidereal time begin	Hour, Minute, Second
I_{12}, I_{13}, I_{14} ...	Sidereal time end	Hour, Minute, Second
I_{15}	Direction of frequency switching	
R_1	Baseline coefficient	
R_2	Baseline coefficient	
R_3	Baseline coefficient	
R_4	Baseline coefficient	
R_5	Baseline coefficient	
R_6	Baseline coefficient	
R_7	Baseline fit descriptor	
R_8	Baseline fit descriptor	
R_9	Baseline fit descriptor	
R_{10}	Baseline fit descriptor	
R_{11}	Baseline fit descriptor	

and $n_{\rm lsr}$ is the number of the channel falling on 0 kms^{-1} LSR. The baseline fit descriptors include R_7, the rms of all channels farther than nine channels from the 0 kms^{-1} LSR channel; R_8, the sum of the absolute value of the residuals of the channels used in the wide-band baseline fit; R_9, the number of channels with temperatures greater than 3× rms in the wide-band spectrum; R_{10}, 3× the rms of the channels used in the narrow-band baseline fit; and R_{11}, the number of channels used in the narrow-band fit.

APPENDIX B

FITS FORMAT DATA

28800

The survey is available as sets of images on a FITS format tape on either a nine track 6250 bpi or on 8 mm videotape (Exabyte compatible). These tapes have been written with a block size of 2880 bytes. The data consist of four types of images: (1) Whole sky images in Galactic (l, b) coordinates in which the displayed data consist of integrations over a 10 kms^{-1} velocity range. The 145 images have central (LSR) velocities ranging from −360 to +360 kms^{-1} in steps of 5 kms^{-1}. (2) North polar cap images and (3) South polar cap images showing each hemisphere in polar Galactic coordinates. In this display, the Galactic equator ($b = 0$) is mapped into a circle at the outer edge of the image while the Galactic poles are in the center of the image. The velocity integration range and step size is identical to the whole sky images. Finally, (4) 67 spatial velocity images are provided in which the horizontal axis is R.A. and the vertical axis is the uninterpolated channel data displayed as LSR velocity. The individual spectra can be recovered from these images since the data at points falling on the original survey grid consist of uninterpolated survey spectra, and the data are oversampled in R.A., so the interpolation between sampled points is unaliased.

Table 4 shows a sample FITS header from one of the images. Standard FITS key words are used and any image display program such as AIPS or IRAF should be able to read, process, and display these images. The various image types can be distinguished from the images headers. The polar cap images have `CTYPE1 = 'DX---SIN'` and `CTYPE2 = 'DY---SIN'`. Whole sky images have `CTYPE1 = 'GLON'` and `CTYPE2 = 'GLAT'`. The R.A.–velocity images have `CTYPE1 = 'RA'` and `CTYPE2 = 'FELO-LSR'`. The `HISTORY COMB` gives the value of the declination and the spatial interpolation radius (59′) for these images. For all the spatial images, a spatial interpolation radius of 200′ was used. In these images, the `HISTORY COMB` line gives the velocity range included in the image.

Table 5 describes the contents of the 8 mm and nine track tapes. For the spatial maps, the first image is centered at $v_{\rm LSR} = -360$ kms^{-1}, and the last at $v_{\rm LSR} = +360$ kms^{-1}, a larger range than the plates described in § 4. Tapes are available from the National Space Science Data Center A, telephone: 301-286-6695, email: `request@NSSDCA.GSSC.NASA.GOV`, upon request.

TABLE 4

A SAMPLE FITS HEADER

```
SIMPLE = T /
BITPIX = 16 /
NAXIS = 3 /
NAXIS1 = 400 /
NAXIS2 = 400 /
NAXIS3 = 1 /
CTYPE1 = 'DX---SIN' /
CRVAL1 = 0.00000000 /
CDELT1 = -0.300751880 /
CRPIX1 = 200.500000 /
CROTA1 = 0.00000000 /
CTYPE2 = 'DY---SIN' /
CRVAL2 = 0.00000000 /
CDELT2 = 0.300751880 /
CRPIX2 = 200.500000 /
CROTA2 = 0.00000000 /
CTYPE3 = 'FELO-LSR' /
CRVAL3 = 0.00000000 /
CDELT3 = 10000.0000 /
CRPIX3 = 0.00000000 /
CROTA3 = 0.00000000 /
BLANK = -32768 /
BSCALE = 0.0212216601 /
BZERO = 709.049054 /
BUNIT = 'K-KM/S ' /
DATAMAX = 1404.41919 /
DATAMIN = 13.6789188 /
DATE = '16/05/91' /
TELESCOP= 'BTL 7M ' /
HISTORY COMB TITLE HI.0 T*dV -5,5
HISTORY COMB PARAM ir:200 gi:  ortho:
END
```

TABLE 5

TAPE CONTENTS

Image Numbers	Data Type
Contents of 8 Millimeter FITS Tapes	
1–145	Whole sky images
146–290	South polar cap
291–435	North polar cap
436–501	R.A.—velocity images
Contents of 9 Track FITS Tape: Volume 1	
1–145	Whole sky images
Contents of 9 Track FITS Tape: Volume 2	
1–66	R.A.—velocity images
67–211	South polar cap images
Contents of 9 Track FITS Tape: Volume 3	
1–145	North polar cap images

REFERENCES

Colgan, S. J. W., Salpeter, E. E., & Terzian, Y. 1990, ApJ, 351, 503
Corbelli, E. & Salpeter, E. E. 1988, ApJ, 326, 551
Crawford, A. B., Hogg, D. C., & Hunt, L. E. 1961, Bell Sys. Tech. J., 40, 975
Davies, R. D. 1972, Nature, 237, 88
Giovanelli, R. 1980, AJ 85, 1155
Giovanelli, R., et al. 1978, ApJ, 219, 60
Henry, P. S. 1976, Rev. Sci. Instr., 47, 1020
Hogg, D. C., & Wilson, R. W. 1965, Bell Sys. Tech. J., 44, 1965
Hulsbosch, A. N. M., & Wakker, B. P. 1973, A&AS, 8, 1
———. 1988, A&AS, 75, 191
Kerr, F. J., & Sullivan, W. J. 1969, ApJ, 158, 115
Lockman, J., Jahoda, K., & McCammon, D. 1986, ApJ, 302, 432 (LJM)
Muller, C. A., Raimond, E., Schwarz, W. J., & Tolbert, C. R. 1966, Bull. Astron. Inst. Netherlands Suppl., 1, 213
Oort, J. H. 1969, Nature, 224, 1158
Penzias, A., Encrenaz, P., & Wilson, R. W. 1969, AJ, 118, 106
Songaila, A., Cowie, L. L., & Weaver, H. 1988, ApJ, 329, 580
van Woerden, H., Schwartz, U. J., & Hulsbosch, A. N. M., eds. 1985, IAU Symp. 106, The Milky Way Galaxy (Dordrecht: Reidel)
Verschuur, G. L. 1971, BAAS, 3, 369
———. 1975, ARA&A, 13, 257
Weaver, H., & Williams, D. R. W. 1973, A&AS, 8, 1
Weinreb, S., Fenstermacher, D. L., & Harris, R. W. 1982, IEEE Trans. Microwave Theory Tech., MTT-30, 849

Copies Figure 6 are not included.
This "figure" is 63 pages of half-tone
plates which do not copy well enough to be useful.

Publications of the Astronomical Society of the Pacific
104: 1256–1265, 1992 December

Far-Sidelobe Contamination of the Bell Laboratories H I Survey

K. D. KUNTZ AND L. DANLY

Space Telescope Science Institute, 3700 San Martin Drive, Baltimore, Maryland 21218
Electronic mail: kuntz@stsci.edu, danly@stsci.edu

Received 1992 May 12; accepted 1992 September 3

ABSTRACT. This paper describes an approximate calculation of the far-sidelobe contamination present in the Bell Laboratories H I survey. The general method is to determine the position of the sidelobe, and to assume that the emission measured at the position of the sidelobe is free of contamination. The maximum possible contamination for a given velocity observed by the main beam is estimated to be the maximum emission within the sidelobe and within a velocity range determined by the motion of the earth, scaled by the antenna response. We have analyzed the errors introduced by saturation in the main beam and found them to be insignificant. The far-sidelobe contamination is shown to be less than 2×10^{16} cm^{-2} per km s^{-1} over most of the entire sky. The low level of far-sidelobe contamination suggests that such contamination does not affect results from studies of H I 21 cm radiation at high latitudes during the Bell Laboratories Survey. In particular, the low-column-density features of high-velocity and intermediate-velocity clouds can be deemed real.

1. INTRODUCTION

The Bell Laboratories H I Survey (Stark et al. 1992) provides complete coverage of the sky accessible from a latitude of 40° with a sensitivity of better than 10^{18} cm^{-2}. Although the beam size is too large ($2\overset{\circ}{.}5\times2\overset{\circ}{.}5$) for investigations of small-scale structure, the survey provides an invaluable tool for studies of the large-scale structure of neutral hydrogen both in the galactic disk and in the galactic halo. As the survey was executed with a horn telescope possessing very low-amplitude far sidelobes, it has been used to correct for sidelobe contamination in H I studies using other telescopes (Lockman et al. 1986; Burton 1992). Therefore, the Bell Laboratories Survey data both directly and indirectly form the basis of much of our understanding of the distribution of H I, particularly at high latitudes, and the uncertainties in the data must be carefully considered. For example, although the far-sidelobe response has a very small amplitude, were a far sidelobe to fall on the galactic disk during the observation of a very low-column-density region of the sky, far-sidelobe contamination could potentially affect the result significantly. Thus, it is important to understand the strength and location of the far-sidelobe contamination.

Developing an understanding of the nature and distribution of H I at high galactic latitudes is important for understanding the structure and evolution of our own galaxy, as well as the nature of other galaxies. For example, the amount of neutral hydrogen distributed at high z strongly affects the amount of ionizing radiation that is able to reach the halo. This parameter is of great importance to all models of the ionization of the Milky Way halo gas, and for determining the ionizing flux in the intergalactic medium. Additionally, much of the halo is occupied by low-column-density features at high and intermediate velocities, whose origin is quite uncertain, but whose presence is likely to be key in understanding the circulation of the galactic ISM through the galactic halo. As the column densities of these features is quite low, a detailed study of the nature of intermediate-velocity (IV) and high-velocity (HV) clouds (Kuntz and Danly 1992) depends on a careful understanding of the contamination by emission falling in the telescope sidelobes.

A complete correction of the Bell Laboratories data set would require the calculation of the earth's velocity vector at the time each spectrum was taken (information not readily available), as well as a detailed map of the beam pattern (which does not exist). As an approximation, we determine the maximum possible contamination for each velocity of each spectrum in the main beam from the spectra for the positions of the far sidelobes over the full range in velocity that could possibly be affected by contamination.

The second section of this paper reviews the method of observation used for the Bell Laboratories Survey, as well as previously published information on the far-sidelobe contamination. The third section contains the mathematical derivation of the beam to sidelobe transformation, the magnitude of the contamination, the uncertainties introduced by receiver saturation, and the computational method used to generate maps of the maximum possible sidelobe contamination. The fourth section presents maps of the far-sidelobe contamination over the entire sky. The contamination is shown to be less than 2×10^{16} cm^{-2} per km s^{-1} over most of the sky.

2. REVIEW OF DATA CHARACTERISTICS

The Bell Laboratories H I Survey was taken with the Crawford Hill horn telescope near Holmdale, New Jersey (latitude=40° $23\overset{\prime}{.}5$). The telescope has an alt-azimuth mounting and was situated such that the main beam was on the prime meridian and the main axis of the horn was due East–West. The beam size is $2\overset{\circ}{.}9\times1\overset{\circ}{.}9$ in the transverse

© 1992. Astronomical Society of the Pacific

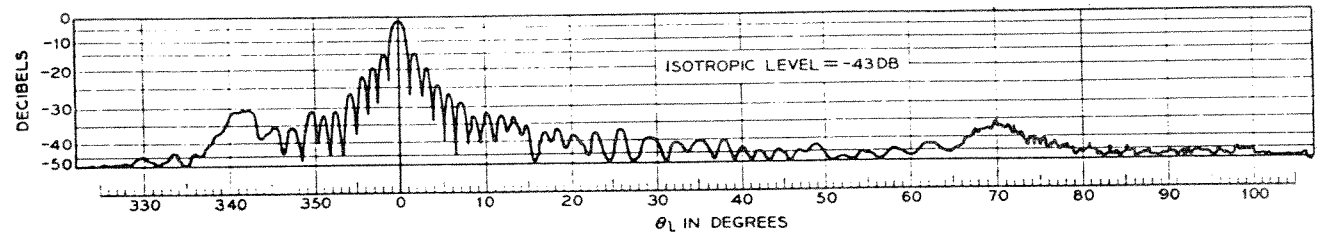

FIG. 1—Response at 6.175 GHz in the longitudinal polarization as a function of angle within the longitudinal plane. This figure is taken from Fig. 11 of Crawford et al. (1961). This is *not* a map of the response at 21 cm (1.420 GHz). (Copyright© 1961 AT&T. Reprinted with permission.)

polarization and $2\overset{\circ}{.}2 \times 2\overset{\circ}{.}4$ in the longitudinal polarization. (Both measurements are $\alpha \times \delta$ in degrees.) The receiver was positioned at the base of the horn such that the contribution from the longitudinal polarization was zero at an altitude of 45°. For observations south of the zenith, the receiver faced east; for observations north of the zenith the telescope was rotated so that the receiver faced west. This minimized the contribution of the longitudinal polarization at the poles. A more complete description of the telescope can be found in Crawford et al. (1961).

The data were taken as drift scans, meaning that the beam was placed at a given altitude and azimuth and the sky allowed to drift past. The data were summed over periods of time representing a drift of the sky by quarter of a beamwidth. The declination spacing of the drift scans was 2°. The data set consists of 22,261 individual spectra, each consisting of position data and spectral data. As the central velocities were not the same for all spectra, all the spectra had been rebinned to a uniform 5 km s^{-1} spacing, a spacing only slightly more narrow than the original 5.27 km s^{-1}. The most complete description of the observation method and the data set is found in Stark et al. (1992).

The absolute calibration agreed to within 2% with that done by Penzias et al. (1970) with the same telescope. The principal source of uncertainty was the baseline correction, which places a lower limit of believability at 3.5×10^{16} cm^{-2} per km s^{-1}. The upper limit of believability is set by the saturation of individual receiver channels at 1.4×10^{19} cm^{-2} per km s^{-1} (Stark et al. 1992). The existence of an upper limit to good data values introduces an inherent uncertainty into the calculation of the *maximum* far-sidelobe contamination. The full implications of this difficulty are addressed in Sec. 3.3.

There are two known far sidelobes. They exist in the longitudinal polarization but are nonexistent in the transverse polarization. The observing strategy minimized the contribution of the longitudinal polarization as much as possible. Given that the longitudinal plane passes through the receiver, the center of the parabolic reflector, and the position of the main beam on the sky, the far sidelobes would fall in that plane at angles of −18° and +70° from the line connecting the beam position and the center of the reflector. Here the negative sign indicates the direction towards the receiver with respect to the reflector. The −18° sidelobe is thought to be caused by the drive wheel or weather cover of the horn; the +70° sidelobe is thought to be caused by diffraction from the edge of the reflector. The geometry of the far sidelobes is described in Lockman et al. (1986) and Diplas and Savage (1991).

The exact position and strengths of the far sidelobes at 21 cm is not precisely known; the sidelobes have been mapped at 2.39 GHz (Fig. 1, taken from Crawford et al. 1961) 3.9 GHz, and 6.175 GHz (Butzien 1981), but have not been mapped at 1.420 GHz (21 cm). We expect the response at 21 cm to have roughly the same pattern with respect to position, but the amplitude of the response is not well determined (see Sec. 3.3).

Stark (1992) describes the far-sidelobe contamination as "present and not negligible" but does not provide a numerical estimate. Diplas and Savage (1991) do not estimate the far-sidelobe contamination, as, for their work, it was not as significant as other systematic problems. Lockman et al. (1986) estimates that the worst possible contamination from the far sidelobes, occurring when the sidelobe is in the galactic disk, would be 8×10^{18} cm^{-2}, but that a "more typical" value would be 5×10^{17} cm^{-2}, where the contamination is presumably integrated over the entire velocity range. The principal difference between our characterization of the far-sidelobe contamination, and that presented by Lockman et al. (1986) is that ours presents the "worst-case" sidelobe contamination as a function of both velocity and position, rather than the average and worst-case contamination for the entire sky. Knowledge of the position and velocity of the far-sidelobe contamination is essential for the evaluation both of the overall distribution of gas at high latitudes and of individual low-column-density features, such as intermediate- and high-velocity clouds.

3. CONSTRUCTING CONTAMINATION MAPS

The far-sidelobe contamination for a particular main beam observation is the emission that falls within the sidelobe multiplied by the antenna response. Of course, the emission measured at the position of a far sidelobe is itself contaminated by its sidelobe response. However, since the far-sidelobe contamination always adds emission, and never removes it, the measure of the emission at the position of a far sidelobe is an upper limit on the contamination of the measure at the position of the main beam. Further, the antenna response at the far sidelobes is several times 10^{-3}, so the "second-order" contamination introduced by an overestimation of emission in the far sidelobe has an equivalent antenna response of 10^{-6}. Thus, the measure-

ment at the position of the far sidelobe, scaled by the antenna response, is a very good upper limit to the true far-sidelobe contamination. To do better one would really need to perform a deconvolution of the entire data set, some 22,261 spectra. Given the uncertainty of the sidelobe position and amplitudes, as well as the saturation at the high-column densities most likely to produce far-sidelobe contamination, such a deconvolution does not seem warranted.

Because of the rotation of the earth and the earth's revolution about the sun, the far-sidelobe response of the telescope adds emission to the main beam at a velocity that is shifted with respect to the main beam velocity scale. The emission detected in the sidelobe can be shifted as much as ± 32.5 km s^{-1} from its true velocity. No attempt is made here to determine the amount by which the sidelobe emission *was* shifted: such a calculation requires information about the time and date of each observation and calculations of the earth's motion. Rather, our analysis determines the maximum amount of emission within the range in which the velocity *could have been* shifted. To construct a map of the contamination at a particular velocity, then, one should take the maximum emission within ± 32.5 km s^{-1} of that velocity. Since the data were binned in 5 km s^{-1} bins, the emission in a far sidelobe at a particular velocity was taken to be the maximum emission within ± 35 km s^{-1} of that velocity.

Constructing a map of the far-sidelobe contamination at a given velocity can be divided into several discrete tasks. The first task is the strictly mathematical operation of determining the position of the far sidelobes from the position of a given main beam and *vice versa*. This derivation is given in Sec. 3.1. The second task is to derive a map of the emission in the far sidelobes from a map of the emission in the main beam, that is, to apply the results of the first task to the entire data set. There are two different approaches to this problem, essentially a question of the direction in which to apply the main beam–far-sidelobe transformation, which are discussed in Sec. 3.2. Finally one must scale the emission in each of the far sidelobes by the antenna response, which is a function of the telescope orientation. This is discussed in Sec. 3.3.

3.1 Derivation of the Beam-to-Lobe Transformation

The relation linking the position of the far sidelobes to the position of the main beam is in telescope coordinates. This relation can be converted to a relation in altitude and azimuth, and thus to right ascension and declination and to galactic coordinates. The derivation given below is from telescope coordinates to altitude and azimuth.

The main beam was always kept on the prime meridian, removing one free variable. Given the altitude of the beam, we wish to determine the altitude and azimuth of the far sidelobes. Both the longitudinal plane and the plane meridian describe great circles on the sky: their intersection is a right angle. The geometry of the relation is simple, and is shown in Fig. 2. If θ is the angle between the main beam and the sidelobe, and z_b is the zenith angle of the main

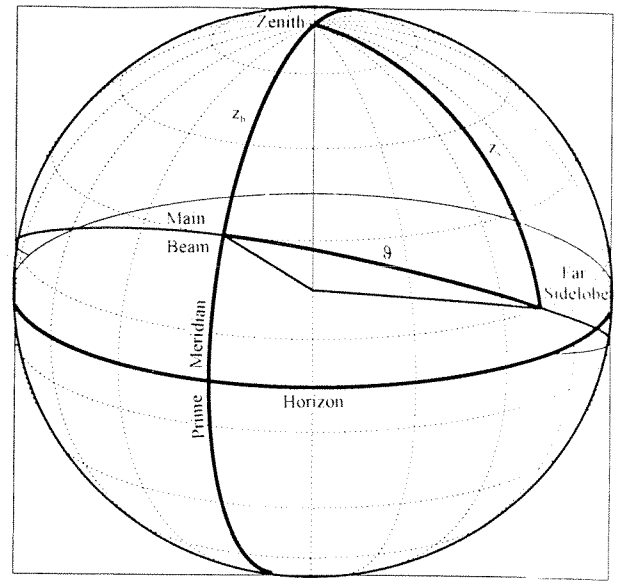

FIG. 2—Geometry of the main beam to far-sidelobe relation in both telescope coordinates and the altitude and azimuth coordinate system.

beam, then the zenith angle of the sidelobe z_s is given by

$$\cos(z_s) = \cos(z_b)\cos\theta + \sin(z_b)\sin\theta\cos(\pi/2),$$

which reduces to

$$\cos(z_s) = \cos(z_b)\cos\theta.$$

The azimuth of the far sidelobe A is given by

$$\sin(A)/\sin\theta = \sin(\pi/2)/\sin(z_s),$$

which reduces to

$$\sin(A) = \sin\theta/\sin(z_s).$$

The position of each spectrum is known, so z_s can be easily calculated from the declination. As the main beam is always on the prime meridian, the transformation of the far-sidelobe position from alt-azimuth coordinates to either celestial or galactic coordinates, given the main beam position in either of those systems, is standard.

Figure 3 is a plot of far-sidelobe position as a function of main-beam position. The central vertical line represents the prime meridian upon which the main beam is always set. Each slanted line connects a main-beam position, in declination and hour angle (always zero since the main beam is always on the prime meridian) with the position of the far sidelobe in declination and hour angle. The plot shows both far sidelobes. The break at a declination of 40°N is the result of the telescope being rotated 180° when observations passed from one side of the zenith to the other. Note that the declinations covered by the +70° far sidelobe is much smaller than the range of declinations covered by the main-beam observations. The range covered by the −18° far sidelobe is also smaller than the range of declinations covered by the main beam, but the restriction is not so extreme. Thus, *not all portions of the sky are able to contribute to the far-sidelobe contamination.*

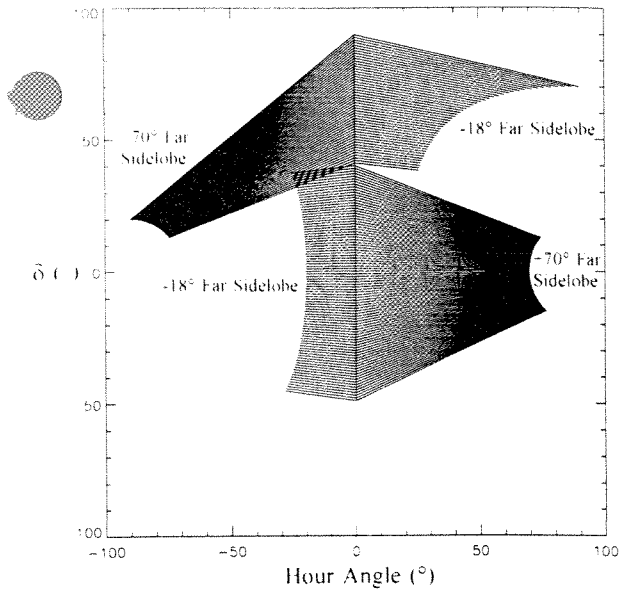

FIG. 3—Plot of the position of the two far sidelobes as a function of the position of the main beam. The horizontal axis is hour angle (in degrees). The vertical axis is declination (in degrees). See text for a full explanation.

3.2 The Computational Method

There are two methods by which one can transform the entire data set from a map of emission in the main beam to a map of the emission in a far sidelobe. The following section describes the two methods and provides a rationale for choosing the computationally more intense.

The first, and computationally simpler method to transform the data set to a map of far-sidelobe emission, is to take the position of each spectrum, assume that that position is in a far sidelobe for *some* main beam, calculate the position of that main beam, and substitute that position for the original position. As there are two far sidelobes, one must take the original data set and transform it once for each sidelobe. The spectra are multiplied by the response and added at a later step in the process.

The second, more computationally intensive method is to take the position of a spectrum in the main beam, determine the position of the sidelobe, find the spectrum closest to that position, and substitute that spectral data for the original spectral data. Again, the original data set must be transformed separately for each sidelobe. This method requires much more computation time than the first, by a factor of about 8.

Since the part of the sky contributing to the far-sidelobe emission is much smaller than the entire sky, mapping the far-sidelobe contamination essentially spreads a small subset of the data points over a much larger area. The first computational method produces the correct sidelobe emission spectrum, but only for a limited number of map points. To produce a complete map of the sidelobe emission, one would have to interpolate all intervening map points. The second computational method provides only the approximate sidelobe emission spectra, but provides spectra for every map point. The second algorithm is not providing any more information; it essentially incorporates a form of interpolation into the transformation process and provides a more convenient product. Thus the preference for the second algorithm.

3.3 The Magnitude of the Contamination

The emission in a far sidelobe must be scaled by two factors to determine the contamination; the response of the far sidelobe, and the contribution of the longitudinal polarization. The latter of these quantities is given by Stark et al. (1992) as the factor

$$\sin^2(\text{elevation} - 45°),$$

where the elevation is that of the main beam. The responses of the far sidelobes used were 0.006 and 0.001 of the total response for the $-18°$ and $+70°$ sidelobes, respectively (Stark et al. 1992).

We formed a data cube of the far-sidelobe emission for each far sidelobe, two of whose axes were spatial dimensions, the third axis being the velocity. The spatial bin was about $2\overset{\circ}{.}5 \times 2\overset{\circ}{.}5$ (similar to the spatial resolution) and contained the sum of two or three spectra; the velocity bin size was 5 km s^{-1}. The longitudinal polarization contribution scaling was done in the process of forming the data cube from the individual spectra. The data cube was then multiplied by the antenna response and divided by the velocity width. The last operation was to convert the emission to the units cm^{-2} per km s^{-1}. Thus, the resultant contamination maps can be easily applied to any (main-beam) map that has the same central velocity and a small ($\Delta v \lesssim 20$ km s^{-1}) velocity width.

Finally, we compute the effects of the velocity shift described in Sec. 3. From the data cube a 70 km s^{-1} wide slice centered upon the velocity of interest was extracted. The maximum possible far-sidelobe contamination for a map position was taken to be the maximum emission at that map position, within the 70 km s^{-1} velocity range.

The saturation at high-column densities introduces an uncertainty into the formulation. Although this uncertainty affects only regions where the emission within the sidelobe is over 1.4×10^{19} cm^{-2} per km s^{-1}, one cannot simply take all the sidelobe emission over a certain threshold to be uncertain, because of both the elevation-dependent factor and the summation of more than one far sidelobe to produce the final far-sidelobe contamination. Instead, the uncertainty due to saturation exists at all intensities of far-sidelobe contamination, but only in certain locations.

The magnitude of the uncertainty introduced by the saturation at high column densities was determined by comparing individual saturated spectra from the Bell Laboratories Survey with spectra taken of four calibration regions by Williams (1973). The Bell Laboratories spectra were not taken at exactly the same positions as the calibration spectra; three are within $0\overset{\circ}{.}5$ of their respective calibration spectra, and the fourth is within $0\overset{\circ}{.}75$. The beam size of the Williams spectra was 35′, and the velocity resolution was 2.11 km s^{-1}, significantly different from the

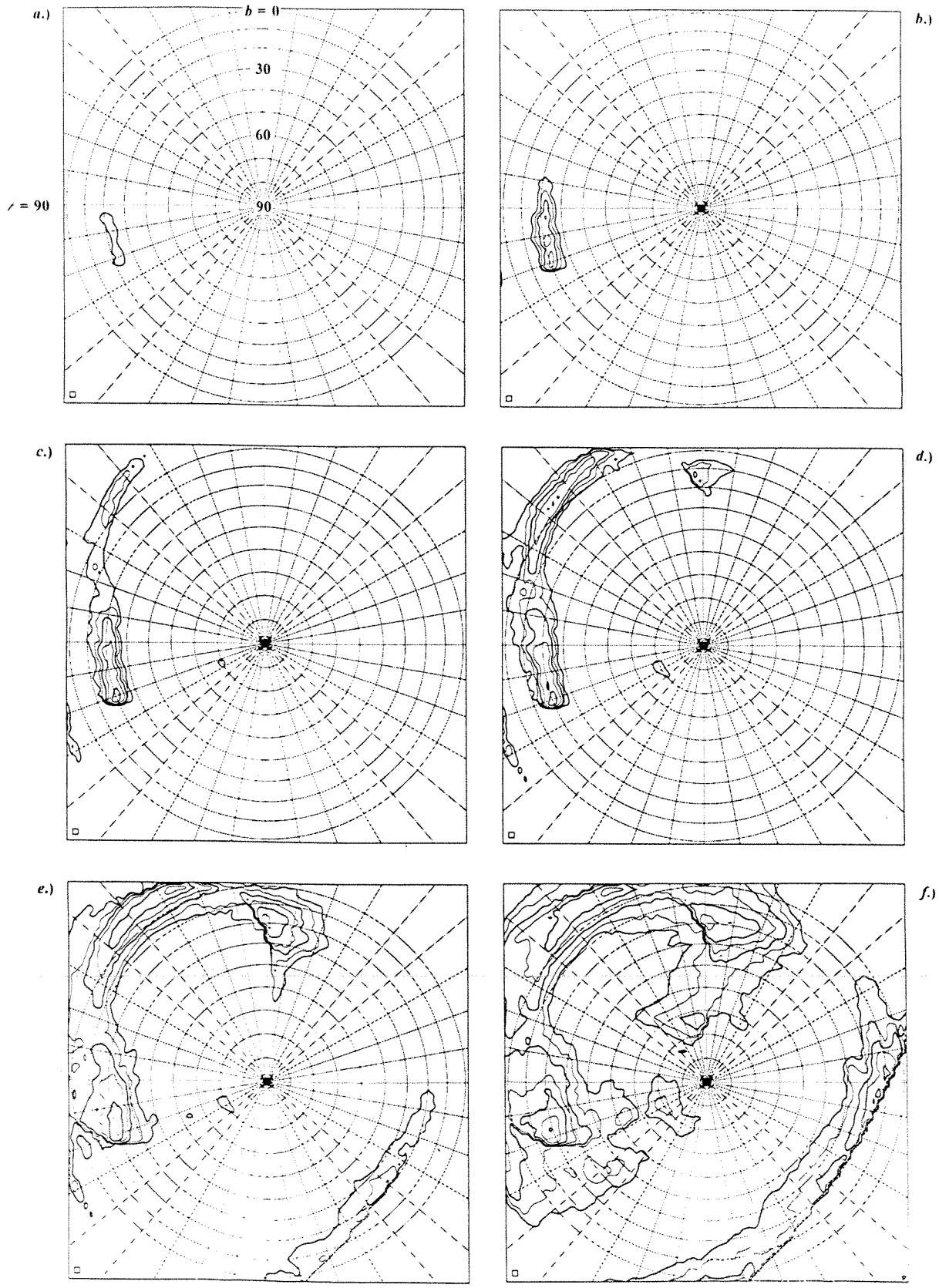

FIG. 4—The sidelobe contamination in the northern galactic hemisphere. Galactic latitude is $l=0°$ at the bottom and increases clockwise. The pole is at the center; the lowest galactic latitude plotted is $b=0°$. The coordinate grid spacing is 10°. The contour levels are 2×10^{16}, 3.6×10^{16}, 6.4×10^{16}, 1.1×10^{16}, 2×10^{17}, 3.6×10^{17}, 6.4×10^{17}, 1.1×10^{17} cm^{-2} per km s^{-1}. The velocity of each panel is (a) -150 km s^{-1}, (b) -125 km s^{-1}, (c) -100 km s^{-1}, (d) -75 km s^{-1}, (e) -50 km s^{-1}, (f) -25 km s^{-1}, (g) 0 km s^{-1}, (h) 25 km s^{-1}, (i) 50 km s^{-1}, (j) 75 km s^{-1}, (k) 100 km s^{-1}, (l) 125 km s^{-1}.

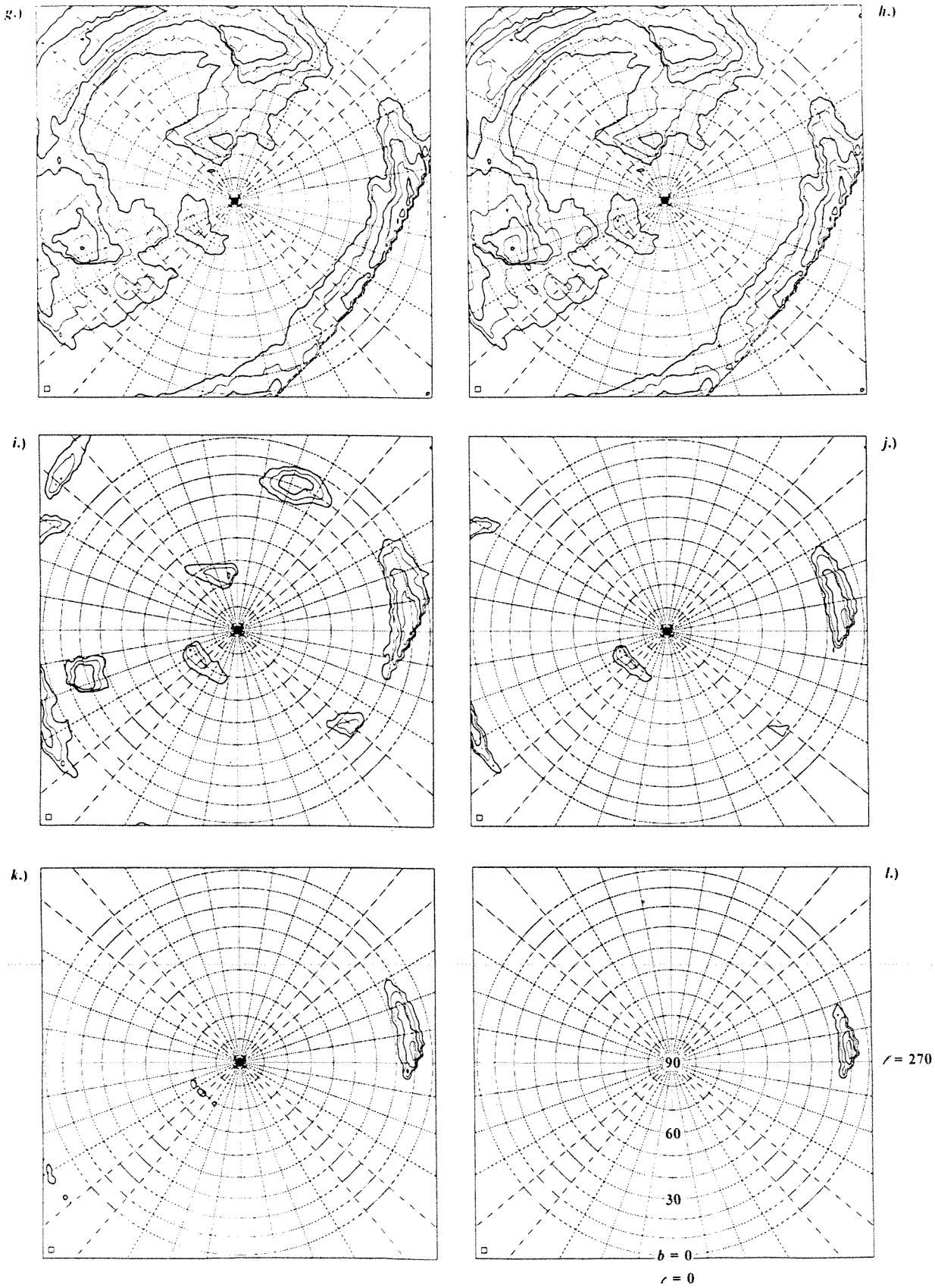

FIG. 4—(Continued)

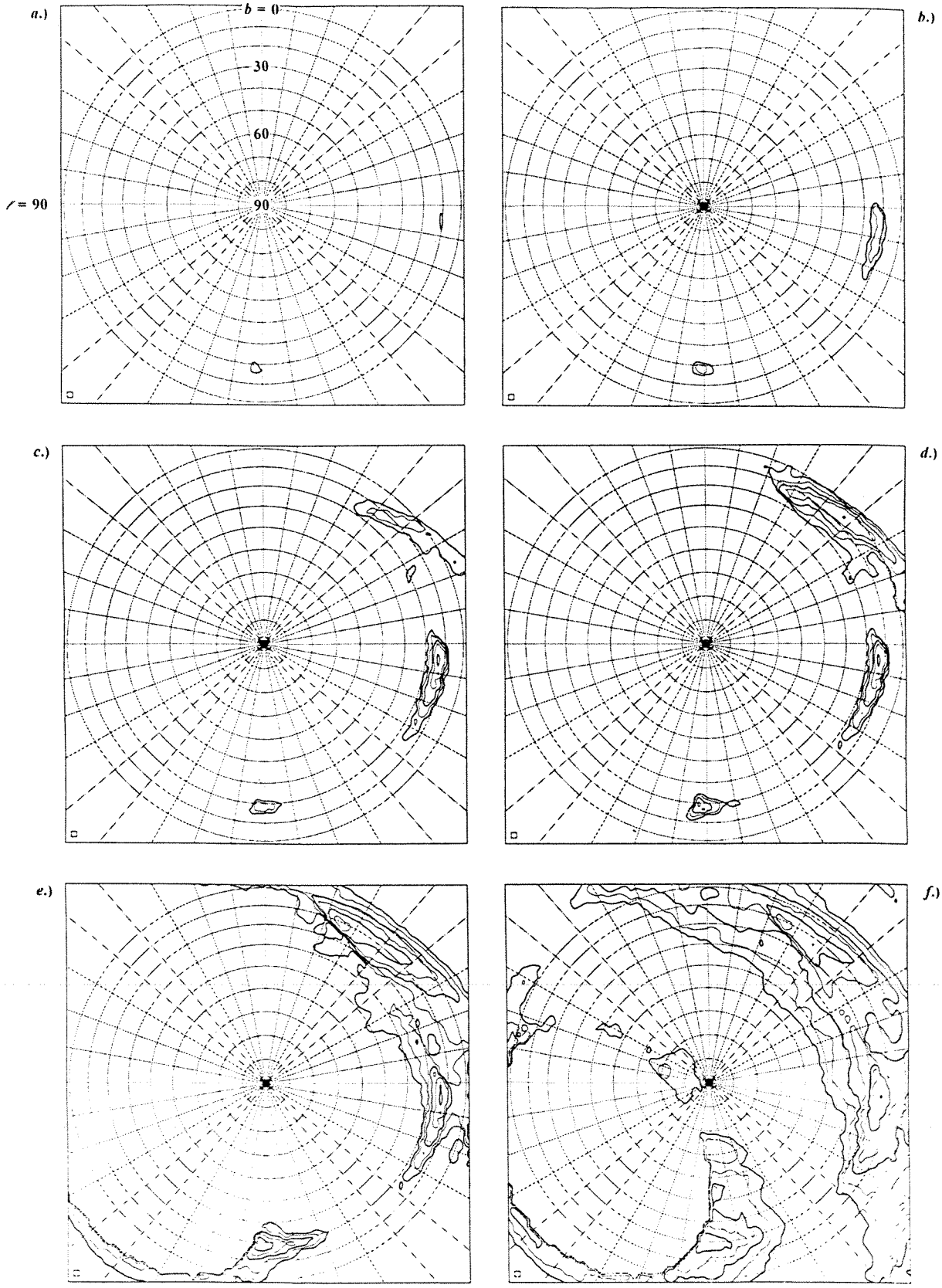

FIG. 5—The sidelobe contamination in the southern galactic hemisphere. Galactic latitude is $l=0°$ at the bottom and increases counter-clockwise. The pole is at the center; the greatest galactic latitude plotted is $b=0°$. The coordinate grid spacing is 10°. The contour levels are 2×10^{16}, 3.6×10^{16}, 6.4×10^{16}, 1.1×10^{16}, 2×10^{17}, 3.6×10^{17}, 6.4×10^{17}, 1.1×10^{17} cm^{-2} per km s^{-1}. The velocity of each panel is (a) -150 km s^{-1}, (b) -125 km s^{-1}, (c) -100 km s^{-1}, (d) -75 km s^{-1}, (e) -50 km s^{-1}, (f) -25 km s^{-1}, (g) 0 km s^{-1}, (h) 25 km s^{-1}, (i) 50 km s^{-1}, (j) 75 km s^{-1}, (k) 100 km s^{-1}, (l) 125 km s^{-1}.

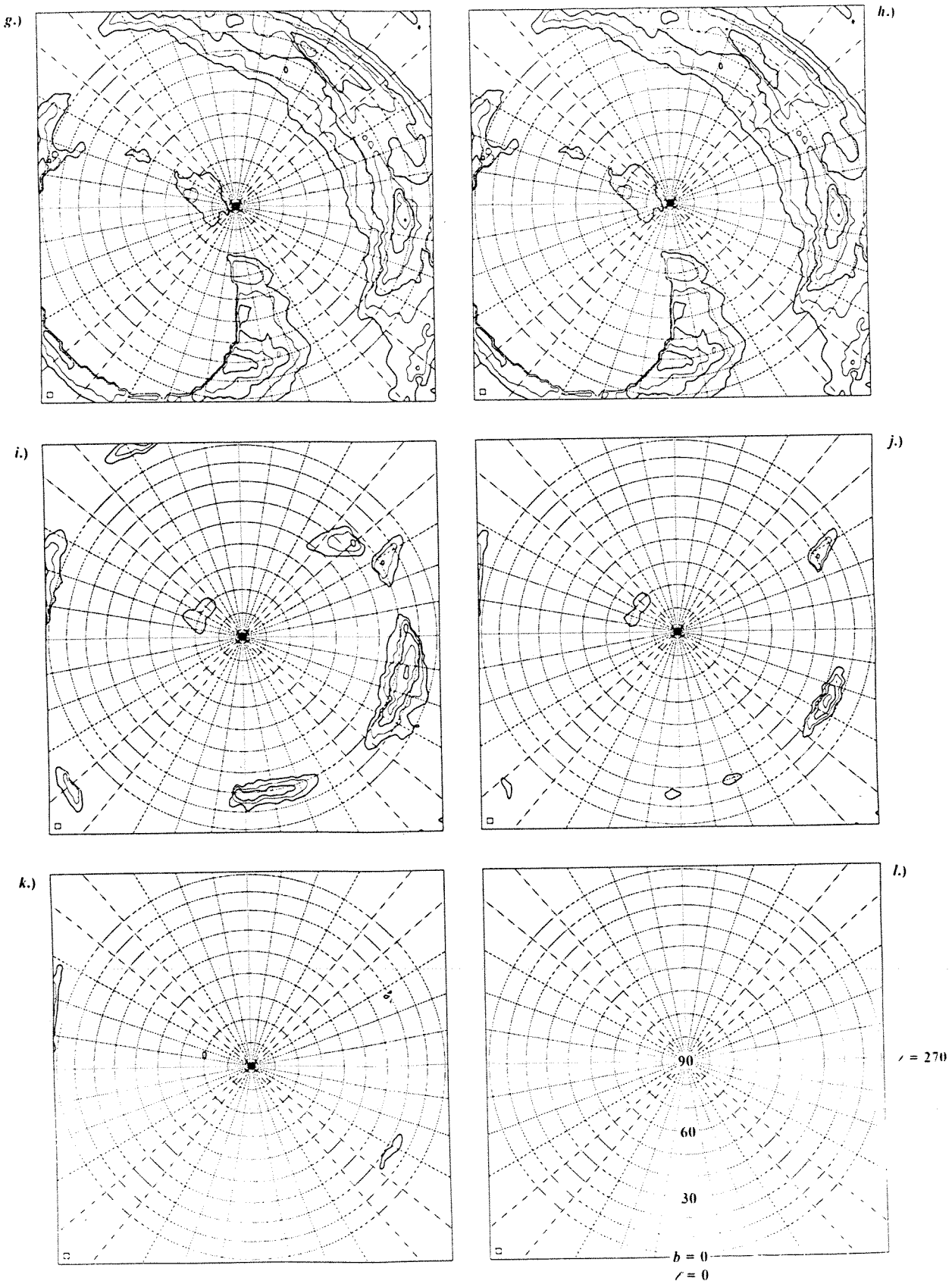

FIG. 5—(Continued)

Bell Laboratories Survey. However, no systematic uncertainties are introduced by these differences. A direct comparison of peak brightness temperatures for the four calibration areas shows that the saturated receiver elements must be increased by only a factor of 1.1–1.6 to match the true brightness temperatures. For no spectrum was the Bell Laboratories flux greater than that of the calibration spectrum, and there was no correlation between brightness temperature and the degree of saturation. As the contour levels in the contamination maps are separated by a factor of 1.78 ($=10^{0.25}$), the uncertainty introduced by saturation must be less than or equal to one contour interval, and the true value will be higher than that shown in the maps.

The saturation affects only limited areas of the sky, and then only at lower velocities. By -50 km s^{-1}, the uncertainty introduced by saturation is virtually nonexistent. Thus, the uncertainty in the far-sidelobe contamination has little, if any, impact on the scientific aims of this study.

4. THE CONTAMINATION MAPS

Figure 4 shows the far-sidelobe contamination at 25 km s^{-1} intervals from -150 to $+125$ km s^{-1} for the North Galactic Pole. Figure 5 presents the same maps for the southern galactic hemisphere. The contour levels are logarithmic: 2×10^{16}, 3.6×10^{16}, 6.4×10^{16}, 1.1×10^{16}, 2×10^{17}, 3.6×10^{17}, 6.4×10^{17}, 1.1×10^{17} cm^{-2} per km s^{-1}. The maps were created by mapping the contamination in both far sidelobes and adding the two sets of maps. The coordinate grid is a polar equal area projection of the galactic coordinate system: $l=0°$ is at the bottom and l increases clockwise for the northern hemisphere, counterclockwise for the southern hemisphere. The lowest galactic

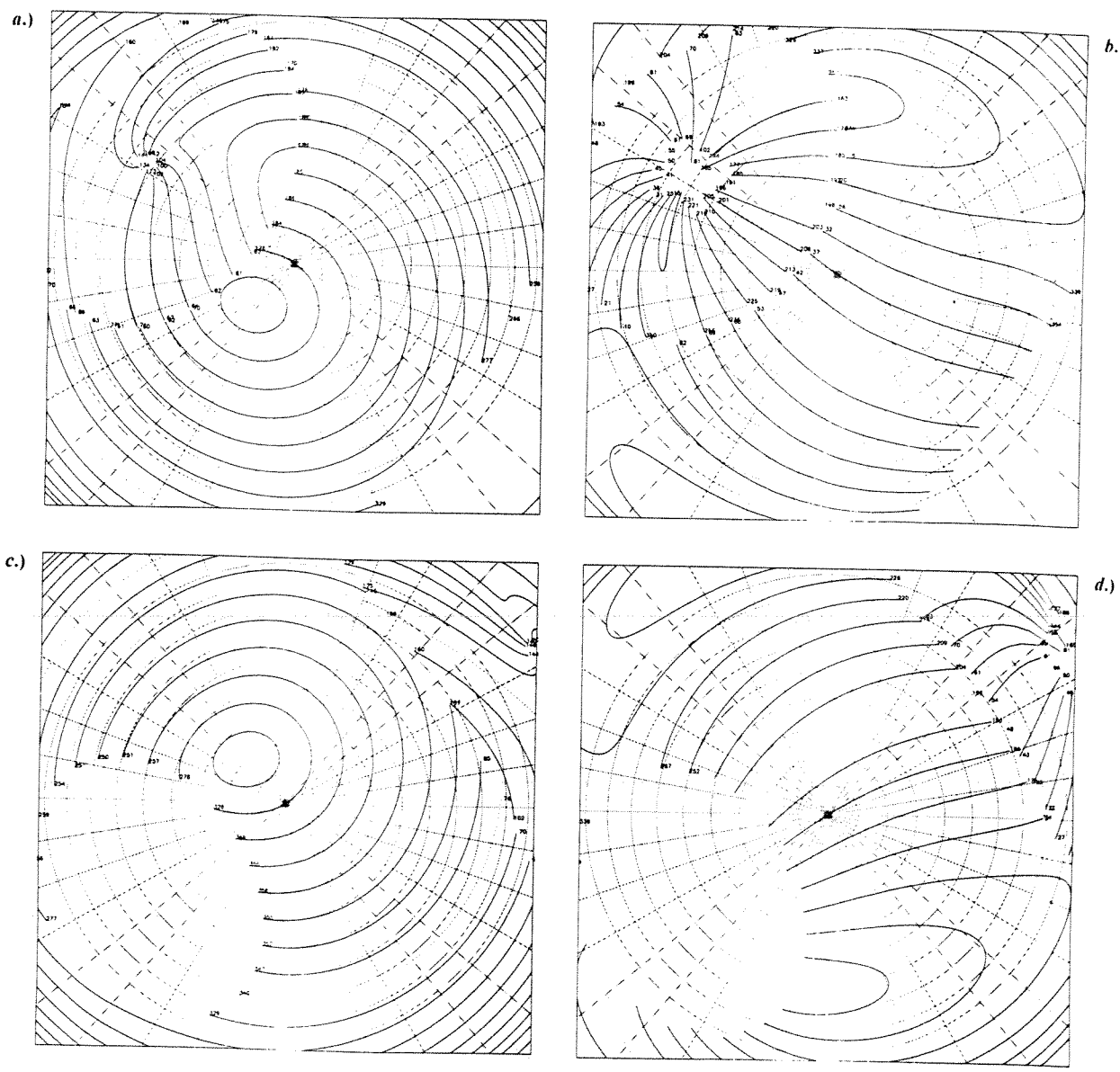

FIG. 6—Plots of the galactic latitude of the far sidelobes as a function of the position of the main beam. The light lines are the galactic coordinate system as in Figs. 5 and 6. The solid lines are lines of constant galactic latitude for the far sidelobe. The dotted line is the galactic equator as it appears in the far sidelobe. (a) Northern galactic hemisphere, $-18°$ sidelobe, (b) northern galactic hemisphere, $+70°$ sidelobe, (c) southern galactic hemisphere, $-18°$ sidelobe, (d) southern galactic hemisphere, $+70°$ sidelobe.

latitude plotted is $b=0°$; the pole is at the center. The coordinate grid interval is 10°. The sharp cutoff in the upper left and lower right of the northern galactic hemisphere maps are due to the horizon. The same is true of the sharp cutoff defining the large elliptical void between $l=250°$ and $l=0°$ in the southern galactic hemisphere maps. Note that due to the geometry of the sidelobes, there are no main-beam observations for which the sidelobes are not measured. Conversely, those regions of the map containing no data about the sidelobes due to the horizon contain no main-beam data either.

To aid the understanding of the contamination maps, Fig. 6(a) depicts the galactic latitude that falls within the $-18°$ far sidelobe. As in Figs. 4 and 5, the polar coordinates trace the position of the main beam. The bold lines show the galactic latitude of the corresponding far sidelobe. This panel contains the northern galactic hemisphere. The dotted line is the galactic equator as observed by the far sidelobe. Figure 6(b) contains a similar plot for the $+70°$ sidelobe. Figures 6(c) and 6(d) contain similar plots for the southern galactic hemisphere. As one might expect, the dotted lines (the galactic equator) in the panels of Fig. 6 are a good guide to the regions of the most intense contamination in Figs. 4 and 5. Figure 6 also indicates the positions of the horizons.

5. DISCUSSION

From Figs. 4 and 5, it can be seen that only very small portions of the sky are afflicted with contamination greater than 2×10^{17} cm^{-2} per km s^{-1}. In fact, for most of the sky, the contamination is less than 2×10^{16} cm^{-2} per km s^{-1}. The baseline uncertainties, although sometimes as large as 0.1 K, are more generally 0.05 K (2×10^{16} cm^{-2} per km s^{-1}) or better (Stark et al. 1992). Thus, for most of the sky, the sidelobe contamination is comparable to or less than the baseline uncertainty.

The restricted area of significant far-sidelobe contamination (column densities $>2\times10^{17}$ cm^{-2} per km s^{-1}) is due to two factors. First, only one far sidelobe contributes the bulk of the contamination. Since the $+70°$ far sidelobe "sees" only a narrow ban of declinations near $\delta=0°$ (Fig. 3), it can only contribute contamination from the very small areas where the celestial equator crosses the galactic disk. The $-18°$ far sidelobe contributes most of the contamination because it "sees" more of the sky, and because it has a larger antenna response. Second, the portion of the galactic disk with column densities greater than 2×10^{20} cm^{-2} per km s^{-1} (and thus capable of providing contamination of 2×10^{17}) is very thin in galactic latitude, has a restricted range of galactic longitudes, as well as a restricted velocity range.

The maps of the far-sidelobe contamination presented here demonstrate the reality of many low-column-density features whose previous existence had been questionable, due to the uncertain nature of the far-sidelobe contamination. Since the far-sidelobe contamination is negligible for $b>30°$, $v>$ 25 km s^{-1}, studies of most high-velocity clouds, the intermediate-velocity complex, and other low-column-density features at high galactic latitudes are essentially free of far-sidelobe contamination. The far-sidelobe contamination calculated here will be important for estimating the uncertainty of small-beam corrections made with the Bell Laboratories data.

We would like to thank K. Jahoda and A. Diplas for several interesting conversations about sidelobe contamination in the Bell Laboratories Survey, A. Stark for sending us a preprint of his paper in advance of publication, and the AT&T Technical Journal for permission to reproduce Fig. 1. We would also like to thank the anonymous referee for his useful comments. This work was supported through NASA grant NAG-1433 to LD.

REFERENCES

Burton, W. B. 1992, private communication
Butzien, P. E. 1981, Bell System Tech. J., 60, 913
Crawford, A. B., Hogg, D. C., and Hunt, L. E. 1961, Bell System Tech. J., 44, 1095
Diplas, A., and Savage, B. D. 1991, ApJ, 377, 126
Kuntz, K. D., and Danly, L. 1992, in preparation
Lockman, F. J., Jahoda, K., and McCammon, D. 1986, ApJ, 302, 432
Penzias, A. A., Wilson, R. W., and Encrenaz, P. J. 1970, AJ, 75, 141
Stark, A. A., Gammie, C. F., Wilson, R. W., Bally, J., Linke, R. A., Heiles, C., and Hurwitz, M. 1992, ApJS, 79, 77
Williams, D. R. W. 1973, A&AS, 8, 505

```
#!/bin/csh
#
# A script file to read FITS files of Bell Labs HI Survey from tape
#
# Usage: bltape tapedev n
# where bltape  is the name of this file
#       tapedev is the non-rewind device name, e.g. /dev/nrst1
#       n       is the number of files you want to read
#
#
mt -f /dev/nrsx0 rew
echo 'finished rewind'
@ i = 1
while ($i <= $2)
        dd if=$1 of=blfits.$i ibs=28800
        @ i = $i + 1
end
```

Dump of device 1MUA81: on 13-MAY-1994 14:59:25.96

Block number 1 (00000001), 28800 (7080) bytes

```
 2F205420 20202020 20202020 20202020 20202020 2020203D 2020454C 504D4953 SIMPLE  =                    T / 000000
 20202020 20202020 20202020 20202020 20202020 20202020 20202020 20202020                                 000020
 20202020 2020203D 20205849 50544942 20202020 20202020 20202020 20202020                 BITPIX  =       000040
 20202020 20202020 20202020 20202020 2F203631 20202020 20202020 20202020             16 /                000060
 20202020 20202020 20202020 20202020 20202020 20202020 20202020 20202020                                 000080
 2F203320 20202020 20202020 20202020 20202020 202020 3D 20202053 4958414E NAXIS   =                    3 / 0000A0
 20202020 20202020 20202020 20202020 20202020 20202020 20202020 20202020                                 0000C0
 20202020 2020203D 20203153 4958414E 20202020 20202020 20202020 20202020                 NAXIS1  =       0000E0
 20202020 20202020 20202020 20202020 2F203030 38202020 20202020 20202020            800 /                000100
 20202020 20202020 20202020 20202020 20202020 20202020 20202020 20202020                                 000120
 2F203030 34202020 20202020 20202020 20202020 2020203D 20203253 4958414E NAXIS2  =                  400 / 000140
 20202020 20202020 20202020 20202020 20202020 20202020 20202020 20202020                                 000160
 20202020 2020203D 20203353 4958414E 20202020 20202020 20202020 20202020                 NAXIS3  =       000180
 20202020 20202020 20202020 20202020 2F203120 20202020 20202020 20202020              1 /                0001A0
 20202020 20202020 20202020 20202020 20202020 20202020 20202020 20202020                                 0001C0
 2F202020 20202020 20202020 27202020 204E4F4C 4727203D 20203145 50595443 CTYPE1  = 'GLON    '           / 0001E0
 20202020 20202020 20202020 20202020 20202020 20202020 20202020 20202020                                 000200
 20202020 2020203D 2020314C 41565243 20202020 20202020 20202020 20202020                 CRVAL1  =       000220
 20202020 20202020 20202020 20202020 2F203030 30303030 30302E30 20202020     0.00000000 /                000240
 20202020 20202020 20202020 20202020 20202020 20202020 20202020 20202020                                 000260
 2F203430 32333635 3035342E 302D2020 20202020 2020203D 20203154 4C454443 CDELT1  =         -0.450563204 / 000280
 20202020 20202020 20202020 20202020 20202020 20202020 20202020 20202020                                 0002A0
 20202020 2020203D 20203158 49505243 20202020 20202020 20202020 20202020                 CRPIX1  =       0002C0
 20202020 20202020 20202020 20202020 2F203030 30303030 2E303038 20202020     800.000000 /                0002E0
 20202020 20202020 20202020 20202020 20202020 20202020 20202020 20202020                                 000300
 2F203030 30303030 30302E30 20202020 20202020 2020203D 20203141 544F5243 CROTA1  =           0.00000000 / 000320
 20202020 20202020 20202020 20202020 20202020 20202020 20202020 20202020                                 000340
 2054414C 4727203D 20203245 50595443 20202020 20202020 20202020 20202020                 CTYPE2  = 'GLAT 000360
 20202020 20202020 20202020 20202020 2F202020 20202020 20202020 27202020     '                  /        000380
 20202020 20202020 20202020 20202020 20202020 20202020 20202020 20202020                                 0003A0
 2F203030 30303030 30302E30 20202020 20202020 2020203D 2020324C 41565243 CRVAL2  =           0.00000000 / 0003C0
 20202020 20202020 20202020 20202020 20202020 20202020 20202020 20202020                                 0003E0
 20202020 2020203D 20203254 4C454443 20202020 20202020 20202020 20202020                 CDELT2  =       000400
 20202020 20202020 20202020 20202020 2F203032 38373231 3135342E 30202020     0.451127820 /               000420
 20202020 20202020 20202020 20202020 20202020 20202020 20202020 20202020                                 000440
 2F203030 30303035 2E303032 20202020 20202020 2020203D 20203258 49505243 CRPIX2  =           200.500000 / 000460
 20202020 20202020 20202020 20202020 20202020 20202020 20202020 20202020                                 000480
 20202020 2020203D 20203241 544F5243 20202020 20202020 20202020 20202020                 CROTA2  =       0004A0
 20202020 20202020 20202020 20202020 2F203030 30303030 30302E30 20202020     0.00000000 /                0004C0
 20202020 20202020 20202020 20202020 20202020 20202020 20202020 20202020                                 0004E0
 2F202020 20202020 20202020 2752534C 2D4F4C45 4627203D 20203345 50595443 CTYPE3  = 'FELO-LSR'          / 000500
 20202020 20202020 20202020 20202020 20202020 20202020 20202020 20202020                                 000520
 20202020 2020203D 2020334C 41565243 20202020 20202020 20202020 20202020                 CRVAL3  =       000540
 20202020 20202020 20202020 20202020 2F203030 302E3030 30303633 2D202020    -360000.000 /                000560
 20202020 20202020 20202020 20202020 20202020 20202020 20202020 20202020                                 000580
 2F203030 30302E30 30303031 20202020 20202020 2020203D 20203354 4C454443 CDELT3  =           10000.0000 / 0005A0
 20202020 20202020 20202020 20202020 20202020 20202020 20202020 20202020                                 0005C0
 20202020 2020203D 20203358 49505243 20202020 20202020 20202020 20202020                 CRPIX3  =       0005E0
 20202020 20202020 20202020 20202020 2F203030 30303030 30302E30 20202020     0.00000000 /                000600
 20202020 20202020 20202020 20202020 20202020 20202020 20202020 20202020                                 000620
 2F203030 30303030 30302E30 20202020 20202020 2020203D 20203341 544F5243 CROTA3  =           0.00000000 / 000640
 20202020 20202020 20202020 20202020 20202020 20202020 20202020 20202020                                 000660
 20202020 2020203D 2020204B 4E414C42 20202020 20202020 20202020 20202020                 BLANK   =       000680
 20202020 20202020 20202020 20202020 2F203836 3732332D 20202020 20202020         -32768 /                0006A0
 20202020 20202020 20202020 20202020 20202020 20202020 20202020 20202020                                 0006C0
 2F203530 2D453137 38303534 34312E32 20202020 2020203D 2020454C 41435342 BSCALE  =       2.14450871E-05 / 0006E0
```

```
20202020 20202020 20202020 20202020 20202020 20202020 20202020 20202020                                  000700
20202020 2020203D 2020204F 52455A42 20202020 20202020 20202020 20202020                 BZERO   =        000720
20202020 20202020 20202020 20202020 2F203839 36353436 3831312E 30202020    0.118645698 /                 000740
20202020 20202020 20202020 20202020 20202020 20202020 20202020 20202020                                  000760
2F202020 20202020 20202020 27202053 2F4D4B2D 4B27203D 20202054 494E5542 BUNIT   = 'K-KM/S  '           / 000780
20202020 20202020 20202020 20202020 20202020 20202020 20202020 20202020                                  0007A0
20202020 2020203D 2058414D 41544144 20202020 20202020 20202020 20202020                 DATAMAX =        0007C0
20202020 20202020 20202020 20202020 2F203536 38363333 3132382E 30202020    0.821336865 /                 0007E0
20202020 20202020 20202020 20202020 20202020 20202020 20202020 20202020                                  000800
2F203037 34353430 3438352E 302D2020 20202020 2020203D 204E494D 41544144 DATAMIN =         -0.584045470 / 000820
20202020 20202020 20202020 20202020 20202020 20202020 20202020 20202020                                  000840
35302F38 3127203D 20202020 45544144 20202020 20202020 20202020 20202020                 DATE    = '18/05 000860
20202020 20202020 20202020 20202020 2F202020 20202020 20202020 2731392F /91'           /                 000880
20202020 20202020 20202020 20202020 20202020 20202020 20202020 20202020                                  0008A0
2F202020 20202020 20202020 2720204D 37204C54 4227203D 504F4353 454C4554 TELESCOP= 'BTL 7M  '           / 0008C0
20202020 20202020 20202020 20202020 20202020 20202020 20202020 20202020                                  0008E0
54495420 424D4F43 2059524F 54534948 20202020 20202020 20202020 20202020                 HISTORY COMB TIT 000900
20202020 20202020 20353533 2D2C3536 332D2056 642A5420 20302E49 4820454C LE HI.0  T*dV -365,-355          000920
20202020 20202020 20202020 20202020 20202020 20202020 20202020 20202020                                  000940
6372203A 69672030 30323A72 69204D41 52415020 424D4F43 2059524F 54534948 HISTORY COMB PARAM ir:200 gi: rc 000960
20202020 20202020 20202020 20202020 20202020 20202020 20202020 2020203A :                               000980
20202020 20202020 20202020 20444E45 20202020 20202020 20202020 20202020                 END              0009A0
20202020 20202020 20202020 20202020 20202020 20202020 20202020 20202020                                  0009C0
20202020 20202020 20202020 20202020 20202020 20202020 20202020 20202020                                  0009E0
20202020 20202020 20202020 20202020 20202020 20202020 20202020 20202020                                  000A00
20202020 20202020 20202020 20202020 20202020 20202020 20202020 20202020                                  000A20
20202020 20202020 20202020 20202020 20202020 20202020 20202020 20202020                                  000A40
20202020 20202020 20202020 20202020 20202020 20202020 20202020 20202020                                  000A60
20202020 20202020 20202020 20202020 20202020 20202020 20202020 20202020                                  000A80
20202020 20202020 20202020 20202020 20202020 20202020 20202020 20202020                                  000AA0
20202020 20202020 20202020 20202020 20202020 20202020 20202020 20202020                                  000AC0
20202020 20202020 20202020 20202020 20202020 20202020 20202020 20202020                                  000AE0
20202020 20202020 20202020 20202020 20202020 20202020 20202020 20202020                                  000B00
20202020 20202020 20202020 20202020 20202020 20202020 20202020 20202020                                  000B20
6CDB6CDB 6CDB6CDB 6CDB6CDB 6CDB6CDB 6CDB6CDB 6CDB6CDB 6CDB6CDB 6CDB6CDB 0101010101010101010101010101010101 000B40
6CDB6CDB 6CDB6CDB 6CDB6CDB 6CDB6CDB 6CDB6CDB 6CDB6CDB 6CDB6CDB 6CDB6CDB 0101010101010101010101010101010101 000B60
6CDB6CDB 6CDB6CDB 6CDB6CDB 6CDB6CDB 6CDB6CDB 6CDB6CDB 6CDB6CDB 6CDB6CDB 0101010101010101010101010101010101 000B80
6CDB6CDB 6CDB6CDB 6CDB6CDB 6CDB6CDB 6CDB6CDB 6CDB6CDB 6CDB6CDB 6CDB6CDB 0101010101010101010101010101010101 000BA0
6CDB6CDB 6CDB6CDB 6CDB6CDB 6CDB6CDB 6CDB6CDB 6CDB6CDB 6CDB6CDB 6CDB6CDB 0101010101010101010101010101010101 000BC0
DDD9DDD9 DDD9DDD9 DDD9DDD9 6CDB6CDB 6CDB6CDB 6CDB6CDB 6CDB6CDB 6CDB6CDB 0101010101010101010101D9D9D9D9D9D9 000BE0
DDD9DDD9 DDD9DDD9 DDD9DDD9 DDD9DDD9 DDD9DDD9 DDD9DDD9 DDD9DDD9 DDD9DDD9 D9D9D9D9D9D9D9D9D9D9D9D9D9D9D9D9D9 000C00
DDD9DDD9 DDD9DDD9 DDD9DDD9 DDD9DDD9 DDD9DDD9 DDD9DDD9 DDD9DDD9 DDD9DDD9 D9D9D9D9D9D9D9D9D9D9D9D9D9D9D9D9D9 000C20
DDD9DDD9 DDD9DDD9 DDD9DDD9 DDD9DDD9 DDD9DDD9 DDD9DDD9 DDD9DDD9 DDD9DDD9 D9D9D9D9D9D9D9D9D9D9D9D9D9D9D9D9D9 000C40
DDD9DDD9 DDD9DDD9 DDD9DDD9 DDD9DDD9 DDD9DDD9 DDD9DDD9 DDD9DDD9 DDD9DDD9 D9D9D9D9D9D9D9D9D9D9D9D9D9D9D9D9D9 000C60
DDD9DDD9 DDD9DDD9 DDD9DDD9 DDD9DDD9 DDD9DDD9 DDD9DDD9 DDD9DDD9 DDD9DDD9 D9D9D9D9D9D9D9D9D9D9D9D9D9D9D9D9D9 000C80
DDD9DDD9 DDD9DDD9 DDD9DDD9 DDD9DDD9 DDD9DDD9 DDD9DDD9 DDD9DDD9 DDD9DDD9 D9D9D9D9D9D9D9D9D9D9D9D9D9D9D9D9D9 000CA0
DDD9DDD9 DDD9DDD9 DDD9DDD9 DDD9DDD9 DDD9DDD9 DDD9DDD9 DDD9DDD9 DDD9DDD9 D9D9D9D9D9D9D9D9D9D9D9D9D9D9D9D9D9 000CC0
00800080 00800080 00800080 00800080 00800080 00800080 0080DDD9 DDD9DDD9 D9D9D9.......................... 000CE0
00800080 00800080 00800080 00800080 00800080 00800080 00800080 00800080 ................................ 000D00
00800080 00800080 00800080 00800080 00800080 00800080 00800080 00800080 ................................ 000D20
00800080 00800080 00800080 00800080 00800080 00800080 00800080 00800080 ................................ 000D40
00800080 00800080 00800080 00800080 00800080 00800080 00800080 00800080 ................................ 000D60
00800080 00800080 00800080 00800080 00800080 00800080 00800080 00800080 ................................ 000D80
00800080 00800080 00800080 00800080 00800080 00800080 00800080 00800080 ................................ 000DA0
33E50080 00800080 00800080 00800080 00800080 00800080 00800080 00800080 ...............................83 000DC0
33E533E5 33E533E5 33E533E5 33E533E5 33E533E5 33E533E5 33E533E5 33E533E5 8383838383838383838383838383838383 000DE0
33E533E5 33E533E5 33E533E5 33E533E5 33E533E5 33E533E5 33E533E5 33E533E5 8383838383838383838383838383838383 000E00
33E533E5 33E533E5 33E533E5 33E533E5 33E533E5 33E533E5 33E533E5 33E533E5 8383838383838383838383838383838383 000E20
95D495D4 95D433E5 33E533E5 33E533E5 33E533E5 33E533E5 33E533E5 33E533E5 8383838383838383838383838383836.6.6. 000E40
95D495D4 95D495D4 95D495D4 95D495D4 95D495D4 95D495D4 95D495D4 95D495D4 6.6.6.6.6.6.6.6.6.6.6.6.6.6.6.6.6.6. 000E60
```

```
95D495D4 95D495D4 95D495D4 95D495D4 95D495D4 95D495D4 95D495D4 95D495D4 ö.ö.ö.ö.ö.ö.ö.ö.ö.ö.ö.ö.ö.ö.ö.ö. 000E80
95D495D4 95D495D4 95D495D4 95D495D4 95D495D4 95D495D4 95D495D4 95D495D4 ö.ö.ö.ö.ö.ö.ö.ö.ö.ö.ö.ö.ö.ö.ö.ö. 000EA0
95D495D4 95D495D4 95D495D4 95D495D4 95D495D4 95D495D4 95D495D4 95D495D4 ö.ö.ö.ö.ö.ö.ö.ö.ö.ö.ö.ö.ö.ö.ö.ö. 000EC0
95D495D4 95D495D4 95D495D4 95D495D4 95D495D4 95D495D4 95D495D4 95D495D4 ö.ö.ö.ö.ö.ö.ö.ö.ö.ö.ö.ö.ö.ö.ö.ö. 000EE0
95D495D4 95D495D4 95D495D4 95D495D4 95D495D4 95D495D4 95D495D4 95D495D4 ö.ö.ö.ö.ö.ö.ö.ö.ö.ö.ö.ö.ö.ö.ö.ö. 000F00
95D495D4 95D495D4 95D495D4 95D495D4 95D495D4 95D495D4 95D495D4 95D495D4 ö.ö.ö.ö.ö.ö.ö.ö.ö.ö.ö.ö.ö.ö.ö.ö. 000F20
1AD91AD9 1AD91AD9 1AD91AD9 1AD995D4 95D495D4 95D495D4 95D495D4 95D495D4 ö.ö.ö.ö.ö.ö.ö.ö.ö.ö.ö.ö.ö.ö.ö.ö. 000F40
1AD91AD9 1AD91AD9 1AD91AD9 1AD91AD9 1AD91AD9 1AD91AD9 1AD91AD9 1AD91AD9 ö.ö.ö.ö.ö.ö.ö.ö.ö.ö.ö.ö.ö.ö.ö.ö. 000F60
1AD91AD9 1AD91AD9 1AD91AD9 1AD91AD9 1AD91AD9 1AD91AD9 1AD91AD9 1AD91AD9 ö.ö.ö.ö.ö.ö.ö.ö.ö.ö.ö.ö.ö.ö.ö.ö. 000F80
1AD91AD9 1AD91AD9 1AD91AD9 1AD91AD9 1AD91AD9 1AD91AD9 1AD91AD9 1AD91AD9 ö.ö.ö.ö.ö.ö.ö.ö.ö.ö.ö.ö.ö.ö.ö.ö. 000FA0
84DA84DA 84DA84DA 84DA84DA 84DA84DA 84DA1AD9 1AD91AD9 1AD91AD9 1AD91AD9 ö.ö.ö.ö.ö.ö.ö.ö.ö.ö.ö.ö.ö.ö.ö.ö. 000FC0
84DA84DA 84DA84DA 84DA84DA 84DA84DA 84DA84DA 84DA84DA 84DA84DA 84DA84DA ö.ö.ö.ö.ö.ö.ö.ö.ö.ö.ö.ö.ö.ö.ö.ö. 000FE0
84DA84DA 84DA84DA 84DA84DA 84DA84DA 84DA84DA 84DA84DA 84DA84DA 84DA84DA ö.ö.ö.ö.ö.ö.ö.ö.ö.ö.ö.ö.ö.ö.ö.ö. 001000
84DA84DA 84DA84DA 84DA84DA 84DA84DA 84DA84DA 84DA84DA 84DA84DA 84DA84DA ö.ö.ö.ö.ö.ö.ö.ö.ö.ö.ö.ö.ö.ö.ö.ö. 001020
84DA84DA 84DA84DA 84DA84DA 84DA84DA 84DA84DA 84DA84DA 84DA84DA 84DA84DA ö.ö.ö.ö.ö.ö.ö.ö.ö.ö.ö.ö.ö.ö.ö.ö. 001040
84DA84DA 84DA84DA 84DA84DA 84DA84DA 84DA84DA 84DA84DA 84DA84DA 84DA84DA ö.ö.ö.ö.ö.ö.ö.ö.ö.ö.ö.ö.ö.ö.ö.ö. 001060
B8D9B8D9 B8D9B8D9 B8D9B8D9 B8D9B8D9 B8D9B8D9 B8D9B8D9 84DA84DA 84DA84DA ö.ö.ö.ö.ö°ö°ö°ö°ö°ö°ö°ö°ö°ö°ö°ö°ö° 001080
B8D9B8D9 B8D9B8D9 B8D9B8D9 B8D9B8D9 B8D9B8D9 B8D9B8D9 B8D9B8D9 B8D9B8D9 ö°ö°ö°ö°ö°ö°ö°ö°ö°ö°ö°ö°ö°ö°ö°ö° 0010A0
6CDB6CDB 6CDB6CDB 6CDB6CDB 6CDB6CDB 6CDB6CDB 6CDB6CDB 6CDBB8D9 B8D9B8D9 ö°ö°ö°ö¡ö¡ö¡ö¡ö¡ö¡ö¡ö¡ö¡ö¡ö¡ö¡ 0010C0
6CDB6CDB 6CDB6CDB 6CDB6CDB 6CDB6CDB 6CDB6CDB 6CDB6CDB 6CDB6CDB 6CDB6CDB ö¡ö¡ö¡ö¡ö¡ö¡ö¡ö¡ö¡ö¡ö¡ö¡ö¡ö¡ö¡ö¡ 0010E0
6CDB6CDB 6CDB6CDB 6CDB6CDB 6CDB6CDB 6CDB6CDB 6CDB6CDB 6CDB6CDB 6CDB6CDB ö¡ö¡ö¡ö¡ö¡ö¡ö¡ö¡ö¡ö¡ö¡ö¡ö¡ö¡ö¡ö¡ 001100
6CDB6CDB 6CDB6CDB 6CDB6CDB 6CDB6CDB 6CDB6CDB 6CDB6CDB 6CDB6CDB 6CDB6CDB ö¡ö¡ö¡ö¡ö¡ö¡ö¡ö¡ö¡ö¡ö¡ö¡ö¡ö¡ö¡ö¡ 001120
6CDB6CDB 6CDB6CDB 6CDB6CDB 6CDB6CDB 6CDB6CDB 6CDB6CDB 6CDB6CDB 6CDB6CDB ö¡ö¡ö¡ö¡ö¡ö¡ö¡ö¡ö¡ö¡ö¡ö¡ö¡ö¡ö¡ö¡ 001140
6CDB6CDB 6CDB6CDB 6CDB6CDB 6CDB6CDB 6CDB6CDB 6CDB6CDB 6CDB6CDB 6CDB6CDB ö¡ö¡ö¡ö¡ö¡ö¡ö¡ö¡ö¡ö¡ö¡ö¡ö¡ö¡ö¡ö¡ 001160
E7DBE8DB E9DBEADB EBDBEBDB ECDBEDDB EEDBEFDB EFDBF0DB F1DBF2DB F3DBF3DB ö°ö°ö°ö°ö°ö°ö°ö°ö°ö°ö°ö°ö°ö°ö°ö° 001180
D9DBDADB DBDBDBDB DCDBDDDB DEDBDFDB E0DBE1DB E2DBE3DB E4DBE5DB E5DBE6DB ö°ö°ö°ö°ö°ö°ö°ö°ö°ö°ö°ö°ö°ö°ö°ö° 0011A0
C8DBC9DB CBDBCCDB CDDBCEDB CFDBD0DB D1DBD2DB D3DBD4DB D5DBD6DB D7DBD8DB ö°ö°ö°ö°ö°ö°ö°ö°ö°ö°ö°ö°ö°ö°ö°ö° 0011C0
B7DBB8DB B9DBBADB BCDBBDDB BEDBBFDB C0DBC1DB C2DBC3DB C4DBC5DB C6DBC7DB ö°ö°ö°ö°ö°ö°ö°ö°ö°ö°ö°ö°ö°ö°ö°ö° 0011E0
A5DBA6DB A7DBA9DB AADBABDB ACDBADDB AEDBAFDB B1DBB2DB B3DBB4DB B5DBB6DB ö°ö°ö°ö°ö°ö°ö°ö°ö°ö°ö°ö°ö°ö°ö°ö° 001200
DDD9DDD9 DDD9DDD9 DDD9DDD9 9ADB9BDB 9CDB9DDB 9EDBA0DB A1DBA2DB A3DBA4DB ö°ö°ö°ö°ö°ö°ö°ö°ö°ö°ö°ö°ö°ö°ö°ö° 001220
DDD9DDD9 DDD9DDD9 DDD9DDD9 DDD9DDD9 DDD9DDD9 DDD9DDD9 DDD9DDD9 DDD9DDD9 ö°ö°ö°ö°ö°ö°ö°ö°ö°ö°ö°ö°ö°ö°ö°ö° 001240
DDD9DDD9 DDD9DDD9 DDD9DDD9 DDD9DDD9 DDD9DDD9 DDD9DDD9 DDD9DDD9 DDD9DDD9 ö°ö°ö°ö°ö°ö°ö°ö°ö°ö°ö°ö°ö°ö°ö°ö° 001260
DDD9DDD9 DDD9DDD9 DDD9DDD9 DDD9DDD9 DDD9DDD9 DDD9DDD9 DDD9DDD9 DDD9DDD9 ö°ö°ö°ö°ö°ö°ö°ö°ö°ö°ö°ö°ö°ö°ö°ö° 001280
DDD9DDD9 DDD9DDD9 DDD9DDD9 DDD9DDD9 DDD9DDD9 DDD9DDD9 DDD9DDD9 DDD9DDD9 ö°ö°ö°ö°ö°ö°ö°ö°ö°ö°ö°ö°ö°ö°ö°ö° 0012A0
DDD9DDD9 DDD9DDD9 DDD9DDD9 DDD9DDD9 DDD9DDD9 DDD9DDD9 DDD9DDD9 DDD9DDD9 ö°ö°ö°ö°ö°ö°ö°ö°ö°ö°ö°ö°ö°ö°ö°ö° 0012C0
DDD9DDD9 DDD9DDD9 DDD9DDD9 DDD9DDD9 DDD9DDD9 DDD9DDD9 DDD9DDD9 DDD9DDD9 ö°ö°ö°ö°ö°ö°ö°ö°ö°ö°ö°ö°ö°ö°ö°ö° 0012E0
DDD9DDD9 DDD9DDD9 DDD9DDD9 DDD9DDD9 DDD9DDD9 DDD9DDD9 DDD9DDD9 DDD9DDD9 ö°ö°ö°ö°ö°ö°ö°ö°ö°ö°ö°ö°ö°ö°ö°ö° 001300
00800080 00800080 00800080 00800080 00800080 00800080 0080DDD9 DDD9DDD9 ö°ö°ö°.......................... 001320
00800080 00800080 00800080 00800080 00800080 00800080 00800080 00800080 ................................ 001340
00800080 00800080 00800080 00800080 00800080 00800080 00800080 00800080 ................................ 001360
00800080 00800080 00800080 00800080 00800080 00800080 00800080 00800080 ................................ 001380
00800080 00800080 00800080 00800080 00800080 00800080 00800080 00800080 ................................ 0013A0
00800080 00800080 00800080 00800080 00800080 00800080 00800080 00800080 ................................ 0013C0
00800080 00800080 00800080 00800080 00800080 00800080 00800080 00800080 ................................ 0013E0
E7F60080 00800080 00800080 00800080 00800080 00800080 00800080 00800080 ................................ö¢ 001400
D5F6D7F6 D8F6DAF6 DBF6DDF6 DEF6DFF6 E0F6E2F6 E3F6E4F6 E4F6E5F6 E6F6E7F6 öçöæößöàöáöâöäöàöåöæöçöèöéöêöëöìöíöîöïöðöñ 001420
B3F6B6F6 B8F6BBF6 BDF6C0F6 C2F6C4F6 C6F6C8F6 CAF6CCF6 CEF6D0F6 D2F6D4F6 öööööö°ö¹ö²ö³öö£öö€öö¥öö¦öö§öö¨öö©öö»ö°ö¶ö¾ 001440
81F685F6 88F68CF6 8FF693F6 96F699F6 9CF69FF6 A2F6A5F6 A8F6ABF6 AEF6B0F6 ö°ö°ö°ö«ö¤ö¥ö¢ö.ö.ö.ö.ö.ö.ö.ö.ö.ö.ö. 001460
DDE7E6E7 F0E74EF6 53F657F6 5BF65FF6 63F667F6 6BF66FF6 73F676F6 7AF67EF6 ö~özövösöoökögöcö_öÖöWöSöNö°öæö° 001480
35E740E7 4BE756E7 61E76CE7 77E782E7 8CE797E7 A1E7ABE7 B5E7BFE7 C9E7D3E7 çöçÉçÇçµç«çiç.ç.ç.ç¡çºçÇçªçVçKçÉç5 0014A0
72E67FE6 8CE698E6 A5E6B1E6 BEE6CAE6 D6E6E3E6 EFE6FBE6 06E712E7 1EE729E7 ç)ç.ç.ç.æûæïæãæõæÇæªæ¥æ±æ¼æ.æ.æ.ær 0014C0
97E5A6E5 B4E5C2E5 D0E5DEE5 ECE5FAE5 07E615E6 22E630E6 3DE64BE6 58E665E6 æÆæXæKæ=æ0æ"æ.æ.åûå¡åªå¾åºåÅåºåº 0014E0
76E089E0 C8E4D7E4 E6E4F6E4 05E514E5 23E531E5 40E54FE5 5EE56CE5 7BE589E5 à.à{à|à^à0à@à1à#à.à.äöäæäÇäÆà.à| 001500
3ADF4FDF 63DF77DF 8BDF9FDF B3DFC7DF DADFEEDF 02E015E0 29E03CE0 4FE063E0 àçàÚà<à)à.à.à¶àÚàÇà³à.à.à¶àÇà¶à¾à: 001520
F0DD05DE 1ADE2FDE 44DE59DE 6DDE82DE 97DEABDE C0DED5DE E9DEFDDE 12DF26DF ð&ð.ÞÿÞéÞßÞAÞ«Þ.Þ.ÞmÞYÞDÞ/Þ.Þ.ÞÿÞÞ 001540
9DDCB2DC C7DCDDDC F2DC07DD 1CDD32DD 47DD5CDD 71DD87DD 9CDDB1DD C6DDDBDD ÝÜÝÆÝ±Ý.Ý.ÝqÝ\ÝGÝ2Ý.Ý.ÜÜÜÝÜÇÜ²Ü. 001560
AADAB6DA C3DAD0DA DDDAEADA F7DADCDB F1DB07DC 1CDC32DC 47DC5CDC 72DC87DC Ú.ÚrÚ\ÚGÜ2Ü.Ü.ÜÑÜÜæÜêÜÝÜ°ÜÆÜ¶ÜÜê 001580
E9D9F4D9 00DA0BDA 17DA22DA 2EDA3ADA 46DA52DA 5FDA6BDA 77DA84DA 90DA9DDA Ú.Ú.Ú.ÚwÚkÚ_ÚRÚFÚ:Ú.Ú"Ú.Ú.Ú.ÚÚÚé 0015A0
44D94DD9 57D960D9 6AD974D9 7ED988D9 92D99DD9 A7D9B2D9 BDD9C8D9 D3D9DED9 ÙÞÙ`ÙEÙ½Ù²Ù§Ù.Ù.Ù.Ù~ÙtÙjÙ'ÙWÙMÙÞÙ 0015C0
C1D8C8D8 CFD8D7D8 DED8E6D8 EED8F6D8 FED806D9 0ED917D9 20D928D9 31D93AD9 Ù:Ù1Ù(Ù Ù.Ù.Ù.Ø°ØØØ¡Ø¶Ø°ØÆØ¡Ø£ØÀ 0015E0
```

```
04F315F3 10F31BF3 31F349F3 62F37CF3 97F3B4F3 D2F3F2F3 13F436F4 5AF480F4 ò.ò7ò6ò.ò6ò6ò6?ò.ò1ò6ò1ò16.ò.ò.ò. 006880
21F22EF2 61F269F2 71F279F2 82F28BF2 95F29FF2 A9F2B5F2 C8F2D6F2 E4F2F3F2 ò6ò4ò0ò0ò8ò¶ò@ò.ò.ò.ò.ò.ò.ò.ò.ò! 0068A0
77F283F2 8EF2FCF1 00F205F2 09F20DF2 11F215F2 19F21DF2 14F217F2 1BF21EF2 ò.ò.ò.ò.ò.ò.ò.ò.ò.ò.ò.ò.ò.ò.ò.ò.w 0068C0
9FF056F1 57F15AF1 5FF164F1 6BF14FF1 59F165F1 3CF245F2 4EF258F2 62F26DF2 ò.ò.ò.ò.ò.ò.ò.ò.ò.ò.ò.ò.ò.ò.ò.ò.ò. 0068E0
00800080 00800080 00800080 00800080 00800080 00800080 00800080 00800080 ................................ 006900
00800080 00800080 00800080 00800080 00800080 00800080 00800080 00800080 ................................ 006920
00800080 00800080 00800080 00800080 00800080 00800080 00800080 00800080 ................................ 006940
00800080 00800080 00800080 00800080 00800080 00800080 00800080 00800080 ................................ 006960
00800080 00800080 00800080 00800080 00800080 00800080 00800080 00800080 ................................ 006980
00800080 00800080 00800080 00800080 00800080 00800080 00800080 00800080 ................................ 0069A0
00800080 00800080 00800080 00800080 00800080 00800080 00800080 00800080 ................................ 0069C0
00800080 00800080 00800080 00800080 00800080 00800080 00800080 00800080 ................................ 0069E0
00800080 00800080 00800080 00800080 00800080 00800080 00800080 00800080 ................................ 006A00
00800080 00800080 00800080 00800080 00800080 00800080 00800080 00800080 ................................ 006A20
00800080 00800080 00800080 00800080 00800080 00800080 00800080 00800080 ................................ 006A40
00800080 00800080 00800080 00800080 00800080 00800080 00800080 00800080 ................................ 006A60
00800080 00800080 00800080 00800080 00800080 00800080 00800080 00800080 ................................ 006A80
00800080 00800080 00800080 00800080 00800080 00800080 00800080 00800080 ................................ 006AA0
00800080 00800080 00800080 00800080 00800080 00800080 00800080 00800080 ................................ 006AC0
00800080 00800080 00800080 00800080 00800080 00800080 00800080 00800080 ................................ 006AE0
00800080 00800080 00800080 00800080 00800080 00800080 00800080 00800080 ................................ 006B00
00800080 00800080 00800080 00800080 00800080 00800080 00800080 00800080 ................................ 006B20
00800080 00800080 00800080 00800080 00800080 00800080 00800080 00800080 ................................ 006B40
00800080 00800080 00800080 00800080 00800080 00800080 00800080 00800080 ................................ 006B60
00800080 00800080 00800080 00800080 00800080 00800080 00800080 00800080 ................................ 006B80
00800080 00800080 00800080 00800080 00800080 00800080 00800080 00800080 ................................ 006BA0
00800080 00800080 00800080 00800080 00800080 00800080 00800080 00800080 ................................ 006BC0
E507E507 E507E507 E507E507 E507E507 E507E507 E507E507 E507E507 E5070080 ...ª.ª.ª.ª.ª.ª.ª.ª.ª.ª.ª.ª.ª.ª.ª 006BE0
44FCBAFC 30FDA5FD 1AFE8DFE FEFE6EFF DCFF4600 AE001401 7701D601 3202E507 .ª.2.º.w...º.F.Ü.®ºº.º.ÿ¥ÿÖüªüD 006C00
71F5B2F5 F5F53CF6 86F6B4F7 F2F734F8 FFF749F8 95FAF2FA 7DFCCDFC 59FBCEFB ûfûYüfü}úòú.øIø.ø4øòøºö.ö<ßßß²ßq 006C20
DCF104F2 2EF259F2 85F2B3F2 E3F214F3 47F372F3 ABF359F4 8BF4C0F4 F8F433F5 ß3ßøßAß.ßY6«ór6G6.ò3ò³ò.òYò.ò.ßÜ 006C40
FFEF18F0 28F043F0 5FF07BF0 97F0B5F0 D3F0F1F0 11F131F1 53F175F1 8FF1B5F1 ßµß.ßußSß1ß.º%º6ºµº.º{º_ºCºº.º.ï. 006C60
D9EEE0EE E9EEF3EE 13EF1FEF 2DEF3CEF 4CEF5DEF 6FEF82EF 95EFAAEF CFEFE7EF ïçïïïëï.ï.ïoï]ïLï<ï-ï.ï.ïóïéïàïù 006C80
61F02DF0 FDEFD0EF A6EF82EF 62EF47EF 2FEF1BEF F2EED8EE D3EED1EE CEEED1EE îÑîîîÑïóïØïòï.ï/ïGïbï.ïºïºïÿº-ºa 006CA0
AFF545F5 DEF47AF4 19F4B7F3 5DF301F3 A9F254F2 F8F1ACF1 6DF129F1 D7F09AF0 º.º¢ß)ßmßºßøòTò@ó.ó]ó•ß.ßzßºßE®º 006CC0
62FDE3FC 4BFCCAFB 4AFBCAFA 4CFACFF9 54F9D9F8 61F8EAF7 76F704F7 94F61CF6 ö.ö.ø.øvøêøaøùùTùïùLúêûJúêüKüßÿb 006CE0
4B031D03 E602A702 60022002 D4017601 1301AB00 3F00D2FF 49FFCAFE 50FEE0FD ÿàºPºë.I.ò.?.«...v.ò. .'.§.æ...K 006D00
4A00CB00 4101C801 28027E02 CA020A03 40036C03 8603A203 A703A103 90036F03 .o...i.§.¢...l.@...ê.~.(.ê.A.È.J 006D20
C7F4B0F5 7EF64BF7 17F8E2F8 A9F96DFA 2DFBE3FB 9AFC4BFD F5FD98FE 2FFFC2FF .A./º.ÿßÿKü.ûßû-úmù@øâø.øKö~ß°ßÇ 006D40
42EABCEA 1DEBA4EB 33ECCBEC 6BED11EE CBEE7CEF 30F0EDF0 ADF185F2 4AF312F4 ß.ßJò.ßººíºOïlîëî.íkîëî3ëºë.ë¼ëB 006D60
1CE803E8 FFE7F0E7 E8E7E8E7 EFE700E8 0DE832E8 5DE895E8 D6E821E9 76E9D4E9 éòévé!èòè.è]è2è.è.çïçèçèçºç.è.è. 006D80
E8EAD0EA A8EA79EA 4BEA19EA E6E9B1E9 7BE944E9 2AE9F8E8 D0E8A1E8 76E84EE8 èNèvèíèºèøé*éDé{é±é¤è.èKéyéxéºèè 006DA0
15EB3DEB 4CEB5EEB 6DEB79EB 82EB8CEB 8FEB8CEB 85EB7AEB 6AEB56EB 3DEB21EB ë!ë=ëVéjézë.ë.ë.ë.ë.ëyëmë^ëLë=ë. 006DC0
F8E822E9 46E96EE9 A6E9B1E9 D3E9F8E9 1DEA40EA 62EA84EA 9EEABEEA DDEAFAEA éúéºéºé.é.ébê@ê.éøéóé±éºéníFé"èø 006DE0
58E67FE6 A7E6D0E6 F0E61EE7 66E794E7 C0E7ECE7 17E842E8 76E88CE8 B7E8E1E8 èáè•è.èvèBè.çìçÀç.çfç.æºæºæ§æ.æX 006E00
19E6EEE5 CBE5B1E5 9FE594E5 92E57EE5 85E594E5 A9E5C2E5 DFE5ECE5 0EE632E6 æ2æ.åïåßåAå@å.å.å~å.å.å.å±åëåîæ. 006E20
BBEDFFEC 5DECB5EB 13EB64EA CCE93EE9 BDE852E8 E4E780E7 25E7D4E6 8CE64EE6 æNæ.æóç%ç.çäèRè½é>éïédë.ëµìî].í» 006E40
AFF73FF7 C6F643F6 B9F548F5 A9F404F4 59F3C0F2 0FF257F1 A1F0EAEF 34EF7FEE î.ï4ïèºïñWò.òAóYó.ó@ßHß¹öCöÆø?øº 006E60
ACF9CDF9 EEF900FA 0AFA0BFA 0AFAF5F9 DCF9BAF9 8EF958F9 18F9CEF8 7BF81EF8 ø.ø{øïù.ùXù.ùºùùùßú.ú.ú.ú.ùïùîùº 006E80
E8F52AF6 70F6ACF6 E0F61FF7 64F7AAF7 EFF740F8 73F8B2F8 EDF824F9 57F984F9 ù.ùWù$øíø²øsø@øìøëødø.ùàùºùpö*ßè 006EA0
AFF3BAF3 C7F3D7F3 EAF314F4 2FF44DF4 6EF493F4 BBF4E7F4 17F54AF5 81F5A8F5 ßxß.ßJß.ßçß»ß.ßnßMß/ß.ßèßCßÇßºßº 006EC0
20F4D7F3 C8F3B9F3 ACF39FF3 93F390F3 88F380F3 9CF39AF3 9AF39CF3 A0F3A7F3 ß§ß.ß.ß.ß.ß.ß.ß.ß.ß.ß.ßºßïßèßCß  006EE0
1AF508F5 F6F4E3F4 CFF4BBF4 A8F493F4 7FF46BF4 57F443F4 2FF41BF4 33F425F4 ß%ß3ß.ß/ßCßWßkß.ß.ßxß»ßïßãßßß.ß. 006F00
52F65DF6 67F670F6 78F67FF6 86F68CF6 91F696F6 9AF69DF6 A0F6A3F6 3CF52CF5 ß,ß<ßÇß.ß.ß.ß.ß.ß.ß.ß.ßxßpßgßlßR 006F20
00800080 00800080 00800080 00800080 00800080 00800080 00800080 00800080 ................................ 006F40
00800080 00800080 00800080 00800080 00800080 00800080 00800080 00800080 ................................ 006F60
00800080 00800080 00800080 00800080 00800080 00800080 00800080 00800080 ................................ 006F80
00800080 00800080 00800080 00800080 00800080 00800080 00800080 00800080 ................................ 006FA0
00800080 00800080 00800080 00800080 00800080 00800080 00800080 00800080 ................................ 006FC0
00800080 00800080 00800080 00800080 00800080 00800080 00800080 00800080 ................................ 006FE0
```

```
00800080 00800080 00800080 00800080 00800080 00800080 00800080 00800080 ................................ 007000
00800080 00800080 00800080 00800080 00800080 00800080 00800080 00800080 ................................ 007020
00800080 00800080 00800080 00800080 00800080 00800080 00800080 00800080 ................................ 007040
00800080 00800080 00800080 00800080 00800080 00800080 00800080 00800080 ................................ 007060
```